# Iceberg Ploughmarks on the Continental Shelf and Slope of Central West Greenland

**Natalie Sarah Thompson**

Girton College

31st August 2011

Supervisor: Professor Julian Dowdeswell

Scott Polar Research Institute
University of Cambridge
Lensfield Road
Cambridge CB2 1ER

**This dissertation is submitted for the degree of Master of Philosophy**

# DECLARATION

This thesis is the result of my own work, and includes nothing which is the outcome of work done in collaboration, except where specifically indicated in the text. The thesis is no more than 20,000 words in length, excluding the declaration, acknowledgements, table of contents, list of figures, list of tables, captions, and list of references.

# ACKNOWLEDGEMENTS

First and foremost, I would like to thank Prof. Julian Dowdeswell for his supervision and guidance throughout the past year. It has been a privilege to work with him. Many thanks go to Dr Kelly Hogan for providing an introduction to the various software systems used in this thesis, and for doing so with such patience. Thanks also to Toby Benham, for his assistance with all things GIS-related, and to Ruth Mugford, who helped me with statistical analysis.

I would like to thank all those who made my time in Cambridge so memorable, in particular my colleagues at the Scott Polar Research Institute, and my fellow Girtonians. I would also like to thank my family and friends, for their help and encouragement over the past year. A big thank you to my long-suffering partner, Joe Holmes, who has always been there to support me. Above all, thank you to my parents, Fran and Gil Thompson; I could not have written this thesis without their love and (financial) support. Last, but by no means least, I would like to thank the world's greatest Great Aunt, Ivy Marsden, who provided me with the financial means to study at a postgraduate level. This thesis is dedicated to the memory of my Aunt Ivy, with love and gratitude.

# TABLE OF CONTENTS

# LIST OF FIGURES

# LIST OF TABLES

# CHAPTER 1 - INTRODUCTION

## 1.1 Introduction and Aims

Throughout the Quaternary, glaciers and ice sheets have advanced and retreated across polar continental shelves in a series of glacial-interglacial cycles, extending as far as the shelf edge under full-glacial conditions (Fig. 1.1). This cyclic pattern of growth and decay is forced by periodic/quasi-periodic variations in the earth's orbital parameters of eccentricity, obliquity, and axial precession, which drive long-term climate change (Imbrie et al., 1992; 1993). At high latitudes, the effects of orbital forcing are amplified by strong positive feedback systems, which have the potential to drive abrupt climatic change. Terrestrial, marine and ice core records show that the dimensions of ice sheets in both hemispheres have fluctuated on a number of different timescales during the Quaternary, with implications for eustatic sea-level change and ocean circulation patterns. However, dynamic changes in ice sheet behaviour are not well constrained, and so represent a major challenge to ice sheet reconstruction. There is, therefore, a need to develop long-term perspectives on ice sheet behaviour, in order to further our understanding of the environmental controls that drive ice sheet fluctuation.

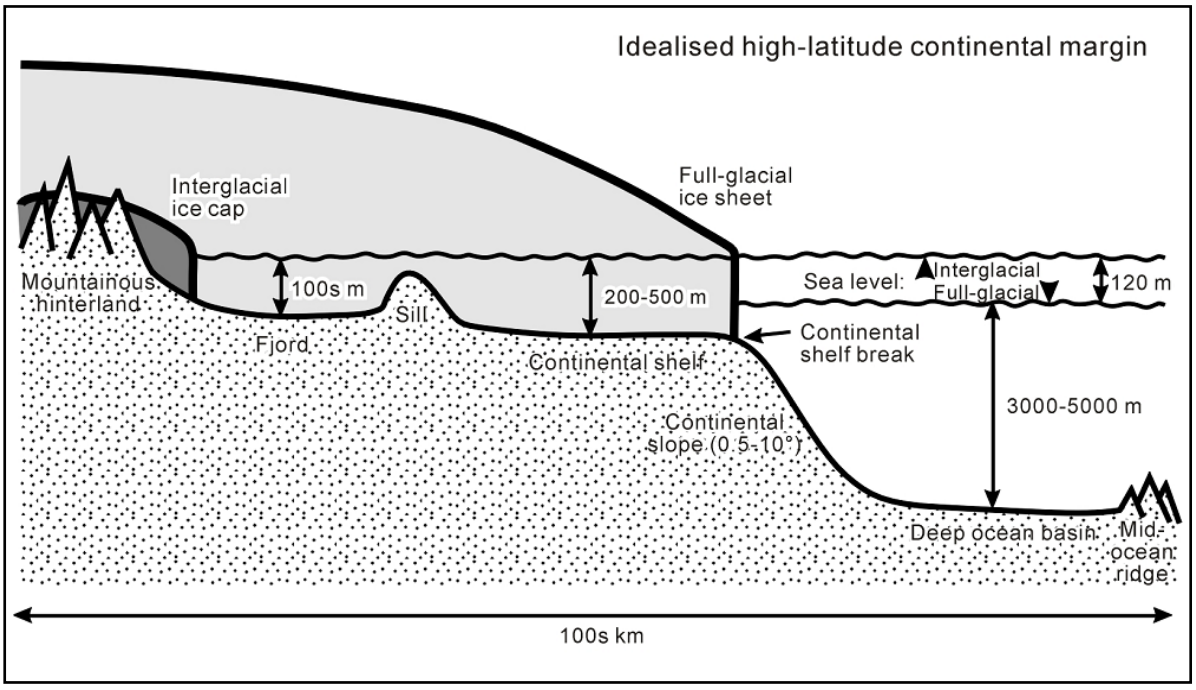


**Figure 1.1.** An idealised high-latitude continental margin, showing full-glacial and interglacial ice sheet extent (from Dowdeswell et al., 2002).

The marine sedimentary record typically preserves a more comprehensive archive of past glacial activity than terrestrial records, since the sea floor below wave base is not subject to the processes of subaerial weathering, fluvial reworking or permafrost degradation. Accordingly, detailed investigations of the morphology of the seafloor provide valuable information on past ice-sheet extent and dynamics, in particular for the most recent glacial cycle (e.g. Ó Cofaigh et al., 2005; Ottesen et al., 2005, 2007; Evans et al., 2006; Winsborrow et al., 2009). Icebergs, produced by glaciers and ice sheets that terminate in marine waters, contribute to the geological record through the release of ice-rafted debris (IRD), and through the disturbance and reworking of seafloor sediments where their keels impact the seabed. Scouring or ploughing of the seafloor by iceberg keels produces characteristic depressions known as ploughmarks (Fig. 1.2). These ploughmarks provide information on the dimensions and drift tracks of icebergs; relict or ancient ploughmarks provide an archive of past iceberg activity, which can be used to reconstruct aspects of the spatial and temporal dynamics of palaeo-ice sheets.

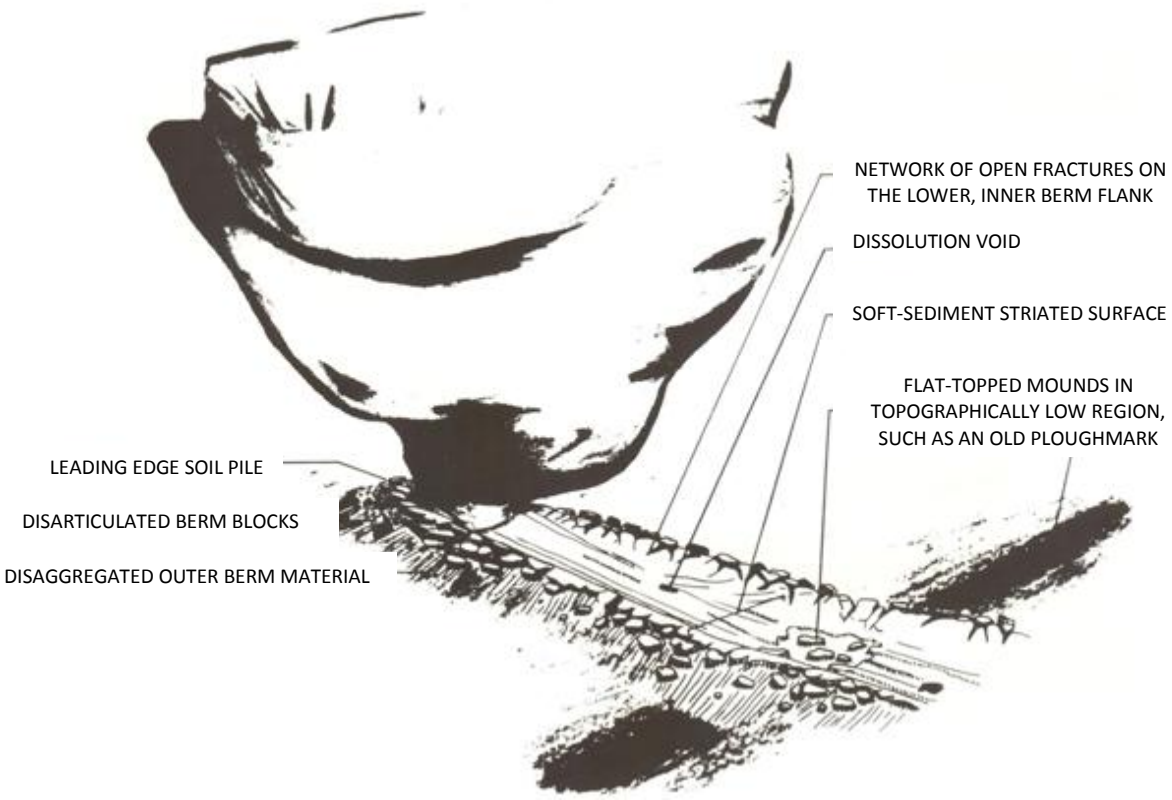


**Figure 1.2.** Diagram to illustrate the key morphological features of an iceberg ploughmark (from Woodworth-Lynas and Dowdeswell, 1994). Note that sometimes only a sub-set of these features is observed on imagery of the seafloor.

The Greenland Ice Sheet is located in a region of significant climatic variability. At present, the ice sheet is experiencing increased mass loss and dynamic change at low elevations; the ice sheet mass deficit has more than doubled since 1996 (Rignot and Kanagaratnam, 2006) and it is predicted that the Greenland Ice Sheet will contribute >0.5 m of global sea-level rise by 2099 (Pfeffer et al., 2008; Long, 2009). These changes may reflect recent warming trends, or, alternatively, they may simply be part of the natural cycle of ice sheet growth and decay. Key to resolving this question is an understanding of long-term changes in the dynamic behaviour of the Greenland Ice Sheet during the Quaternary. However, our understanding of long-term changes in ice sheet behaviour is still poor, and major uncertainties exist with regard to past ice sheet extent and dynamics in many parts of Greenland. This is particularly the case on the West Greenland margin (Fig. 1.3), where a number of fast-flowing outlet glaciers drain the ice sheet into Baffin Bay. The large flux of these glaciers represents a major control on the mass balance and stability of the Greenland Ice Sheet (Rignot and Kanagaratnam, 2006).

This thesis will use multibeam swath-bathymetric and TOPAS sub-bottom profiler records acquired during the JR175 research cruise of the RRS *James Clark Ross* in 2009 to characterise and map iceberg ploughmarks on the West Greenland margin. These data will then be interpreted in the context of the dynamic behaviour of the western sector of the Greenland Ice Sheet and the ocean waters on the Greenland shelf. The main aims of this thesis are, therefore:

(a) To describe the distribution, dimensions and morphological features of iceberg ploughmarks on the West Greenland margin (Fig. 1.3);

(b) To interpret these ploughmarks in the context of the behaviour of outlet glaciers of the Greenland Ice Sheet, both past and present.

## 1.2 Thesis Structure

This thesis contains the following elements. A short introduction, outlining the main aims and objectives of the investigation, was provided in this chapter. Background on previous scientific studies of icebergs, and the process of iceberg ploughing of seafloor sediments, is

presented in Chapter 2. This chapter also describes the modern physiographic, glaciological and oceanographic setting of the study area on the West Greenland margin, and summarises the recent glacial history of this region. The acquisition, processing and interpretation of the geophysical datasets used in this thesis are explained in Chapter 3. Observations on the dimensions, orientations and characteristics of iceberg ploughmarks on the West Greenland margin are presented in Chapter 4, and used to map the nature and intensity of iceberg ploughing in the region. In Chapter 5, these results are interpreted in the context of the dynamic behaviour of the western sector of the Greenland Ice Sheet. Final conclusions and suggestions for further work are presented in Chapter 6.

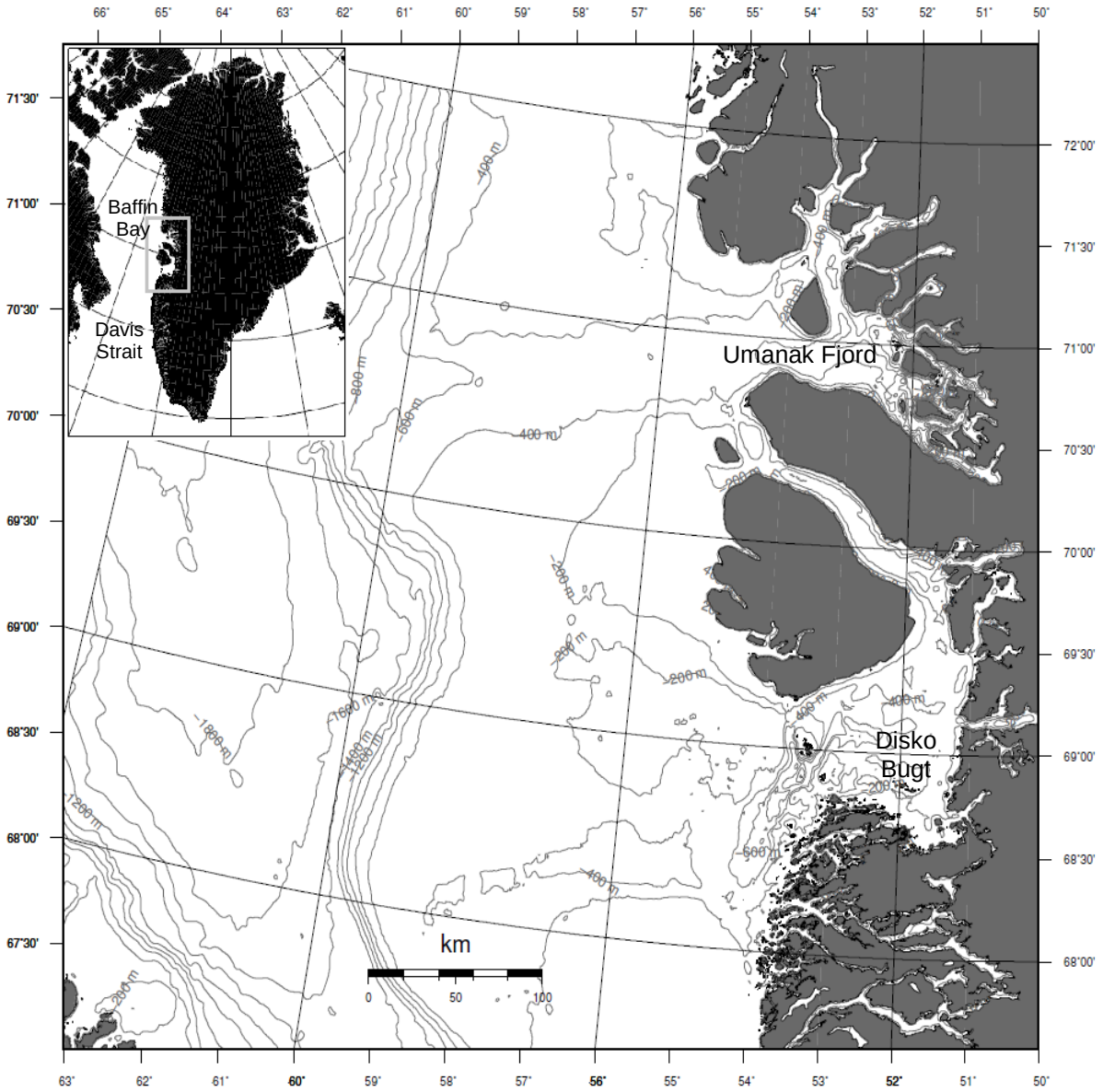


**Figure 1.3.** Map depicting the location and regional bathymetry of the study area on the West Greenland margin. Bathymetric contours are derived from the IBCAO dataset (Jakobsson et al., 2008).

# CHAPTER 2 - SCIENTIFIC BACKGROUND AND STUDY AREA ON THE WEST GREENLAND MARGIN

This chapter provides background on both previous scientific studies of icebergs, and on the study area on the West Greenland margin. This information provides an important context for the research on iceberg ploughing of the West Greenland shelf contained in subsequent chapters of this thesis.

## 2.1 Icebergs

### 2.1.1 Iceberg Production

Icebergs are produced at the marine margins of glaciers and ice sheets through the process of calving. Calving occurs when tensile or compressive stresses close to a glacier terminus exceed the fracture strength of the ice. This allows fractures (crevasses) to penetrate right through the ice, detaching blocks from the main body of the glacier, which are then released to drift in the marine waters offshore (Fig. 2.1; Benn et al., 2007a, b). Crevasses form largely in response to the internal stress patterns within a glacier. Stresses large enough to drive fracture propagation are generated by the following mechanisms: (i) longitudinal stretching associated with spatial variations in velocity; (ii) force imbalances at terminal ice cliffs; (iii) undercutting of the glacier terminus by subaqueous melting; (iv) bending at the junction between grounded and buoyant ice and (v) buoyancy-driven calving of projecting, submerged ice feet (Fig. 2.1; Benn et al., 2007b). Crevasse propagation is greatly facilitated by the presence of water (Benn et al., 2007a, b; Scambos et al., 2008), because water opposes the cryostatic pressure of the ice, preventing creep closure. Additional stresses caused by, for example, tides, storm-generated swell waves, or collisions between icebergs, may also facilitate the calving process (e.g. Robin, 1979; MacAyeal et al., 2006, 2008).

Iceberg calving provides a mechanism for rapid mass transfer from ice sheets to the oceans, with implications for global sea-level rise. For example, if $3.6 \times 10^{14}$ kg of icebergs were to calve and melt, this would result in a global sea level rise of 1 mm (Metz, 2005). Calving is estimated to account for 77% of mass loss from the Antarctic ice sheets (Jacobs et al., 1992)

and contributes to around two-thirds of mass loss from the Greenland Ice Sheet (Rignot and Kanagaratnam, 2006). Calving is also believed to have played a major role in the growth and decay of palaeo-ice sheets. The importance of calving during the last glacial period is demonstrated by layers of IRD in marine sediment cores from the North Atlantic, which record major calving events (Benn et al., 2007b; Metz et al., 2008; Mottram, 2008). The rate of iceberg production is controlled by several factors, including the net snow accumulation rate, the area of the ice sheet drainage basin, and the cross-sectional area at the terminus (Dowdeswell et al., 1995; Pfeffer et al., 2008). Calving flux from the margins of the Greenland Ice Sheet is currently estimated at ~357 $km^3$ $yr^{-1}$ (Rignot and Kanagaratnam, 2006); for Antarctica, calving flux is estimated somewhere between 500 and 2400 $km^3$ $yr^{-1}$ (Long and Roberts, 2003).

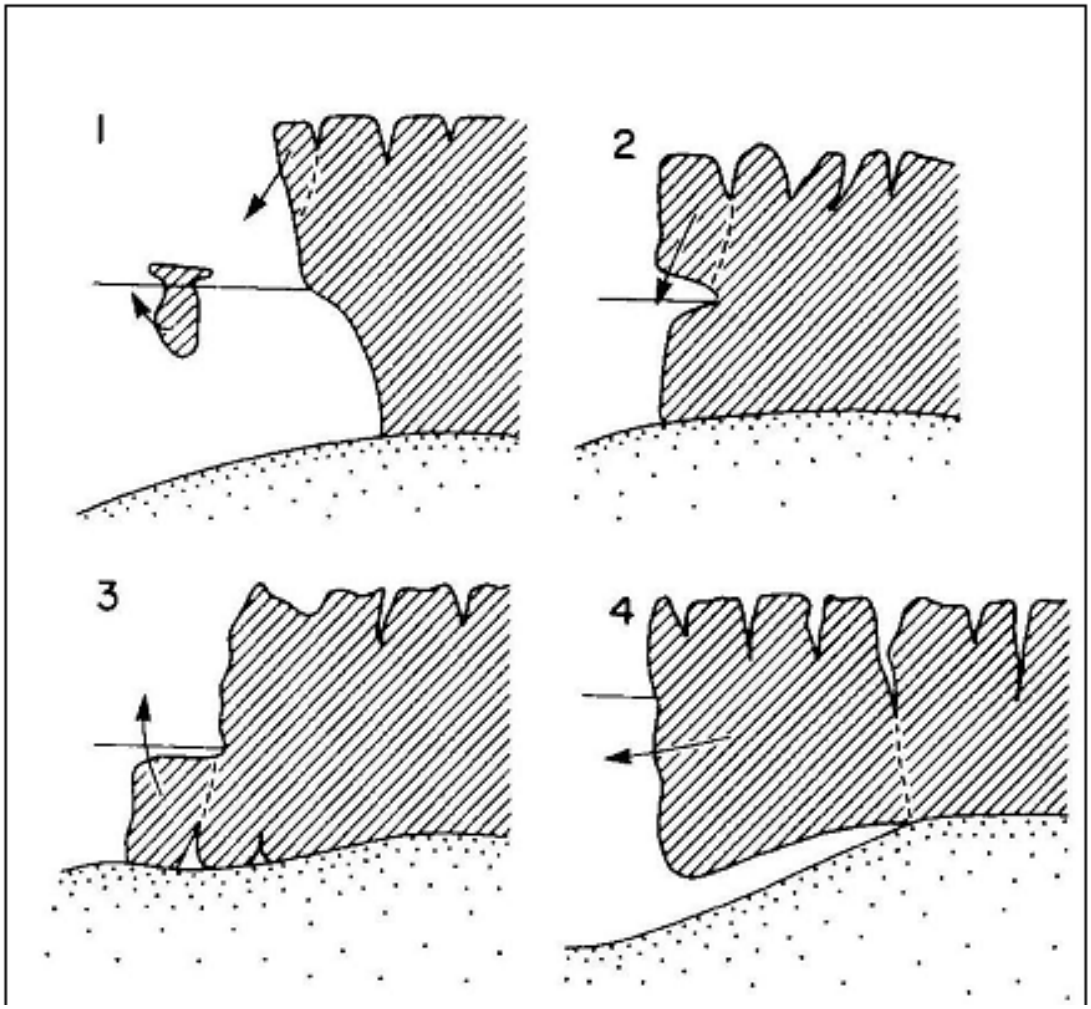


**Figure 2.1.** Iceberg calving processes at grounded ice margins. 1: calving due to force imbalances at the margin. 2: calving due to the formation of a meltwater notch. 3: buoyancy-driven calving of a submerged ice foot. 4: calving in response to bending forces at the junction between grounded and buoyant ice (Syvitski et al., 1987, reproduced in Benn and Evans, 2010).

### 2.1.2 Iceberg Dimensions

The above-water dimensions (length, width and freeboard) of icebergs are highly variable. The main control on iceberg size is the nature of the source environment (Dowdeswell et al., 1992; Meier, 1997). Grounded, fast-flowing tidewater glaciers tend to calve small, irregular icebergs of <50 m in length (Dowdeswell, 1989). Dowdeswell and Forsberg (1992) made observations on the dimensions of 295 icebergs derived from tidewater glaciers in Kongsfjorden, northwest Spitsbergen. Iceberg widths in the fjord ranged from <0.5 m to 30 m and the maximum freeboard was 6 m. Fast-flowing, partially buoyant outlet glaciers, some with floating tongues, can produce much larger icebergs; examples from the Greenland margin have lengths of up to a few kilometres and maximum freeboards in excess of 70 m (Dowdeswell et al., 1992, 1993).

Icebergs typically range from a few metres to several kilometres in width (e.g. Neshyba, 1980; Dowdeswell, 1989; Dowdeswell et al., 1992). Neshyba (1980) recorded a modal width of 200-600 m for Antarctic icebergs. This is comparable with observations made by Wadhams (1988), who noted a modal width of 400-600 m for 174 icebergs in the South Atlantic. Only 6% of these icebergs were less than 200 m wide. The widths of 1900 icebergs in the Scoresby Sund fjord system of East Greenland were measured by Dowdeswell et al. (1992). They found that the majority (70%) of icebergs were less than 200 m wide. Only 5 exceeded 1 km in width and the largest was 2.7 km wide. The size-frequency distribution for an independent sample of these icebergs demonstrates a progressive decay of iceberg frequency with size (Fig. 2.2).

### 2.1.3 Iceberg Keel Depths

Iceberg keel depth is defined as the distance that an iceberg extends below the waterline. Icebergs with keels as deep as ~500 m are currently produced in large numbers at the margins of the Greenland and Antarctic ice sheets (e.g. Dowdeswell et al., 1992, 1993; Dowdeswell and Bamber, 2007). Dowdeswell et al. (1993) calculated the keel depths of 254 icebergs in the Scoresby Sund fjord system, East Greenland. The modal keel depth for the inner fjord (Nordvestfjord) was 400-500 m, decreasing to 100-200 m at the mouth of Scoresby Sund. Two icebergs with keel depths in excess of 600 m were recorded. The shift towards smaller

keel depths in Scoresby Sund likely reflects the changing bathymetry of the fjord system, from deep, narrow inner fjords to a broad and relatively shallow outer fjord.

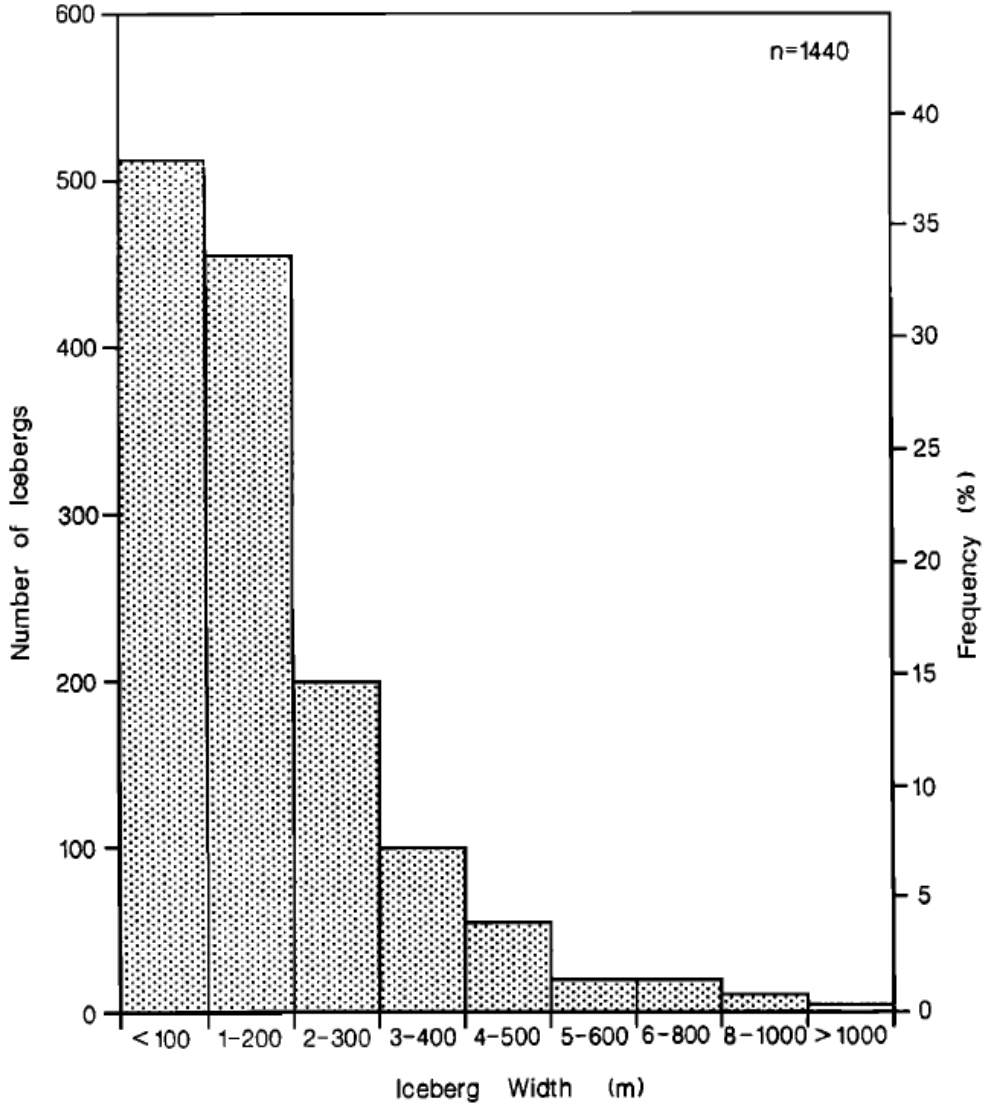


**Figure 2.2.** Size-frequency distribution for an independent sample of icebergs observed by radar in the Scoresby Sund fjord system, East Greenland (from Dowdeswell et al., 1992).

Different types of ice margin produce icebergs of a characteristic keel depth. This has been shown by Dowdeswell and Bamber (2007) in their work on the frequency distribution of Antarctic iceberg keel depths. The frequency distribution of mean keel depth in the Antarctic has three peaks: at 150-200 m, 250-300 m and 550-600 m (Fig. 2.3). Small ($10^3$ $km^2$) ice shelves fringing the Antarctic Peninsula typically calve icebergs with keel depths in the range of 150-200 m. Major ice shelves ($10^5 km^2$), such as the Ronne, Ross and Amery, produce icebergs with mean keel depths of 250-300 m. Fast-flowing outlet glaciers (e.g. Dibble and

Pine Island glaciers), along with the topographically confined Filchner Ice Shelf, calve icebergs with keel depths of between 450 and 650 m and account for the peak at 550-600 m (Fig. 2.3). The main controls on iceberg keel depth are the thickness of ice at the grounding line, the distance from the grounding line to the calving margin and the nature of melting and freezing at the ice-ocean interface. Most ice shelves do not produce icebergs thicker than ~350 m, because creep thinning reduces ice shelf thickness with distance from the grounding line. It is, thus, widely accepted that fast-flowing ice streams and outlet glaciers with deep-water grounding lines, short floating tongues and high mass flux provide the optimal conditions to produce deep-keeled icebergs (e.g. Dowdeswell et al., 1992, 1993; Dowdeswell and Bamber, 2007).

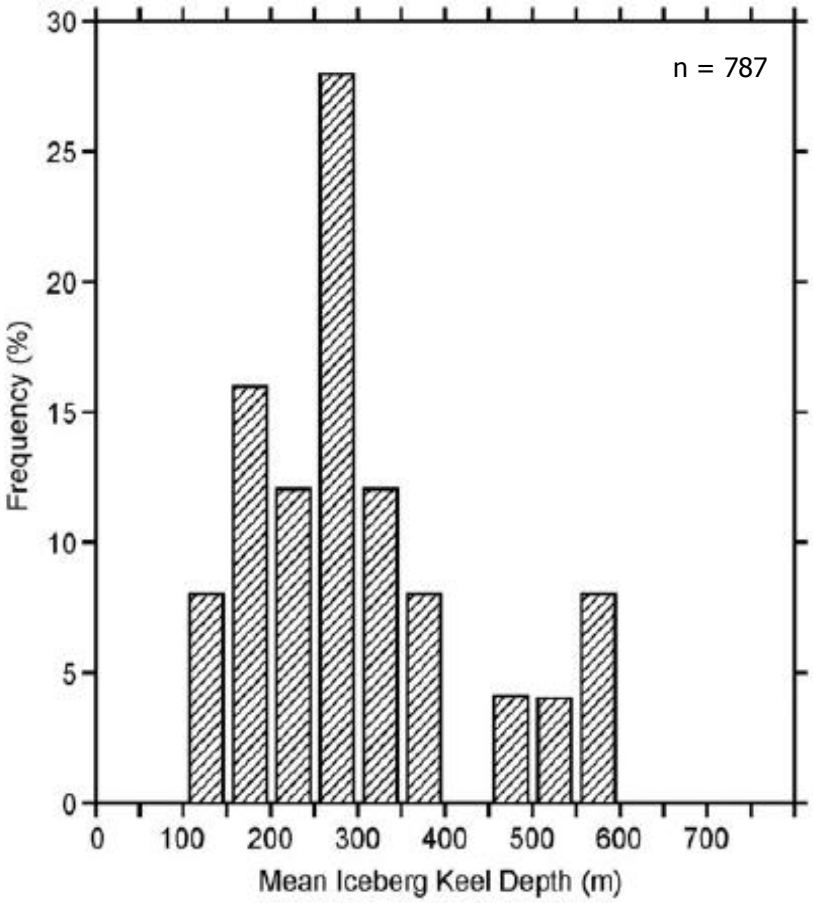


**Figure 2.3.** The frequency-distribution of mean Antarctic iceberg keel depths, derived from satellite radar-altimeter measurements of marginal ice thickness (from Dowdeswell and Bamber, 2007).

Very few modern icebergs have keels deeper than about 650 m (Dowdeswell and Bamber, 2007). Icebergs with keel depths significantly greater than 500-600 m are most likely to be the result of overturn, and readjustment to a more stable position after calving (Dowdeswell,

et al., 1993). Iceberg draft modelling has shown that icebergs can increase their drafts significantly by rolling (e.g. Bass and Peters, 1984; Lewis and Bennett, 1984). Bass and Peters (1984) documented iceberg draft increases of up to 50%, with an average increase of 25%. However, the models indicate that draft change of this magnitude is a rare event, and overturn is therefore unlikely to produce large numbers of deep-keeled icebergs.

## 2.2 Icebergs and the Geological Record

Icebergs affect the geological record through the release of IRD, and the disturbance and reworking of seafloor sediments by iceberg keels (Fig. 2.4). The latter process is the main focus of this investigation, and will be described in more detail below. A comprehensive review of debris rafting is not possible within the scope of this thesis; for an in-depth discussion of iceberg sedimentation processes the reader is referred to Dowdeswell and Dowdeswell (1989).

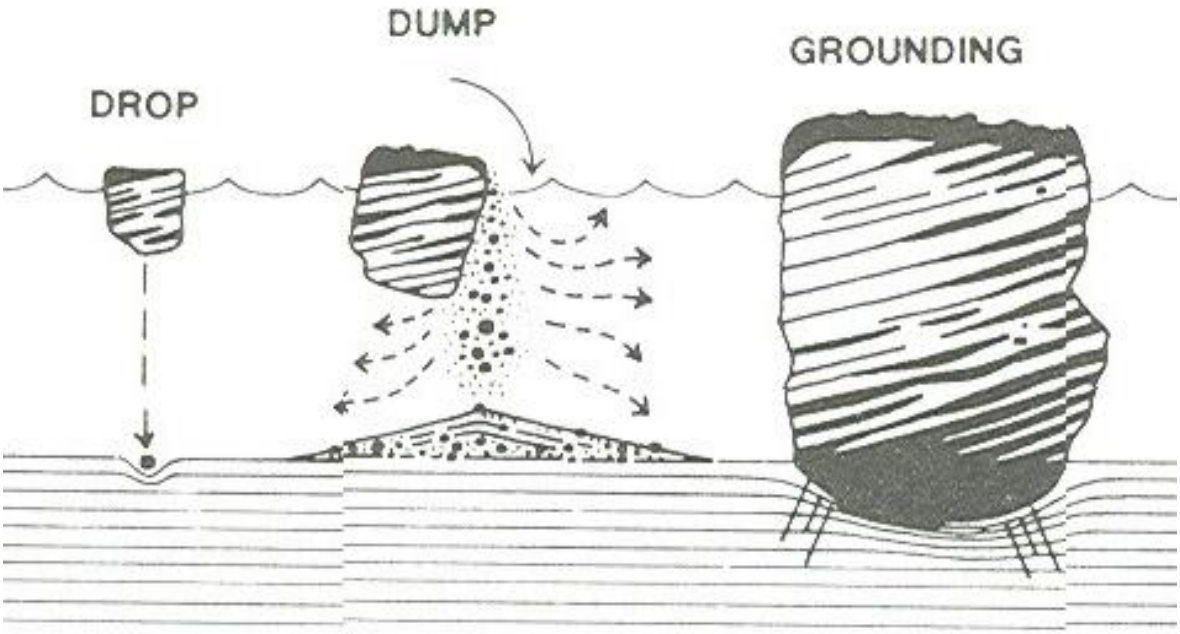


**Figure 2.4.** The effects of iceberg processes on the marine sedimentary record: deposition (dropping and dumping) of ice-rafted sediments, and deformation of seafloor sediments by an iceberg keel (from Thomas and Connell, 1985).

### 2.2.1 Iceberg Ploughmarks

Scouring or ploughing of the seafloor occurs when iceberg keels extend through the full depth of the water column and impact the seafloor, displacing sediments to form a series of depressions (known variously as ploughmarks, scours or furrows) in the seabed. Individual ploughmarks can be tens of kilometres in length, hundreds of metres wide and tens of metres deep, but are typically much smaller. The main controls on ploughmark size are iceberg mass and dimensions (Syvitski et al., 2001). Ploughmarks may be linear, curvilinear, cross-cutting, or any combination thereof. Sets of ploughmarks generally display an irregular pattern on the seafloor, reflecting the wandering drift tracks of individual icebergs (Syvitski et al., 2001; Dowdeswell and Bamber, 2007). The drift track of an iceberg is largely determined by the prevailing current direction, and, to a lesser extent, by wind, waves and tidal currents (Belderson et al., 1973; Belan et al., 2004).

Iceberg ploughmarks are characterised by lateral berms (Fig. 2.5), which range in height from a few centimetres to as much as 6 m above the general level of the seafloor (Woodworth-Lynas et al., 1991). Ploughmark troughs often contain ridge and groove microtopography, formed at the trailing edge of the keel by clastic material embedded in the ice (Woodworth-Lynas and Guigné, 1990; Woodworth-Lynas et al., 1991). A pile of mounded sediment at one end of a ploughmark indicates a grounding event; such features can be used to infer the direction of travel at the time of grounding (Syvitski et al., 2001; Kuijpers et al., 2007). Alternatively, icebergs may produce isolated circular depressions (iceberg pits) as they impact the sea floor (Fig. 2.4; Syvitski et al., 2001).

The intensity of iceberg ploughing is controlled by several factors, including the rate of production and the drift tracks of icebergs, the nature of the substrate, and the relationship between keel depth and bathymetry (Dowdeswell et al., 1993). The bathymetry of the seafloor provides a major control on the distribution of iceberg ploughmarks. The keel depth required to form a ploughmark is constrained by the bathymetric features of the continental shelf. An iceberg will float freely, providing that its keel depth does not exceed the water depth. However, if keel depth is greater than water depth, the iceberg may plough the seafloor. ‘Skipping’ ploughmarks, where an iceberg drifts across a shallowing seafloor and eventually grounds, demonstrate the interplay between keel depth and bathymetry (Syvitski et al., 2001). Woodworth-Lynas et al. (1985) showed that icebergs may traverse significant (40-

50 m) ranges in bathymetry, both upslope and downslope. They attribute this to the continual re-equilibration of icebergs by gradual rotation about a horizontal axis normal to the direction of travel. In this way, icebergs may continue to plough sediments for long distances over undulating seabeds.

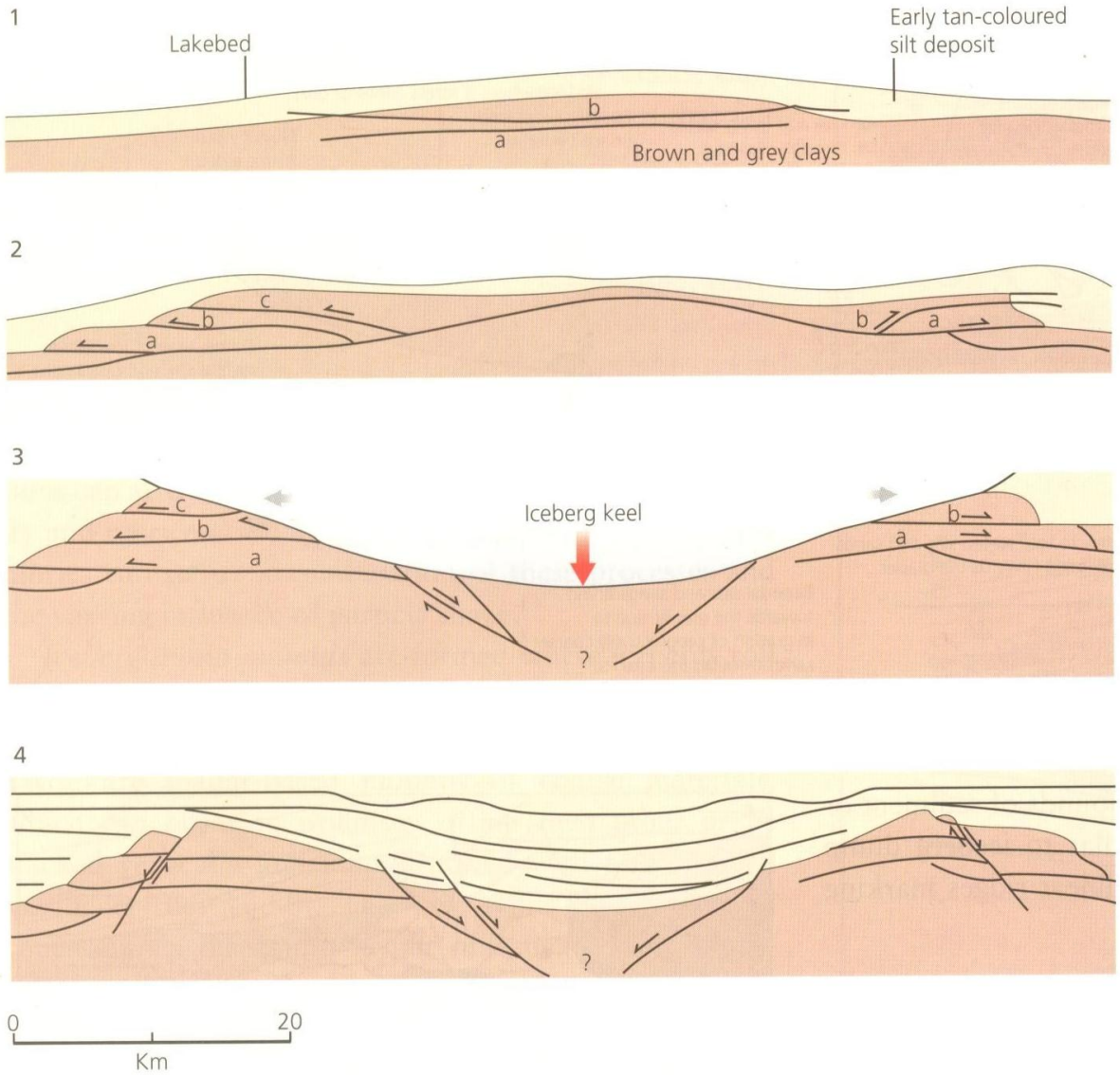


**Figure 2.5.** Conceptual sequence of the development of berms and fault structures during iceberg ploughing. (1) Sediment is compacted in front of the ploughing iceberg keel and as a result the sediment surface bulges and develops horizontal faults. (2) As ploughing continues, berms are produced by the horizontal displacement of seafloor sediments. (3) As the iceberg keel passes over, final emplacement of sediment takes place at the ploughmark margins. (4) As the keel moves past, stress release causes high-angle normal faulting on the berm margins. Sediment then fills the ploughmark trough, and faults may be reactivated by the resultant overburden pressure (Woodworth-Lynas and Guigné, 1990; reproduced in Benn and Evans, 2010).

### 2.2.2 The Effects of Iceberg Ploughing on the Geological Record

Reworking of seafloor sediments by iceberg keels has been, and continues to be, a major glacimarine process on high-latitude continental margins. Both modern and relict ploughmarks have been observed on high-latitude shelves in the northern hemisphere (e.g. Dowdeswell et al., 1993; Syvitski et al., 2001; Dowdeswell et al., 2010c) and Antarctica (e.g. Barnes and Lien, 1988; Ó Cofaigh et al., 2005). Ancient ploughmarks have also been reported from mid-latitude continental shelves (e.g. Belderson et al., 1973), reflecting iceberg drift under full glacial conditions.

The intensity of iceberg ploughing varies inversely with water depth. Factors affecting the maximum depth to which this process occurs include glaciological constraints on iceberg keel dimensions, global eustatic sea level rise, and local sea level adjustments to isostatic and tectonic effects (Dowdeswell and Bamber, 2007). The lower limit of iceberg ploughing, based on observations of modern iceberg dimensions, is generally found at water depths of less than 650 m (e.g. Dowdeswell et al., 1993; Dowdeswell and Bamber, 2007). Ploughmarks at present-day water depths in excess of 700 m may be attributed to a temporary increase in iceberg draft by unstable roll (Dowdeswell et al., 1993), but are more commonly interpreted as relict features, produced by deep-keeled palaeo-icebergs (Syvitski et al., 2001). Ancient ploughmarks have been reported down to water depths of ~1100 m (e.g. Syvitski et al., 2001; Kuijpers et al., 2007; Metz et al., 2008; Dowdeswell et al., 2010c; Pedrosa et al., 2011). Datasets derived from swath bathymetry show evidence of seafloor ploughing by deep-keeled icebergs on the flanks of the Yermak Plateau, north of Svalbard, in water depths of up to 1000 m. Some of these ploughmarks are more than 1 km wide, and several tens of metres deep. Currently, only small icebergs with keel depths typically less than 100 m are calved from ice cliffs in the region of the Yermak Plateau. The large ploughmarks on the Plateau, therefore, must be relict features, most probably formed by large, deep-keeled icebergs calved from major ice streams draining a former Eurasian Ice Sheet (Dowdeswell et al., 2010c).

Where unmodified by sediment reworking processes, iceberg ploughmarks provide a comprehensive archive of past iceberg activity. The dimensions of relict ploughmarks are proxy indicators of palaeo-iceberg dimensions, and can be used to reconstruct aspects of the spatial and temporal dynamics of past ice sheets (e.g. Dowdeswell and Bamber, 2007). The

trajectories of relict ploughmarks reflect iceberg drift patterns, and can be used to make inferences on the direction(s) of palaeo-currents. The relative age of ploughmarks can be inferred, based on the principle of superposition, which states that sedimentary layers are deposited in chronological order, with the oldest at the bottom and the youngest on top; therefore, if one ploughmark crosscuts another, that cross-cutting ploughmark must be the younger feature (Dowdeswell et al., 1993; Dowdeswell et al., 2008). The most recent ploughmarks are likely to appear 'acoustically fresh' (Polyak, 1997), whereas relict ploughmarks may be winnowed by current action, or masked by sedimentary drape (Syvitski et al., 2001). Sediment accumulation rates are the main control on the preservation of iceberg ploughmarks; low rates of sedimentation favour preservation (Polyak, 1997; Syvitski et al., 2001). Ploughmarks formed in a compact deposit, such as till, may retain a fresh appearance for several thousand years in areas with low sedimentation rates (Polyak, 1997). The preservation potential of ploughmarks is also high in areas where the continental shelf is well below the wave base (Syvitski et al., 2001).

## 2.3 Ice Sheet Dynamics and the Greenland Ice Sheet

### 2.3.1 Quaternary Ice Sheet Dynamics

The Quaternary (2.588 Myr-present; Gibbard et al., 2010) has been characterised by the repeated growth and decay of large ice sheets across continental shelves over a series of glacial-interglacial cycles (Fig. 1.1). These cycles are forced by variations in the Earth's orbital parameters of eccentricity, obliquity, and axial precession, which operate on timescales of 100 kyr, 41 kyr and 23 kyr respectively (Imbrie et al., 1992, 1993). Under full-glacial conditions, when global sea-levels were significantly lower than at present, glacier ice advanced as far as the shelf break, where increased mass loss by iceberg calving into deepening water prevented further expansion (Fig. 1.1; Dowdeswell et al., 2002). Quaternary ice sheet dynamics are further characterised by short-term fluctuations of the ice margin in response to significant and often rapid changes in climate, sea-level, and oceanographic regime.

Ice sheet dynamics are not uniform over space (Dowdeswell et al., 2002). Instead, ice sheets are partitioned into fast-flowing ice streams, bounded by regions of slower moving ice. This

pattern is thought to be typical of both modern and Quaternary ice masses (e.g. Ottesen et al., 2007; Ottesen and Dowdeswell, 2009). Ice streams and fast-flowing outlet glaciers currently drain ~80-90% of the Greenland and Antarctic ice sheets, and their large flux has a significant impact on ice sheet mass balance. Furthermore, ice streams control ice, fresh water and sediment flux to the oceans, thereby affecting ocean circulation, and, through this, climate (Ó Cofaigh, 2009; Roberts et al., 2010). Palaeo-ice streams thus hold great potential, both in terms of advancing our understanding of past ice sheet dynamics, and in order to address questions regarding the likely response of ice sheets to ongoing, and future, climatic change.

### 2.3.2 Dynamic History of the Greenland Ice Sheet

The Greenland Ice Sheet has existed in some form at least since the Middle Miocene, around 14 Myr (Funder et al., 2001), and is the only ice sheet in the northern hemisphere to have survived the last glacial-interglacial transition (Fleming and Lambeck, 2004; Kelly and Long, 2009). Palaeoclimatic records indicate that, throughout the Quaternary, the ice sheet has consistently lost mass in response to warming and gained mass in response to cooling (Alley et al., 2010). The dimensions of the Greenland Ice Sheet during the Early and Middle Pleistocene, however, are still largely unresolved. It is only the most recent (Saalian and Weichselian) glacial stages that can be reconstructed with any degree of confidence. Based on the stratigraphic record, the Late Saalian glaciation (ca. 160-140 kyr) produced the most extensive ice advance of the Quaternary. Ice surface elevation on Greenland at this time was at least 1000 m above sea level (e.g. Funder, 1989; Roberts et al., 2009) and the ice sheet likely expanded as far as the outer shelf break (Roberts et al., 2009). Around 130 kyr, the Saalian glaciation was succeeded by the Eemian interglacial. The climate during the Eemian is known to have been warmer than the Holocene; ice cores indicate peak summertime temperatures up to 5ºC warmer than at present (Alley et al., 2010). The ice margin retreated significantly, to leave one main ice sheet covering the central and northern parts of Greenland, and a smaller ice cap over the southern highlands (Fig. 2.6). Proxy records indicate that global sea-level was 5-6 m higher than at present during the Eemian. Tarasov and Peltier (2003) suggested that the Greenland Ice Sheet contributed somewhere in the range of 2.7-4.5 m to this eustatic sea-level rise; Otto-Bliesner et al. (2006) proposed a minimum contribution of 2.2 m and a maximum of 3.4 m.

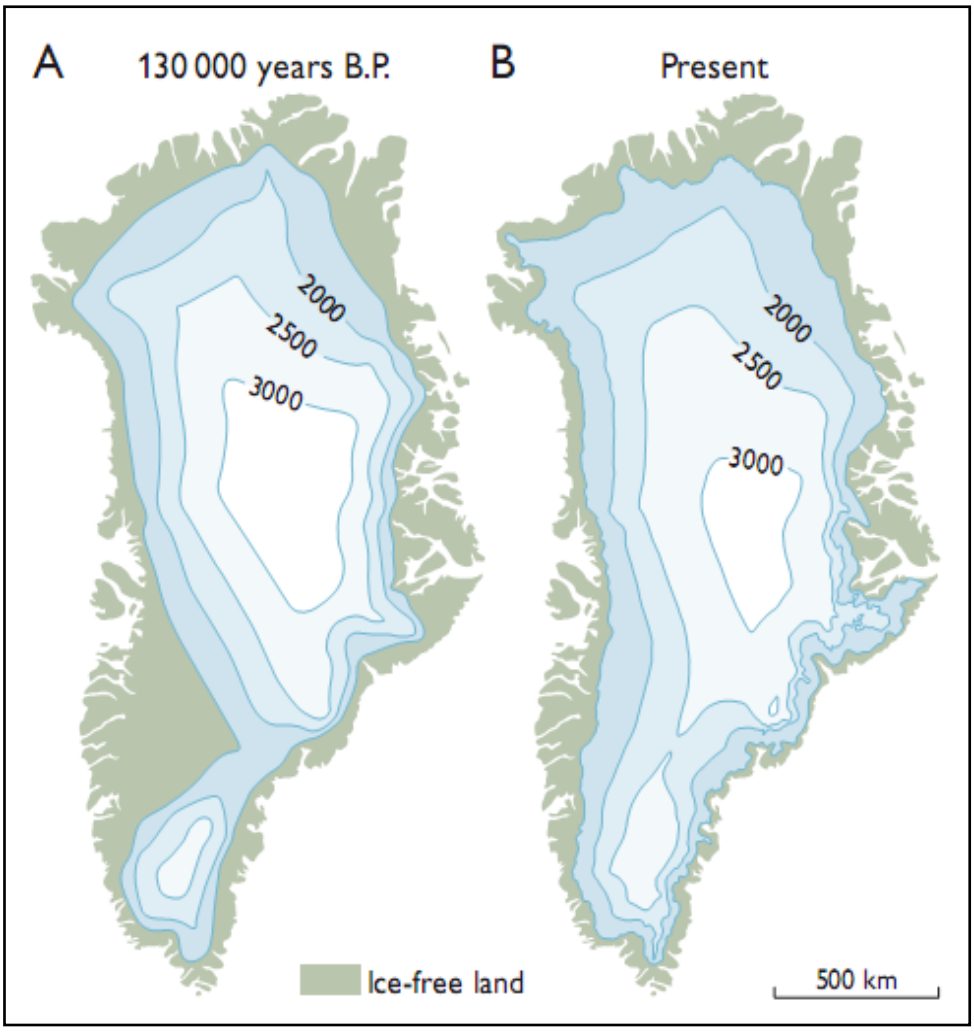


**Figure 2.6.** A: Model of the surface elevation of the Greenland Ice Sheet during the last interglacial according to Létreguilly et al. (1991). B: Modern-day surface elevation (from Weidick and Bennike, 2007).

The last glacial period, the Weichselian, dates from ca. 120-10 kyr, and includes three separate phases of glaciation. The most recent advance (the Late Weichselian) reached a maximum around 21 kyr. This corresponds with a global eustatic sea-level depression of between ca. 125-135 m below the present level (Huybrechts, 2002). Funder and Hansen (1996) used published onshore field studies to reconstruct the dimensions of the Greenland Ice Sheet at the Last Glacial Maximum (LGM). Their model depicts a relatively thin ice sheet, with ice advance in Northeast Greenland restricted to the inner shelf. However, more recent studies (e.g. Evans et al., 2009; Roberts et al., 2009; Winkelmann et al., 2010) indicate that the LGM ice sheet was thick, and extended to at least a mid-shelf position in most regions. Simpson et al. (2009) constrained a thermomechanical model of ice sheet evolution from the LGM to the present day, using observations of relative sea-level. This model

projects the northeastern sector of the ice sheet to a mid- or outer shelf position, indicating a more extensive ice advance than previously assumed (Fig. 2.7). Ice streams were an important glacio-dynamic feature of the Greenland Ice Sheet during the LGM, draining extensive sectors of the Inland Ice across the continental shelf (Evans et al., 2009; Roberts et al., 2010). In many cases, fjord systems acted as tributaries, routing ice streams onto the continental shelf, where they converged to form large, cross-shelf, composite ice streams (Roberts et al., 2009, 2010).

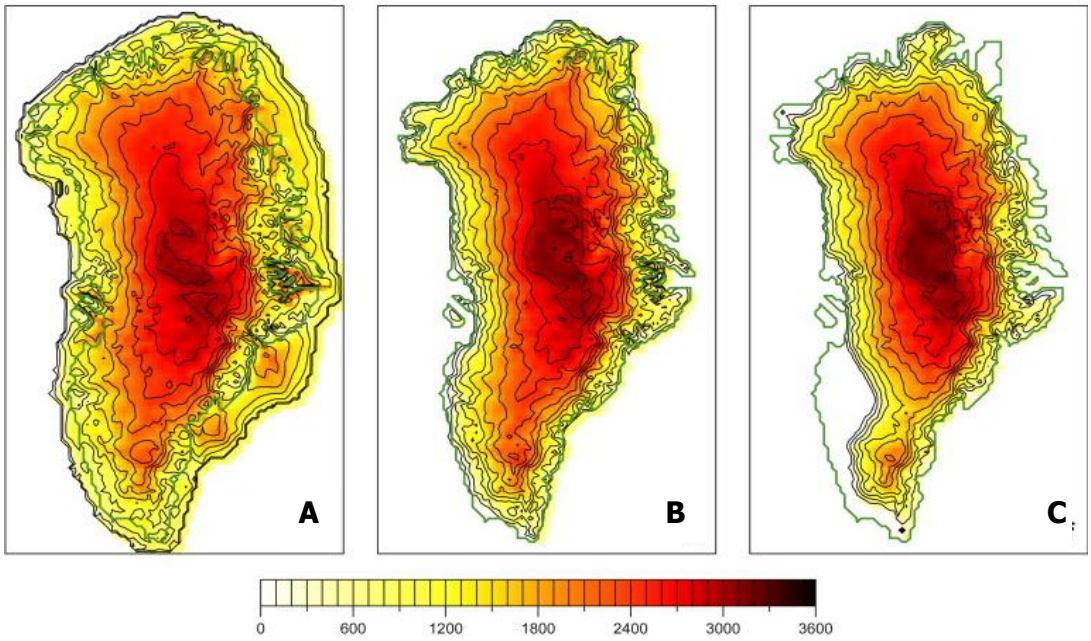


**Figure 2.7.** Ice thickness evolution in metres for the Greenland Ice Sheet. A: 18 kyr BP (LGM). B: 10 kyr BP. C: 4 kyr BP. Present day coastline is marked in green (from Simpson et al., 2009).

Deglaciation following the LGM took place in two stages. Initial retreat was driven by eustatic sea-level rise, which destabilised marine-based sections of the ice sheet, resulting in a high calving flux. This stage commenced around 15 kyr, and by 10 kyr, the Greenland Ice Sheet was essentially at, or inland of, the present coastline (Fig. 2.7; Siegert, 2001). The second phase of retreat began around 10 kyr, and was driven primarily by surface melting. North of latitude 69ºN, a major readvance of fjord glaciers, the Milne Land Stade, occurred at the Weichselian-Holocene transition (Funder, 1989). The Early Holocene was characterised by a period of rapid ice retreat. Warmer temperatures during the Holocene Thermal Maximum (ca. 9-5 kyr) forced ice margins to retreat inland at least 10 km beyond their present margins. The minimum configuration was reached at 4-5 kyr (Fig. 2.7). A non-uniform response of the ice margin to climatic forcing is reflected by clearly defined

sequences of prehistoric moraine systems in all regions. These moraines can be traced over hundreds of kilometres and represent a series of still-stands or minor readvances of the ice margin during the Early Holocene (Funder, 1989). Around 3 kyr, the ice margin began to readvance, and reached a maximum in the late nineteenth century. Ice margin fluctuations of tens of kilometres characterise the Late Holocene dynamics of the Greenland Ice Sheet (Funder, 1989; Kelly and Long, 2009).

### 2.3.3 Present Dynamics of the Greenland Ice Sheet

The Greenland Ice Sheet (Fig. 2.8) covers an area of 1.7 million km², extending as much as 2200 km from north to south (Weidick and Bennike, 2007; Alley et al., 2010). The total ice volume is estimated between 2.6 million and 2.9 million km³ (Weidick and Bennike, 2007) and maximum ice thickness at the centre is in excess of 3200 m (Siegert, 2001). The ice sheet contains 10% of the Earth's total fresh water and, if melted completely, would contribute to a globally-averaged eustatic sea-level rise of ~7 m (e.g. Dowdeswell, 2006; Williams and Ferrigno, 2009). At present, the Inland Ice is separated from the sea by a strip of more or less ice-free land, up to 300 km wide, except in Northwest Greenland, where large sections of the ice sheet margin reach the sea (Weidick and Bennike, 2007). The slow-moving ice sheet interior is drained towards the coasts by fast-flowing outlet glaciers (Fig. 2.8; Funder, 1989; Siegert, 2001; Bamber et al., 2007). The large flux of these glaciers has a profound effect on ice sheet mass balance. Recently, a major increase in ice discharge from several Greenland outlets has resulted in accelerated mass loss from the interior (e.g. Rignot and Kanagaratnam, 2006; Holland et al., 2008; Nick et al., 2009). The ice sheet mass deficit has more than doubled, from 90 $km^3\ yr^{-1}$ in 1996, to 220 $km^3\ yr^{-1}$ in 2006, and its contribution to sea-level rise has increased from 0.23 ± 0.08 mm $yr^{-1}$ in 1996 to 0.57 ± 0.1 mm $yr^{-1}$ in 2005 (Rignot and Kanagaratnam, 2006). It remains to be seen whether these changes represent a dynamic response to climate forcing, or simply natural variability in ice sheet behaviour.

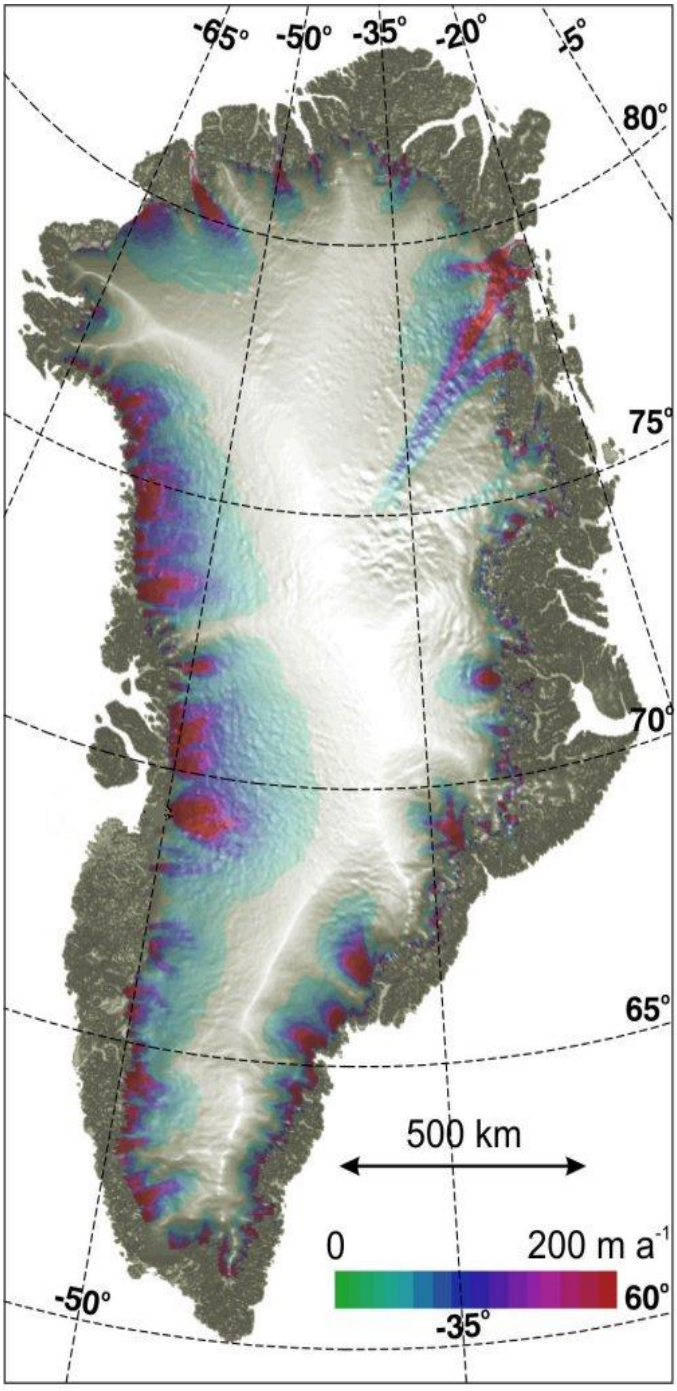


**Figure 2.8.** Surface topography and calculated balance velocities (m $yr^{-1}$) for the Greenland Ice Sheet (from Bamber et al., 2007).

## 2.4 Study Area on the West Greenland Margin

The location of the study area on the West Greenland margin is shown in Figure 1.3. The study area comprises the continental shelf and slope offshore of Disko Bugt and the Vaigat Strait, as well as the trough-mouth fan and adjoining shelf offshore of Umanak Fjord to the

north. Within this region, a number of fast-flowing outlet glaciers currently drain the ice sheet via Disko Bugt and the Umanak Fjord system into Baffin Bay. The process of iceberg calving at the margins of these outlets provides a major mechanism for mass loss (Ó Cofaigh et al., 2010).

Swath-bathymetric data from the continental shelf show the existence of streamlined bedforms, which record the former presence of major fast-flowing ice sheet outlets (Ó Cofaigh et al., 2010). These bedforms indicate that ice streams were an important glacio-dynamic feature of the ice sheet during the LGM and subsequent deglaciation. Despite this, the past extent and dynamic behaviour of ice streams on the West Greenland margin remain poorly understood (Roberts et al., 2009, 2010; Ó Cofaigh et al., 2010).

### 2.4.1 Physiographic Setting

The general bathymetry of the West Greenland margin is shown in Figure 1.3. Shelf width varies from 50 km to a maximum of ~300 km offshore Disko Bugt. Water depth over the shelf is mainly 100-300 m, except where glacially eroded troughs, 600-1000 m deep, extend from fjord systems to the continental slope (Brett and Zarudzki, 1979; Weidick and Bennike, 2007). Characteristic features of the shelf are the large trough-mouth fans at the shelf break. The largest of these is found offshore of Disko Bugt and extends far westwards to reach Canadian waters in Baffin Bay (Weidick and Bennike, 2007). Much of the shelf is underlain by a continuous sedimentary basin. Sediment thickness varies greatly across the basin, from a maximum of 5 km at latitude 69°N to less than 2 km at 71°30'N. Thick deposits of Quaternary marine sediments and till cover large areas of the shelf (Weidick and Bennike, 2007).

A number of workers have described the morphology of the shelf area offshore of Disko Island and Disko Bugt (e.g. Denham, 1974; Brett and Zarudzki, 1979; Chalmers et al., 1999; Weidick and Bennike, 2007). By contrast, far less is known about the morphology of the Umanak Fjord system and adjoining shelf. The bathymetric features of the Disko region are shown in Figure 2.9. Average water depth in Disko Bugt is 200-400 m. Precambrian rocks, heavily glaciated, outcrop over parts of the seafloor, with sediments comprising the remainder (Brett and Zarudzki, 1979). A deep trough, known as Egedesminde Dyb, exits westward from Disko Bugt and extends for ~350 km across the shelf. The south side of

Egedesminde Dyb is bounded by Store Hellefiskebanke, one of the largest offshore banks on the West Greenland margin. At the bank's most shallow locality, water depth is only 8 m. An exploration well drilled on the western slope of the bank has revealed a 200 m thick cover of glacial till, overlying thick deposits of Cenozoic sediments. A similar moraine system has been described from the eastern slopes of Store Hellefiskebanke, and on the banks farther south (Weidick and Bennike, 2007). To the north and northeast Egedesminde Dyb is limited by Disko Banke. The shallowest part of Disko Banke is 150 m below the present sea level. A continuation of the Hellefisk Moraine System is found on the western slopes of Disko Banke. A pronounced basalt escarpement at 200-300 m water depth connects Disko Banke with the easternmost part of Store Hellefiskebanke. This escarpement divides Egedesminde Dyb into a narrow, eastern channel, with depths in excess of 1000 m, and a shallower, western channel, with depths of up to 600 m (Weidick and Bennike, 2007). Vaigat Strait, to the north of Disko Bugt, is a typical glaciated fjord, with depths of up to 600 m in its southeastern part and 200-300 m at its western mouth. Quaternary deposits several hundreds of metres thick are found in the strait (Denham, 1974; Chalmers et al., 1999; Weinrebe et al., 2009).

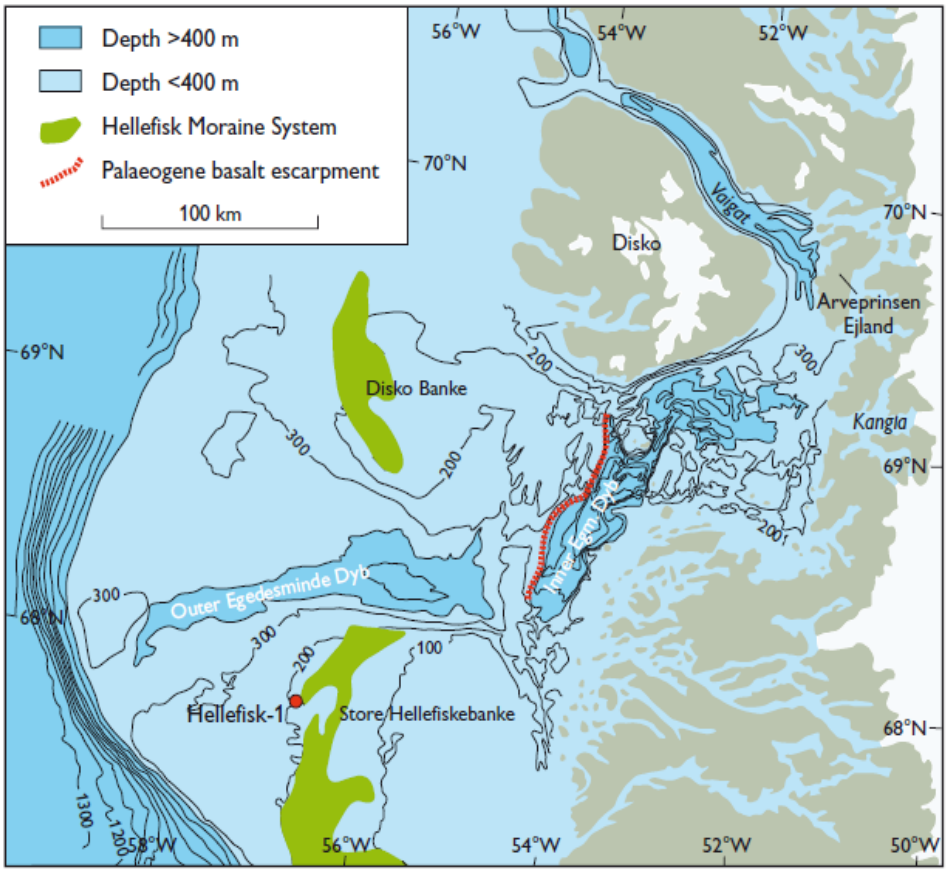


**Figure 2.9.** Bathymetric features of the continental shelf offshore of Disko and Disko Bugt (from Weidick and Bennike, 2007).

### 2.4.2 Glaciological Setting

A number of fast-flowing outlet glaciers currently drain the western sector of the Greenland ice sheet into Baffin Bay (Fig. 2.10). The majority of these outlets are located along a 300 km stretch of coastline between Disko Bugt and the Umanak Fjord system and a high density of icebergs has been observed for this region of the shelf. The calf-ice production of Jakobshavn Isbrae (Fig. 2.10) is of particular importance to the mass balance of the ice sheet. At present, Jakobshavn Isbrae drains 7% of the ice sheet by area and accounts for the greater part of ice flow to the Disko Bugt region; the rate of calf-ice production from Jakobshavn Isbrae is currently estimated at 50 $km^3$ $yr^{-1}$ (Joughin et al., 2004; Holland et al., 2008). Since 1997, Jakobshavn Isbrae has undergone rapid thinning, acceleration and retreat (e.g. Holland et al., 2008; Joughin et al., 2010). Ice flow velocities have roughly doubled, from 5.7 km $yr^{-1}$ in 1992, to a maximum of 12.6 km $yr^{-1}$ in 2003. Several smaller glaciers in the Disko Bugt-Umanak Fjord region have also undergone recent speed-ups (Fig. 2.10; Joughin et al., 2010).

The majority of fjord systems that drain into Disko Bugt are fronted by shallow sills that prevent deep-keeled icebergs from exiting the fjords (Rignot et al., 2010). The Iceberg Bank is a shallow, arch-shaped threshold at the mouth of Illulisat Icefjord, into which Jakobshavn Isbrae drains. This threshold separates the deep Icefjord from the interior of Disko Bugt and prevents icebergs with keels deeper than 200-225 m from entering Disko Bugt (Mikkelsen and Ingerslev, 2002). Brett and Zarudzki (1979) mapped the intensity of iceberg ploughing between 64° and 69°30'N and showed that the region offshore Disko Bugt is ploughed extensively to a maximum depth of 340 m (Fig. 2.11). This depth limit has been attributed to the presence of a basalt escarpement, which prevents icebergs with drafts deeper than ~300 m from exiting Disko Bugt. Most of the ploughmarks appear fresh, but some, particularly in deeper water, are thought to have been produced at a time when the ice margin was to the west of Disko Banke, or when an ice stream was still present in Egedesminde Dyb. Kuijpers et al. (2007) present acoustic evidence for giant iceberg ploughmarks extending sub-parallel to the continental slope at present water depths between 800 and 1085 m. The largest of these ploughmarks are 750 m wide and up to 40 m deep. Allowing for a maximum sea-level lowstand of ~120 m, these ploughmarks must have been produced by palaeo-icebergs with keel depths of at least 950 m. At the southern entrance to Baffin Bay, the Davis Strait sill depth is approximately 650 m. Glacial rebound data from the West Greenland margin

indicate a maximum glacial subsidence of ~100 m for the Davis Strait. This implies that the deep-keeled icebergs were calved from an ice margin in the Baffin Bay region.

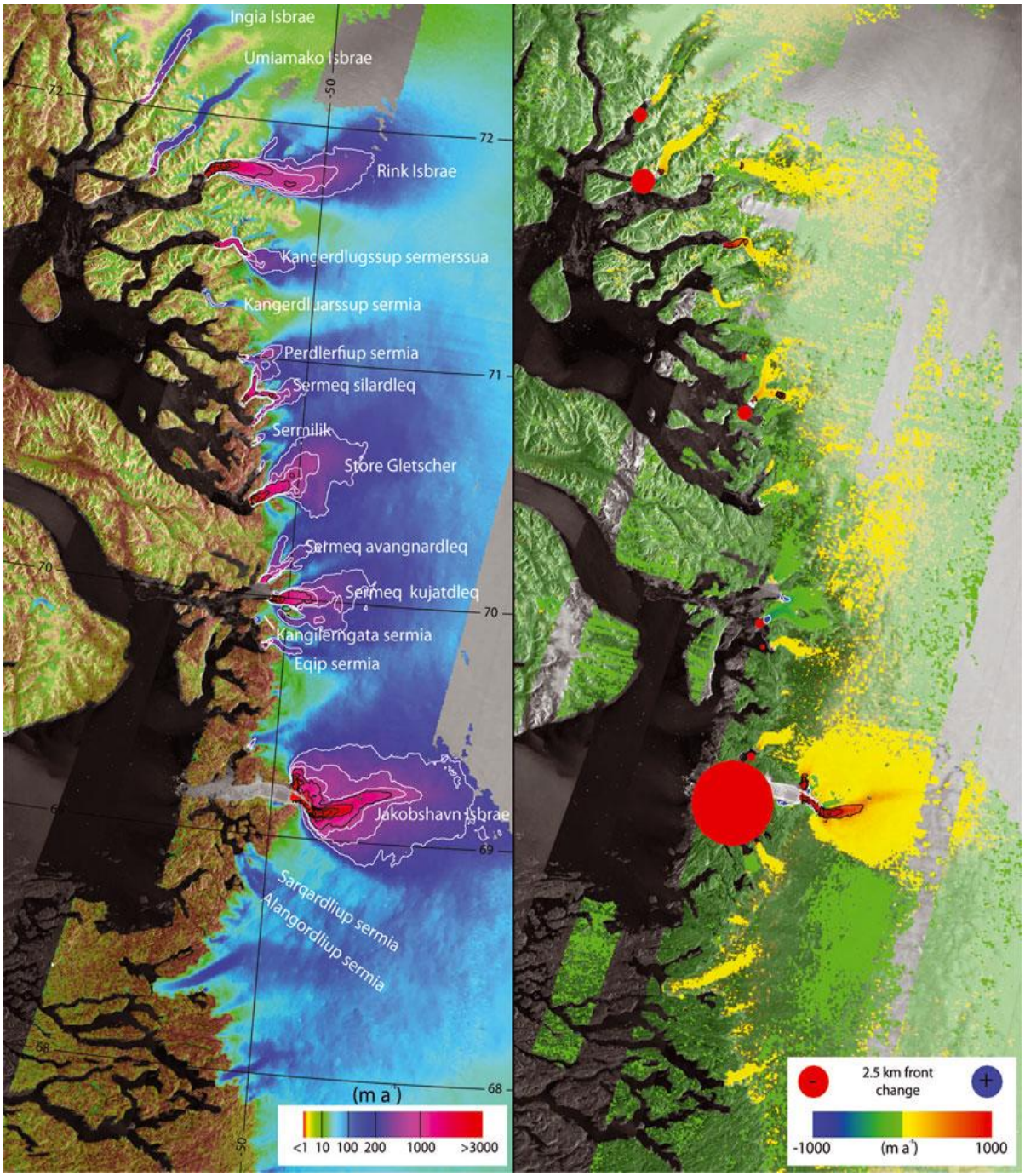


**Figure 2.10.** Map showing the locations of major calving glaciers along the coast of central West Greenland. Flow speeds for 2005/2006 (left) and change in speed from 2000/2001 to 2005/2006 displayed over a 2000/2001 SAR mosaic (right) are also shown. Speed is indicated by colour, white 250 m $yr^{-1}$ contours and black 1000 m $yr^{-1}$ contours. Speed differences are shown with colour (saturation is reduced where speed-up or slowdown is <20 m $yr^{-1}$) and 500 m $yr^{-1}$ black (speed-up) and white (slowdown) contours. Blue dots indicate advance and red dots retreat (from Joughin et al., 2010).

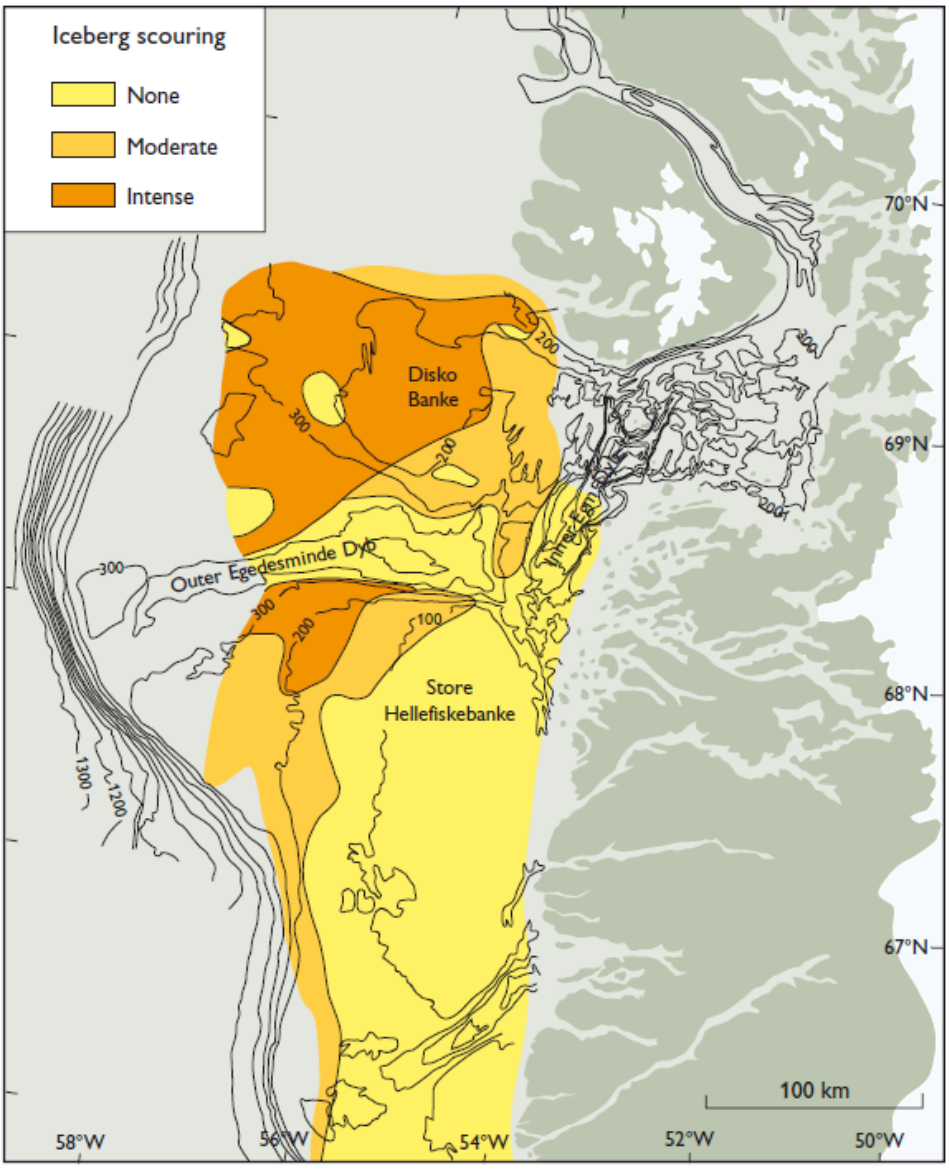


**Figure 2.11.** Intensity of iceberg ploughing on the continental shelf offshore of Disko Bugt, central West Greenland (Brett and Zarudzki, 1979; reproduced in Weidick and Bennike, 2007).

### 2.4.3 Modern Oceanographic Setting

At present, the oceanographic regime of West Greenland (Fig 2.12) is dominated by the West Greenland Current (WGC), which transports relatively warm, saline water northwards across the shelf. The WGC is produced by the mixing of cold, low salinity water from the East Greenland Current (EGC) and warm, saline water from the Irminger Current (IC). The EGC flows southwards from the Arctic Ocean, and is joined by the IC off southeast Greenland. Initially, there is poor mixing; the EGC component of the WGC is concentrated at the surface, whilst the denser IC component is concentrated about 200 m below. The components

of the WGC mix increasingly as they flow north, but are still distinguishable to the south of Disko Bugt. As the WGC flows north it is partly deflected to the west by the flux of cold melt-water from the Inland Ice (Lloyd et al., 2005). In Disko Bugt, the WGC is present as a deep, warm and saline current. Cold melt-water discharge and icebergs are transported northwards by this current, exiting through the Vaigat Strait and drifting westward across the shelf (Andersson, 2008). In Baffin Bay, to the north of Disko Bugt, the WGC is trapped by the cold Baffin Current and circles as a gyre. Along the continental slope a southward counter current has been found (Tang et al., 2004; Kuijpers et al., 2007).

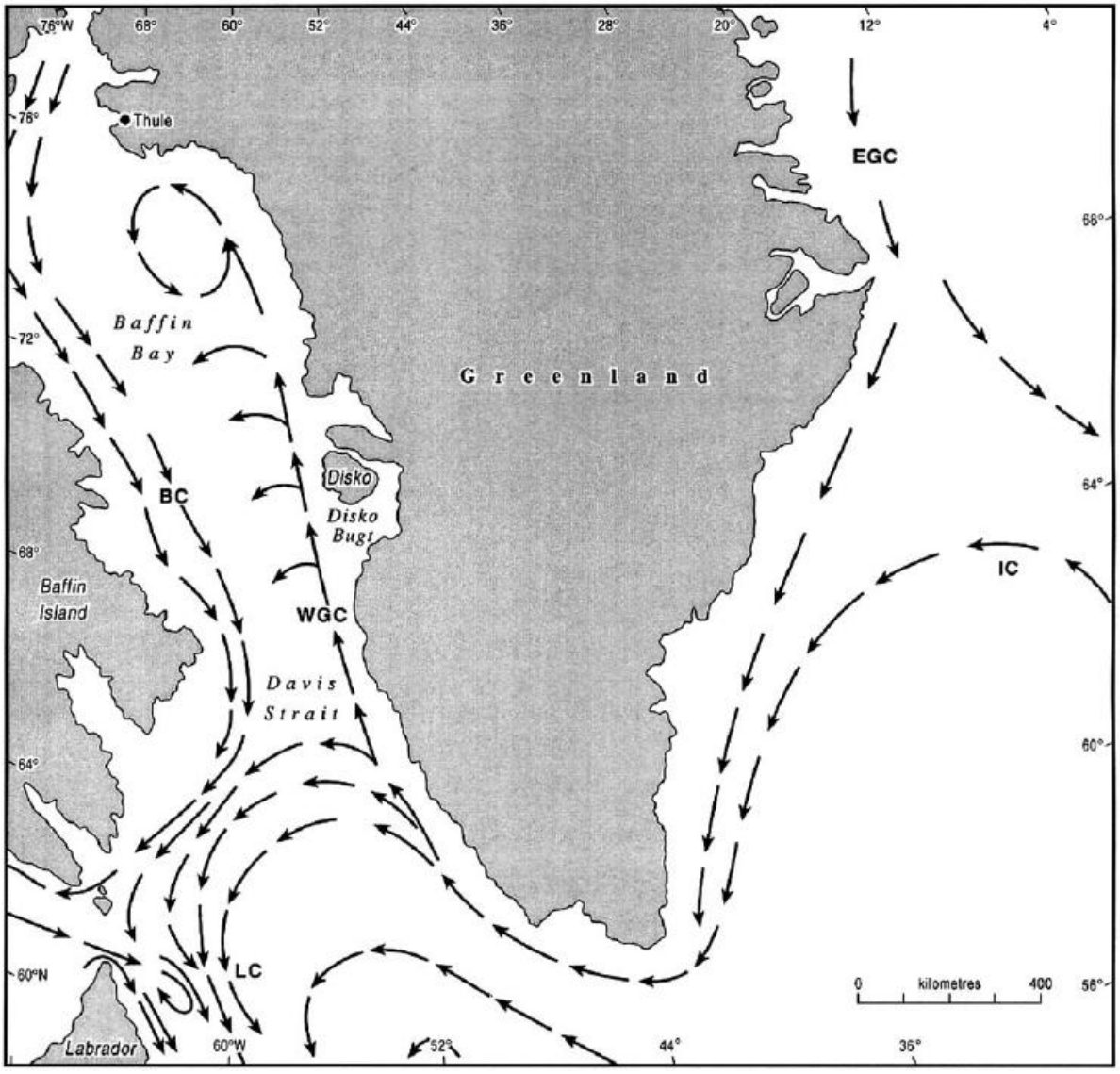


**Figure 2.12.** Map showing present day oceanographic regime influencing the study area of West Greenland. IC = Irminger Current, WGC = West Greenland Current, EGC = East Greenland Current, BC = Baffin Current and LC = Labrador Current (from Lloyd et al., 2005).

The western sector of the Greenland Ice Sheet is highly sensitive to changes in ocean temperature, with the warm WGC driving Holocene and more recent ice margin fluctuations (Roberts et al., 2009). The earliest date for initiation of the WGC is 9.73-10.58 kyr, based on mollusc data from the Thule region of Northwest Greenland (Feyling-Hanssen and Funder, 1990). Lloyd et al. (2005) report a weak WGC signal in southern Disko Bugt by 9.2 kyr. The orientation of relict ploughmarks on the outer continental shelf of West Greenland shows that iceberg drift can be related to a (palaeo)circulation pattern corresponding to the WGC (Belan et al., 2004; Kuijpers et al., 2007).

### 2.4.4 Late Weichselian Glacial History of West Greenland

According to Funder and Hansen (1996), the ice sheet margin in West Greenland during the LGM was grounded on the inner shelf, 30-50 km beyond the present coastline, where a number of moraine-type landforms have been observed. Large outlet glaciers drained ice through cross-shelf troughs towards the shelf edge. The ice sheet filled Disko Bugt, and extended at least as far as the outer part of Vaigat Strait (Weidick and Bennike, 2007). Based on trim-line evidence, Kelly (1985) proposed a relatively thin (300-600 m) LGM ice sheet, which extended to the inner-middle shelf, and left high coastal mountains free of ice. These reconstructions have been challenged by Roberts et al. (2009), who show that maximum ice surface elevation in central West Greenland was in the order of 750-810 m above sea-level, based on cosmogenic surface exposure ages, and that ice advanced to at least a mid-shelf position, and most likely to the Hellefiske moraines at the shelf edge. This concurs with recent modelling work by Simpson et al. (2009), which reconstructs ice sheet thickness to ~900 m above sea-level, and projects the western sector of the ice sheet to a middle or outer shelf position (Fig. 2.8).

Ice streams were major glacio-dynamic features of the West Greenland Ice Sheet during the LGM, draining extensive sectors of the Inland Ice across the continental shelf (Roberts and Long, 2005; Roberts et al., 2009, 2010). Preliminary interpretation of streamlined submarine landforms recorded on swath-bathymetric data acquired during Cruise JR175 in 2009 suggests that ice streams reached the outermost shelf west of Disko Bay and Umanak Fjord at the LGM (J.A. Dowdeswell, pers. comm.). In many cases, fjord systems acted as tributaries, routing ice streams onto the continental shelf, where they converged to form large, cross-shelf, composite ice streams (Roberts et al., 2009, 2010). Roberts and Long (2005) proposed

the coalescence of several outlet glaciers with Jakobshavn Isbrae, to form a composite ice stream, which flowed westwards through Egedesminde Dyb, and formed a distinctive trough-mouth fan at the shelf edge. This ice stream would have provided a major control on LGM ice flow dynamics in central West Greenland.


**Figure 2.13.** Radiocarbon dates pertaining to the last deglaciation of the ice-free areas around Disko Bugt. Dates are given as calibrated thousand years before present (cal. kyr B.P.), using the INTCAL04 datset for calibration. The map also shows the Marrait (M), Tasiussaq (T), Drygalski (D) and Godhavn (G) moraine systems, which mark Holocene fluctuations of the ice margin (from Weidick and Bennike, 2007).

Funder and Hansen (1996) proposed a 2 stage model for deglaciation following the LGM. Initial retreat across the shelf was driven by rapid sea-level rise, which destabilised marine-based sections of the ice sheet. Calving was the primary mechanism of ice loss. This stage commenced around 15 kyr, and was accelerated by the Allerød/Bølling warm interval at

14.7-12.6 kyr. During the Younger Dryas (12.6-11.7 kyr) the ice margin may have halted at the shallow basalt escarpement between Disko Banke and Store Hellefiskebanke (Funder, 1989; Weidick and Bennike, 2007). Relative-sea level records and offshore sediment cores suggest that Jakobshavn Isbrae remained on the outer shelf until 10.5 kyr cal. BP, followed by rapid retreat to a position near the eastern margins of Disko Bugt (Long and Roberts, 2003; Lloyd et al., 2005). The second phase of retreat began around 10 kyr, and was driven primarily by surface melting. During this time, Jakobshavn Isbrae retreated to the shallow bank immediately west of the present-day Ilulisat Icefjord (Lloyd et al., 2005). Radiocarbon dates pertaining to the last deglaciation of the ice-free areas around Disko Bugt are shown in Figure 2.13.

# CHAPTER 3 - METHODOLOGY

## 3.1 Introduction

A range of geophysical techniques, including multibeam echo sounding, side-scan sonar, and sub-bottom profiling, provide information on the seafloor morphology and shallow subsurface stratigraphy of formerly glaciated continental shelves. In this thesis, two types of acoustic record are used to investigate the nature of iceberg ploughing on the continental shelf and slope of central West Greenland. The datasets comprise multibeam swath-bathymetric and TOPAS (TOpographic PArametric Sonar) 3.5 kHz sub-bottom profiler records, acquired during the JR175 research cruise of the RRS *James Clark Ross* to West Greenland and Baffin Bay in August-September 2009.

## 3.2 Multibeam Swath-Bathymetry Data

### 3.2.1 Multibeam Swath Systems

Swath-bathymetry systems operate according to the same basic principles as most seismic and acoustic techniques. An acoustic signal (known as a 'ping') is transmitted downwards from a source instrument on the survey vessel and reflected back from the seafloor. The two-way travel time of this signal can be converted to a single depth measurement, provided that the speed of sound through the water column is known (Jones, 1999).

Multibeam swath systems were developed in order to provide more detailed images of the seafloor over wider areas than single beam systems, which only return bathymetry along the vessel track-line (Renard and Allenou, 1979; Denbigh, 1989). Data from multibeam systems is used to produce digital models of the seabed accurate to <1m vertically (Dowdeswell et al., 2010b); this has greatly facilitated the mapping of seafloor landforms on glacier-influenced margins. A number of recent studies (e.g. Evans et al., 2009; Dowdeswell et al., 2010a, c; Ó Cofaigh et al., 2010) have used multibeam swath images to reconstruct past ice extent and dynamics. Multibeam systems transmit a series of acoustic beams, oriented at known angles in a plane perpendicular to the ship's forward motion (Fig. 3.1). The properties of the reflected beams are converted to depths, given the known configuration of the transducer

array, the position of the survey vessel and the sound velocity profile of the water column. A single depth profile is recorded for every swath ping; as the ship advances, sequential depth profiles are combined to produce a bathymetric map of the seafloor. A differential global positioning system (DGPS) is used to record the ship's position; this allows seafloor features to be located accurately (Jones, 1999).

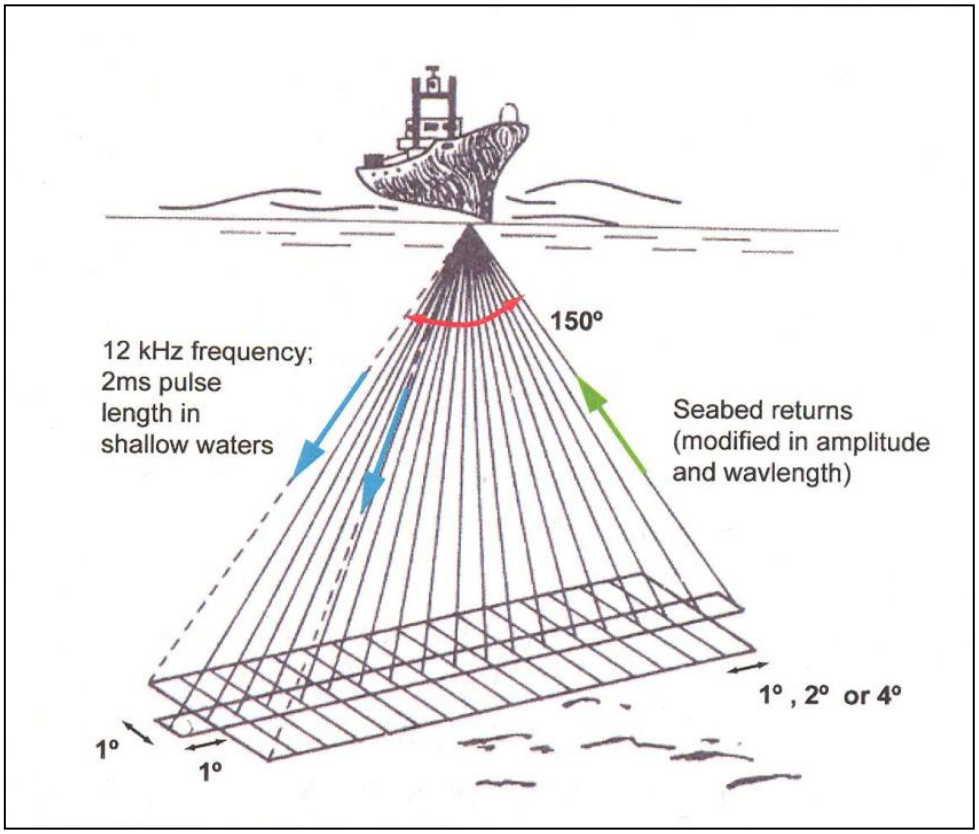


**Figure 3.1.** Schematic of a multibeam swath bathymetric echo sounder system, based on the EM120 system used in this thesis. Larger rectangles represent the total area of seafloor covered by the receiving hydrophones, and smaller rectangles represent the acoustic energy received from 16 square zones on the seafloor. For simplicity, these zones are shown as squares, although in reality they are elliptical, and increase in area with angle of incidence (Hogan, 2008; modified from Renard and Allenou, 1979).

### 3.2.2 The EM120 System

A Kongsberg Simrad EM120 multibeam echo sounder was used to acquire bathymetric data during the JR175 research cruise; swath track-lines from the study area on the West Greenland margin are presented in Figure 3.2. The hull-mounted EM120 system consists of a piezoelectric transducer array, with separate units to transmit and receive (Kongsberg Maritime AS, 2005). It operates at a nominal frequency of 12 kHz, standard for deep-ocean

echo sounding, and records up to 191 narrow (1° by 1°) beams every swath ping, with angular coverage of up to 150° (Fig. 3.1). On a flat seabed, the EM120 can survey maximum swath widths of approximately 5.5 times the water depth (Kongsberg Simrad Subsea AS, 2001; Kongsberg Maritime AS, 2005). During cruise JR175, the system was run in automatic ping mode, with one of five pre-set modes (Very Shallow, Shallow, Medium, Deep or Very Deep) selected according to the water depth. The ping mode defines the optimal swath angle for a given water depth and thereby limits depth errors.

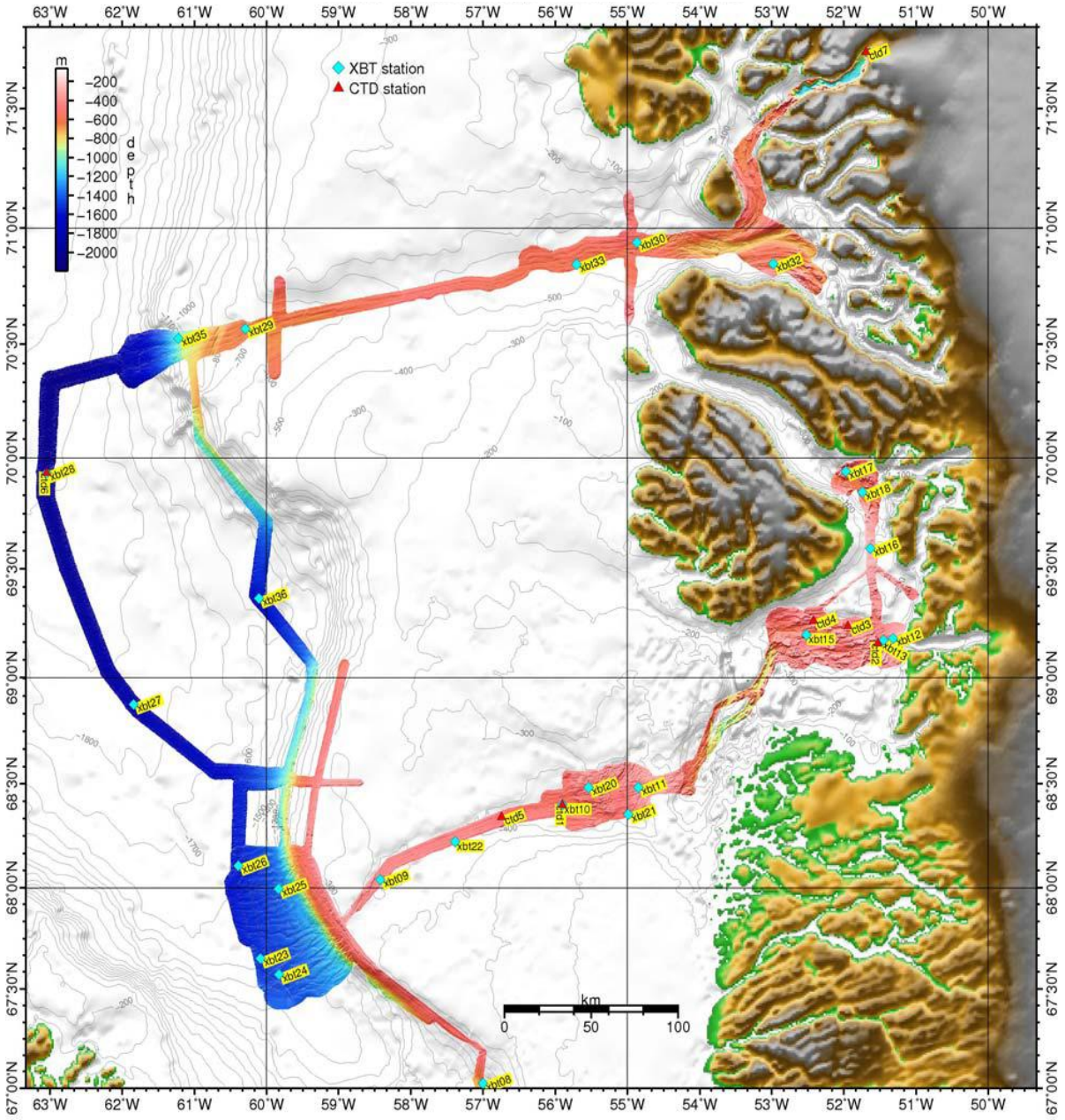


**Figure 3.2.** JR175 EM120 multibeam swath-bathymetric coverage of the West Greenland margin, with XBT (blue) and CTD (red) stations shown.

A number of location-specific sound velocity profiles (SVPs) were constructed to determine the acoustic structure of the water column. The approximate speed of sound through water is 1490 m/s (Stoker et al., 1997; Jones, 1999), but this varies with salinity, temperature and depth. Expendable bathythermographic (XBT) devices were used to calculate local water column temperature variations during cruise JR175; XBT stations are shown in Figure 3.2. XBT casts were made at regular intervals throughout the cruise, and also whenever there was a significant change in water depth. Salinity values were obtained from the Oceanlogger display and input to the XBT system software manually. The calculated SVPs were then imported to the EM120 system to correct the raw swath data (Ó Cofaigh, 2009).

### 3.2.3 Swath Data Processing

The accuracy of the EM120 system depends on a number of external factors, including water depth, seafloor roughness and the precision of the DGPS. During Cruise JR175, positional data were recorded every 1 second with an Ashtech ADU5 DGPS, which acted as a dedicated logging system for the scientific data (Hogan, 2008). Good satellite coverage was available throughout the cruise and no navigational issues were encountered. Environmental factors, such as high winds, large waves, and the presence of sea ice, may disrupt the steady motion of the ship, potentially altering the properties of the reflected signal (e.g. Hogan, 2008; Robinson, 2010). The quality of bathymetric data is also influenced by the speed of the acoustic signal through the water column; poor SVPs disproportionately affect the accuracy of depths recorded by the outer beams in particular; they may appear in swath imagery as 'stripes' running along the edges of swath track-lines. All of these factors must be accounted for prior to interpreting the data.

Limited post-processing (gridding and filtering) of the raw EM120 data was carried out using Kongsberg Simrad NEPTUNE post-processing software. The data files were then archived to DVD, and transported from the ship to the Scott Polar Research Institute, University of Cambridge. Here, the files were transferred to a Linux platform, and processed with MB-system™ software, an open-source software system designed to facilitate the processing, manipulation and visual presentation of swath bathymetry data (Schmidt et al., 2006).

Processing of the bathymetric data was carried out in several stages. First, the raw data files were assessed for coverage and quality. Physical biases of the system during acquisition were

identified and corrected. The automated MB-system™ tool 'mbclean' was then used to remove artefacts and erroneous data segments. This was followed by manual editing of the data in order to remove erroneous data segments left unflagged. Lastly, appropriate SVPs were applied to the data using the 'mbvelocitytool' function, to minimise 'striped' artefacts. The bathymetry was then recalculated, and a 'cleaned' bathymetric dataset consisting of processed swath files was produced (Hogan, 2008).

### 3.2.4 Swath Data Visualisation

The MB-system™ tool 'mbgrid' was used to grid the processed bathymetric data at regular intervals. The data were gridded with horizontal cell sizes of between 10 and 30 m; a cell size appropriate to the resolution of the data and the size of the grid was selected. A cell size of 20-30 m is typical on the continental shelf, but more detailed plots were derived from 10 m grids (Fig. 3.3; Hogan, 2008). Grids were produced in the UTM projection WGS 84 North and visualised with Generic Mapping Tools (GMT) – a free, public domain software package that can be used to manipulate and display gridded data in a variety of forms (Wessel and Smith, 1991). Grids were then exported as ASCII files for use within the GIS software systems ArcView and Erdas Imagine. Final sun-shaded relief maps were produced in Erdas Imagine.

### 3.2.5 Swath Data Interpretation

Interpretation of the swath data was based on both qualitative and quantitative analyses. The swath coverage was divided into five sections, based on geographic location (Fig. 3.4). Each section was further divided into a series of smaller blocks (Figs. 3.5-3.9). The size of these blocks was determined by the average water depth in each section; for this reason, block sizes are not entirely uniform throughout the study area.

Iceberg ploughmarks were identified from visual assessment of PostScript grid images and sun-shaded relief maps. A degree of quantification was made possible through the use of GIS software applications to measure ploughmark dimensions and orientations (Metz et al., 2008). The lengths and average orientation (in degrees north) of the ploughmarks in each block were recorded. The lengths given are the maximum observed lengths, as some of the ploughmarks extended beyond the bounds of the swath-bathymetric coverage. The average modern-day

water depth that the ploughmarks occurred at was also recorded. Finally, the widths of an independent sample of ploughmarks in each section were measured. These results, presented in Chapter 4, are used to map the nature and intensity of iceberg ploughing on the continental shelf and slope of central West Greenland.

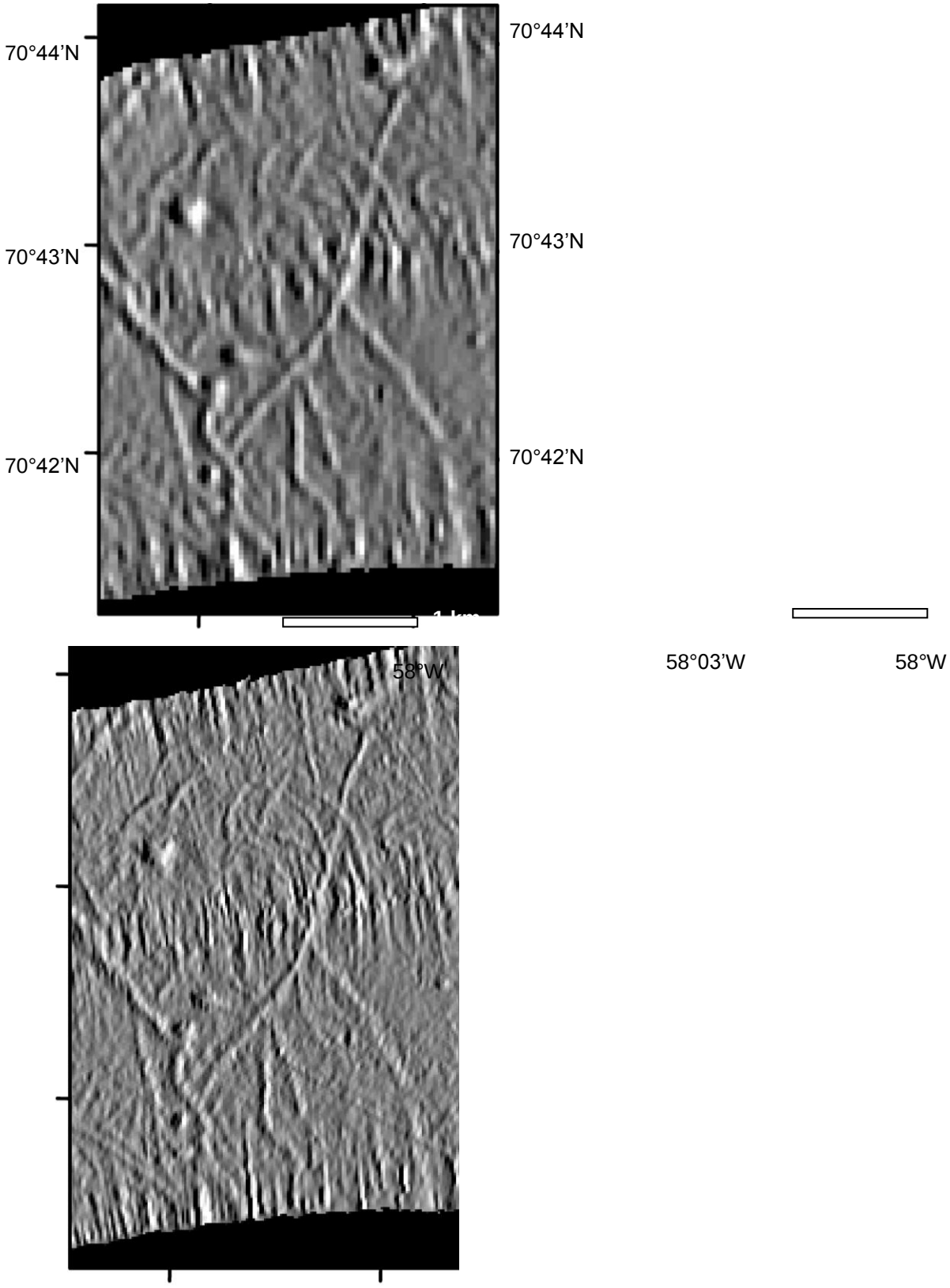


**Figure 3.3.** Greyscale sun-shaded relief maps (illuminated from the west) showing the difference in resolution between images derived from 30 m grids (left) compared with 10 m grids (right). Seafloor features are much easier to distinguish at a higher resolution. Note, however, that gridding at a high resolution enhances swath edge artefacts in the data.

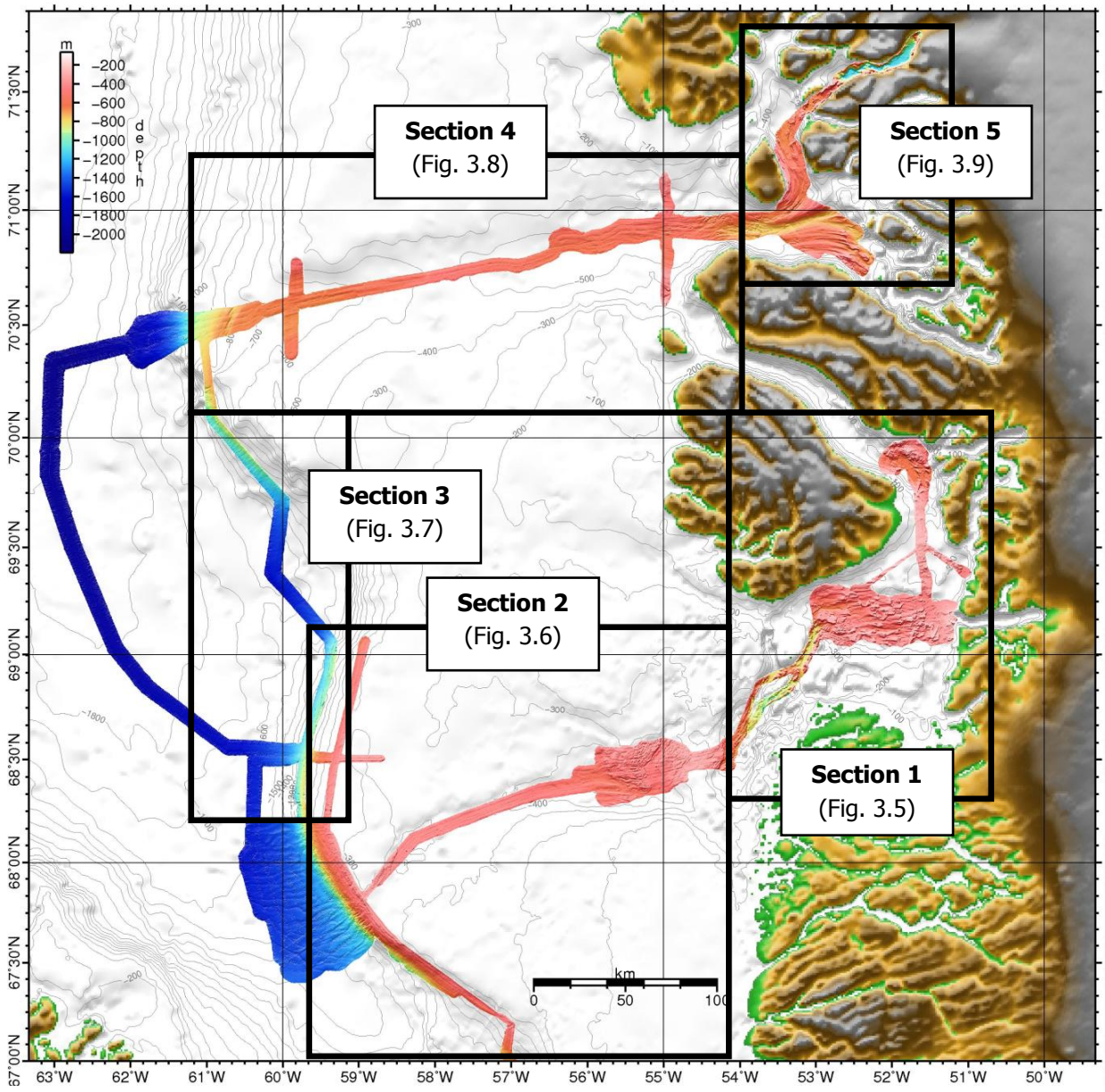


**Figure 3.4.** JR175 swath-bathymetric coverage of the study area on the West Greenland margin, showing the location of each section analysed. A detailed image of each section is shown in Figures 3.5 to 3.9.

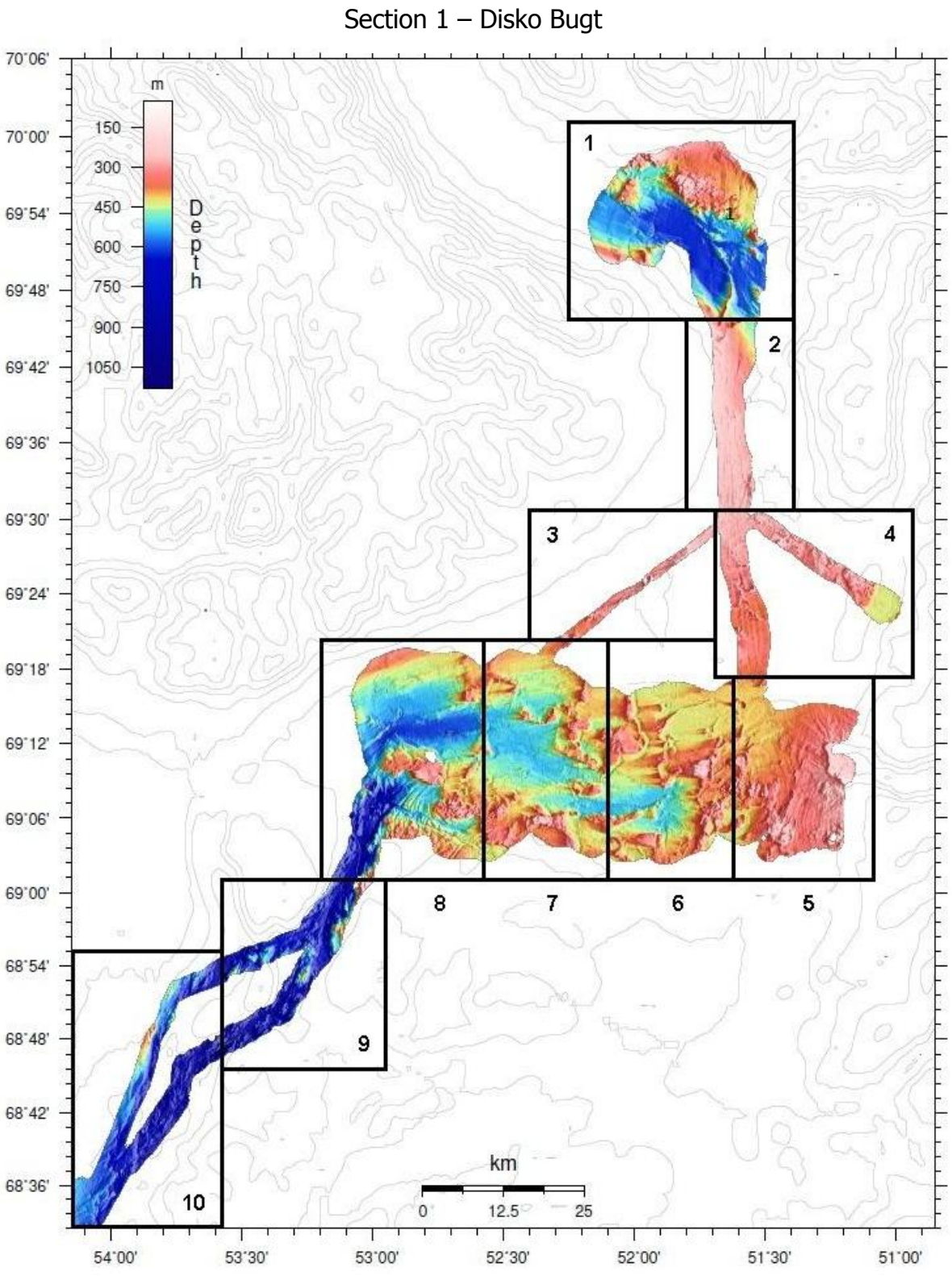


**Figure 3.5.** Swath-bathymetric map of Section 1, showing the locations of blocks within this section (section located in Fig. 3.4; data gridded at 50 m).

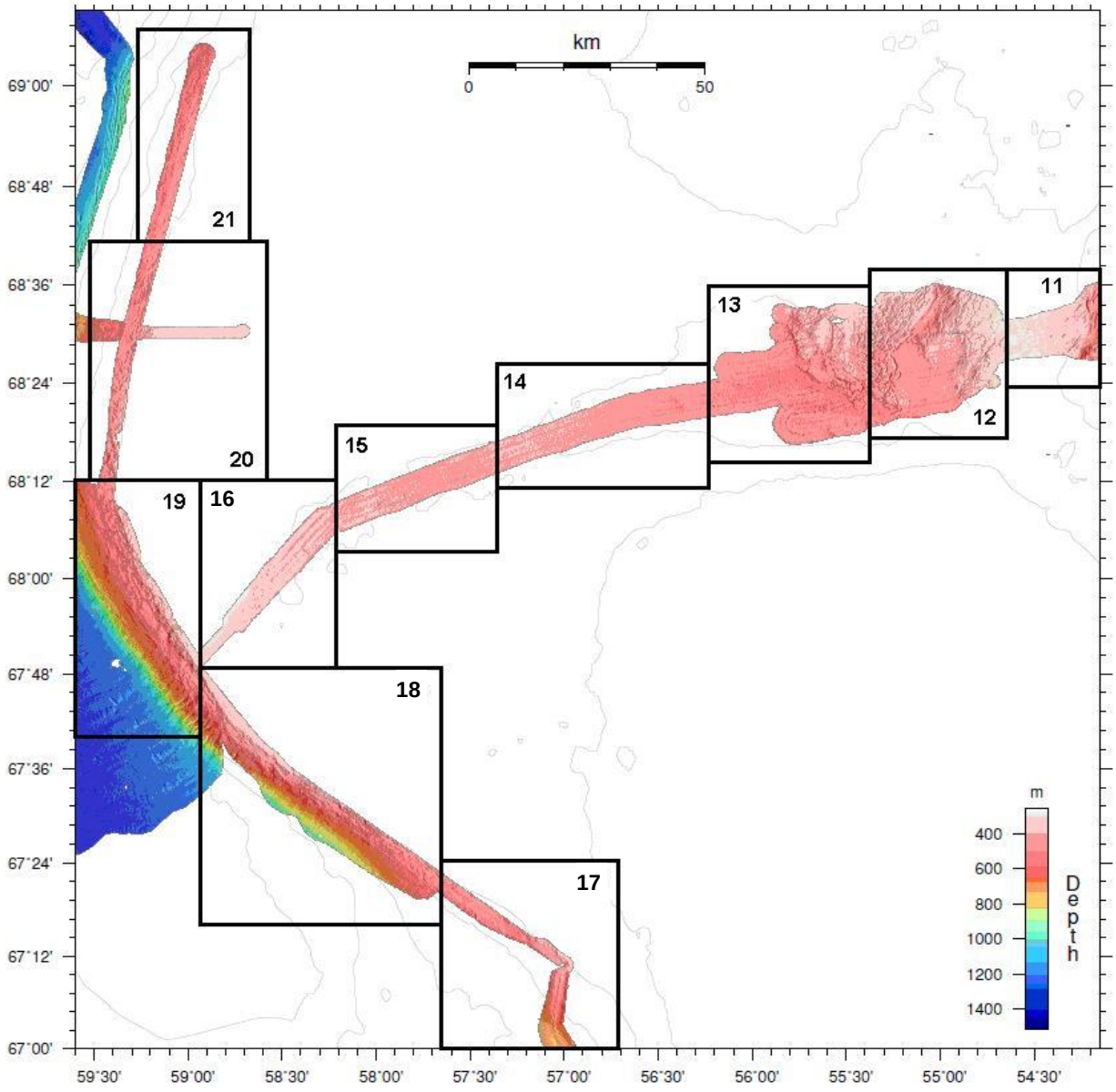


**Figure 3.6.** Swath-bathymetric map of Section 2, showing the locations of blocks within this section (section located in Fig. 3.4; data gridded at 30 m).

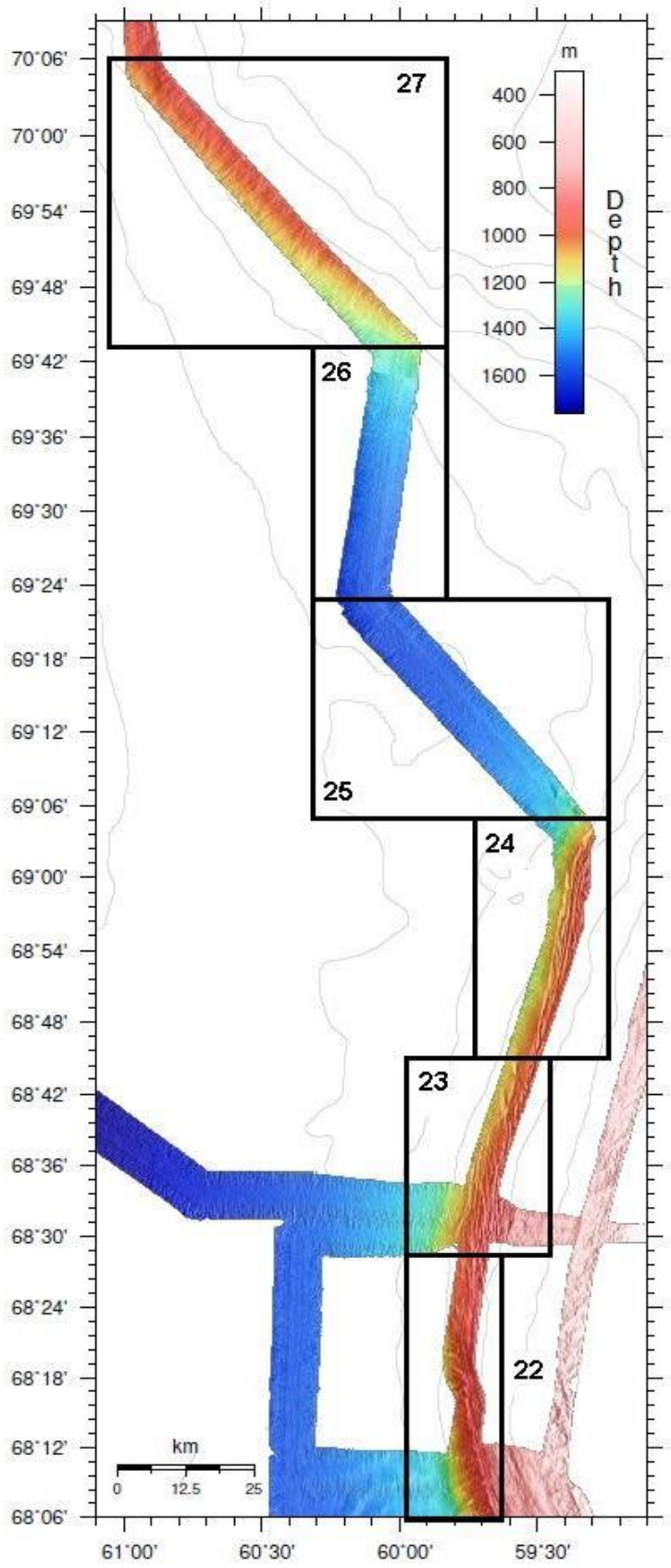


**Figure 3.7.** Swath-bathymetric map of Section 3, showing the locations of blocks within this section (section located in Fig. 3.4; data gridded at 50 m).

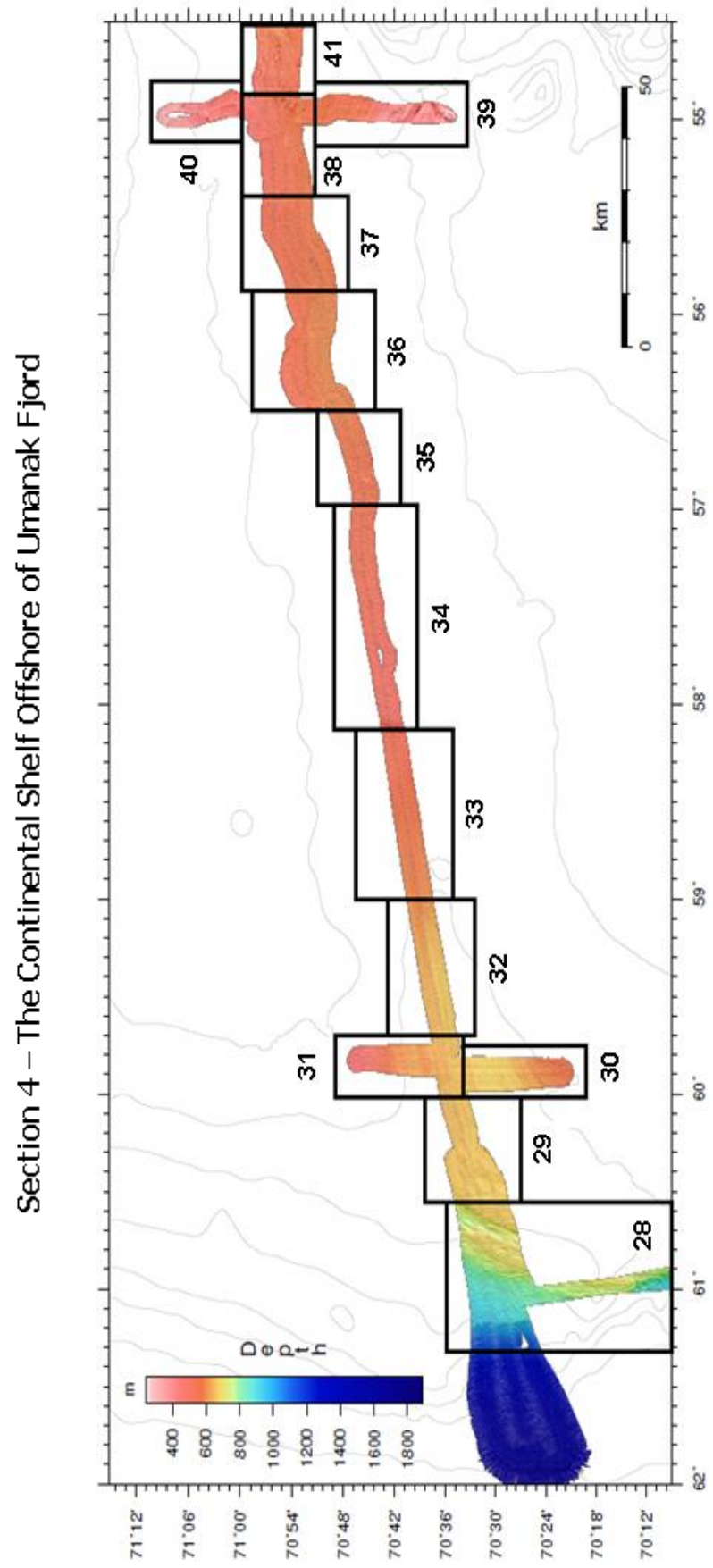


**Figure 3.8.** Swath-bathymetric map of Section 4, showing the locations of blocks within this section (section located in Fig. 3.4; data gridded at 30 m).

Section 5 – Umanak Fjord

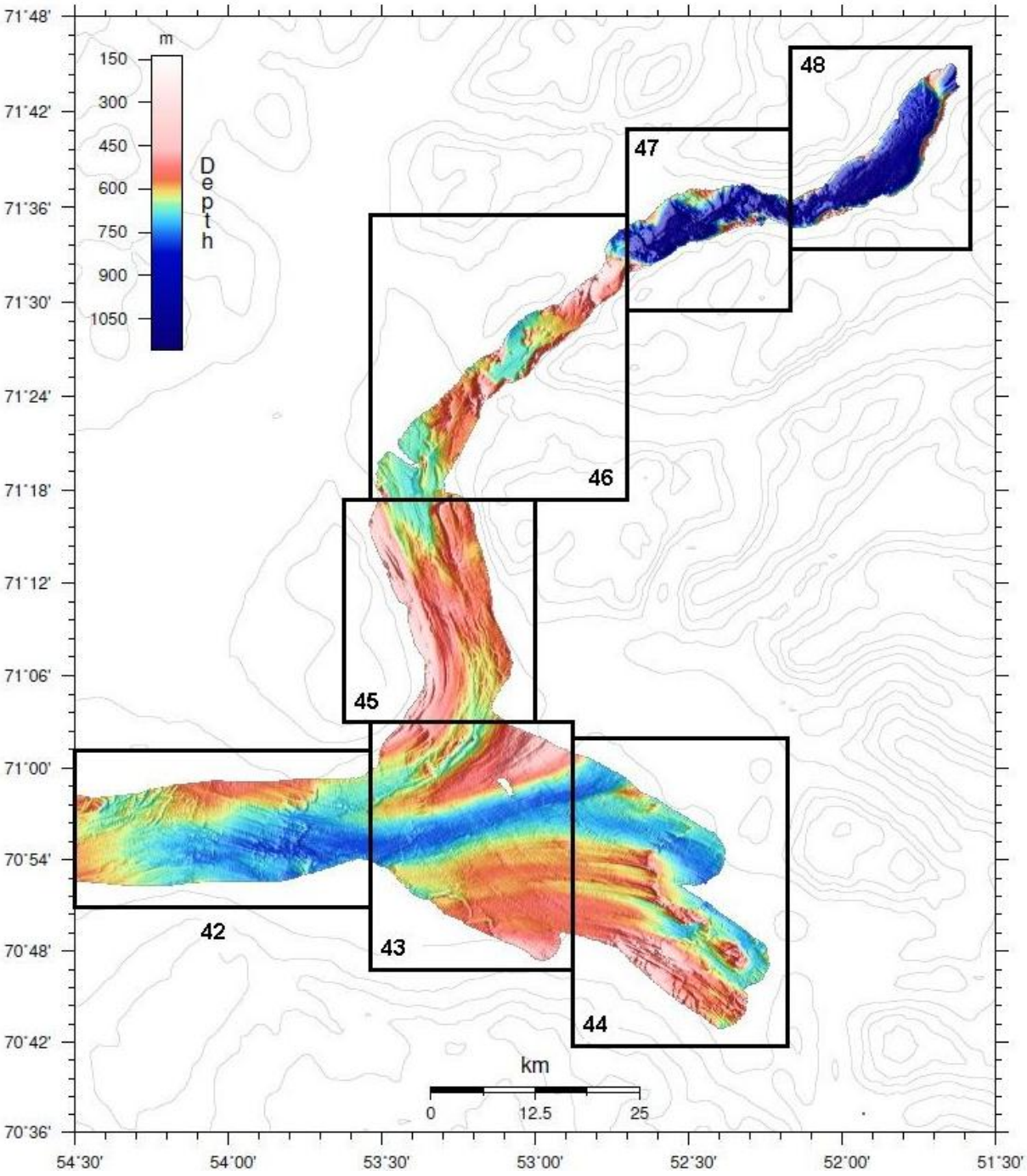


**Figure 3.9.** Swath-bathymetric map of Section 5, showing the locations of blocks within this section (section located in Fig. 3.4; data gridded at 50 m).

## 3.3 TOPAS Sub-Bottom Profiler Data

### 3.3.1 TOPAS Sub-Bottom Profiling and the PS 018 System

Sub-bottom profiling is a seismic technique used to investigate the upper layers of sediment beneath the seafloor. It provides a valuable tool for the study of Quaternary sedimentation processes (e.g. Damuth, 1975, 1980; Melles and Kuhn, 1993; Dowdeswell et al., 1997). A sub-bottom profiler like the TOPAS system transmits an acoustic pulse downwards at timed intervals, which is reflected at the boundaries between materials of differing acoustic impedance. The typical sound source for a sub-bottom profiler is a pressure compensated boomer or sparker (Kenny et al., 2003). Hydrophone receivers record the travel time and properties of the returned signal; two-way travel times are then converted to depth profiles using the known seismic velocities of different earth materials (Table 3.1). TOPAS systems use high frequency sound sources (usually between 2 and 15 kHz) to achieve high resolution in the vertical plane. Penetration is generally limited to the upper few tens of metres below the seafloor, as high-frequency sound waves are rapidly attenuated by sediment and rock (Jones, 1999; Kenny et al., 2003). Penetration depth is dependent on the impedance and internal structure of the seafloor at a given location, with rock and stiff till usually being impenetrable at these frequencies (Jones, 1999).

| MATERIAL | VELOCITY (m $s^{-1}$) |
|---|---|
| Water | 1490 |
| Glacimarine muds | 1500-1800 |
| Glacial till | 1600-2700 |
| Limestone | 3500-6500 |
| Granite | 4600-7000 |

**Table 3.1.** Examples of seismic velocities through different media (after Stoker et al., 1997).

A hull-mounted TOPAS PS 018 sub-bottom profiler was used to acquire shallow acoustic profiles during research cruise JR175. This system transmits two high frequency signals, centred symmetrically on 18 kHz, from a 1.1 m by 1.1 m transducer array. Interference

between the two primary waves generates a secondary beam with a frequency range of 0.5-6 kHz (Kongsberg, 2010). The system typically operates at a frequency of 3.5 kHz, and achieves a resolution of less than 1 m in the vertical plane (Evans et al., 2009). Horizontal resolution is <5° by 5° and, therefore, varies with depth. Some real-time processing was performed on the shipboard operating unit; this included altering acoustic modes to improve the quality of the returned signal, and altering the gain (Hogan, 2008).

### 3.3.2 TOPAS Data Visualisation and Interpretation

The JR175 TOPAS data were visualised with the tool 'swath_profile_utility.exe', developed by Toby Benham at the Scott Polar Research Institute, University of Cambridge. With this tool, TOPAS profiles can be selected from track-lines overlain on a grid of swath-bathymetry data and viewed in a separate window. This ensures that seafloor features of interest can be fully investigated in the context of the subsurface. Acoustic profiles were visualised with the TOPAS program, which replays individual files. Final greyscale images of the profiles were produced with the Kongsberg post-processing software TOPAS MK II (Hogan, 2008).

TOPAS data add a cross-sectional, subsurface dimension to high-resolution bathymetric maps of the seafloor (Jones, 1999). The intensity of iceberg ploughing is reflected by characteristic seafloor irregularities on 3.5 kHz profiles (Fig. 3.10; Josenhans et al., 1986; Solheim et al., 1988; Dowdeswell et al., 1993). These profiles were used in conjunction with swath-bathymetric data to investigate the morphology and verify the dimensions of iceberg ploughmarks on the continental shelf of central West Greenland.

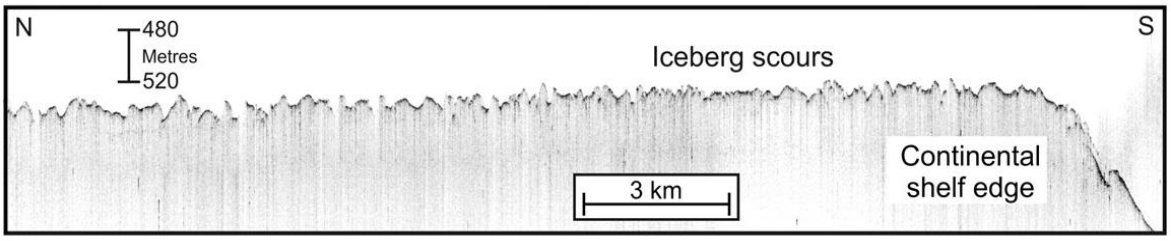


**Figure 3.10.** TOPAS 3.5 kHz sub-bottom profiler record from the outer shelf of the Kangerlussuaq margin, East Greenland, showing the characteristic seabed irregularities associated with intense iceberg ploughing of seafloor sediments (from Dowdeswell et al., 2010a).

# CHAPTER 4 – RESULTS

Analysis of the JR175 swath-bathymetric dataset has shown that over 3900 iceberg ploughmarks are present on the seafloor of the study area on the West Greenland margin. This chapter presents observations on the dimensions, orientations and morphology of ploughmarks within the study area; these data are used to describe and map the distribution of ploughmarks on the West Greenland margin.

## 4.1 Ploughmark Lengths

### 4.1.1 Observations

A wide range of ploughmark lengths were observed across the study area (Table 4.1; Fig. 4.1; Fig. 4.2). The shortest ploughmark identified was 30 m in length, whereas the longest measured at least 20.81 km (Table 4.1). It should be noted that all lengths given are the maximum observed length for each ploughmark; a number of ploughmarks were long enough to extend past the edges of the data coverage and are, therefore, only partially imaged. In fact, the 20.81 km ploughmark extended beyond the bounds of the swath-bathymetric coverage and may therefore have been much longer than 20.81 km.

| **SECTION** (Fig. 3.4) | **MEAN LENGTH (km)** | **MEDIAN LENGTH (km)** | **RANGE OF LENGTHS (km)** |
|---|---|---|---|
| 1<br>Disko Bugt | 0.38 | 0.31 | 0.06 - 3.5 |
| 2<br>Disko Shelf | 1.41 | 1.1 | 0.16 - 9.5 |
| 3<br>Continental Slope | 3.7 | 2.76 | 0.35 - 15.79 |
| 4<br>Umanak Shelf | 0.66 | 0.45 | 0.03 - 20.81 |
| 5<br>Umanak Fjord | 0.93 | 0.72 | 0.4 - 2.74 |

**Table 4.1.** Summary of the mean, median and range of ploughmarks lengths (in kilometres) for each section of the study area (sections located in Figure 3.4).

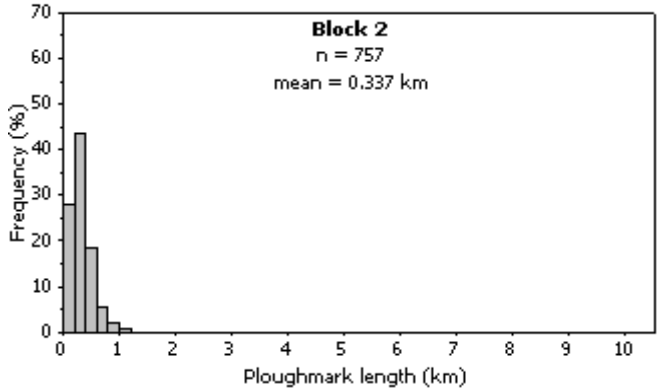
Block 2
n = 757
mean = 0.337 km
Frequency (%)
Ploughmark length (km)

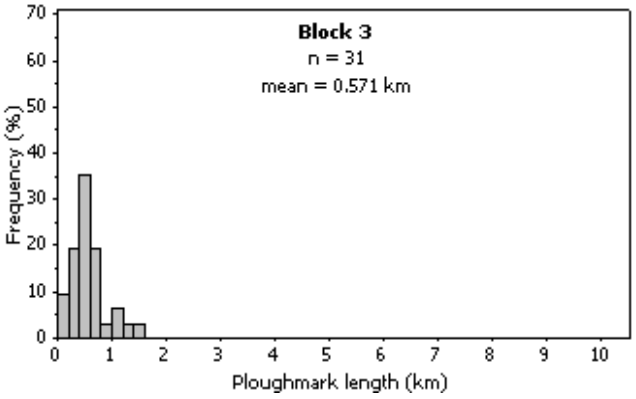
Block 3
n = 31
mean = 0.571 km
Frequency (%)
Ploughmark length (km)

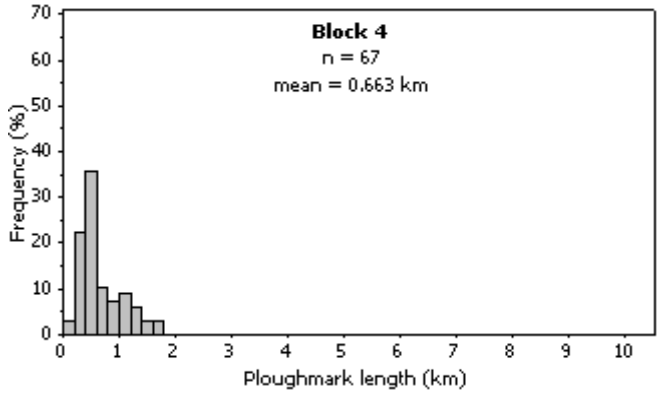
Block 4
n = 67
mean = 0.663 km
Frequency (%)
Ploughmark length (km)

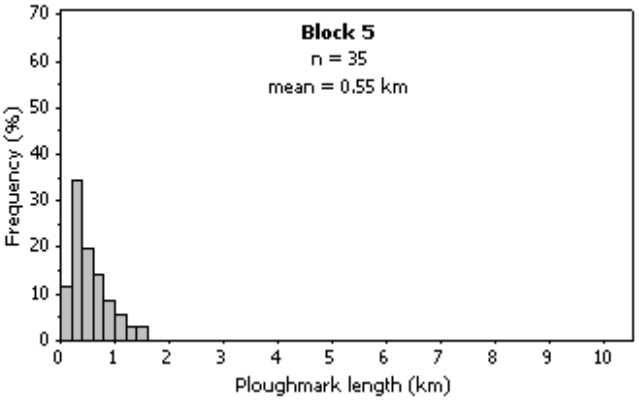
Block 5
n = 35
mean = 0.55 km
Frequency (%)
Ploughmark length (km)

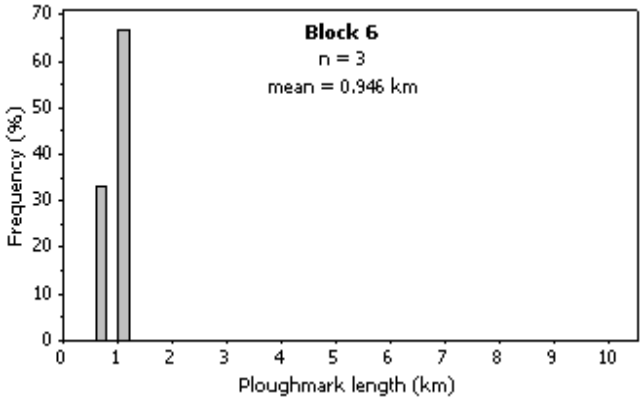
Block 6
n = 3
mean = 0.946 km
Frequency (%)
Ploughmark length (km)

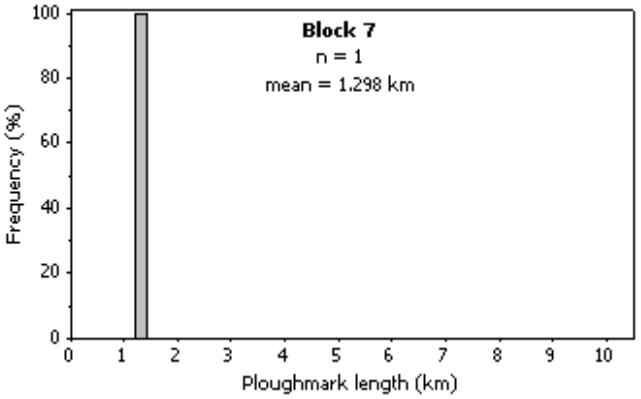
Block 7
n = 1
mean = 1.298 km
Frequency (%)
Ploughmark length (km)

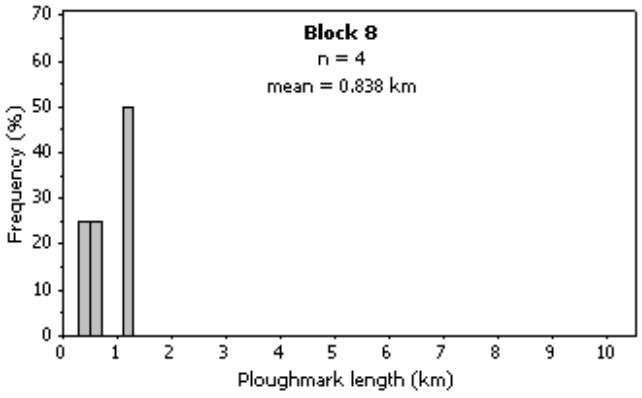
Block 8
n = 4
mean = 0.838 km
Frequency (%)
Ploughmark length (km)

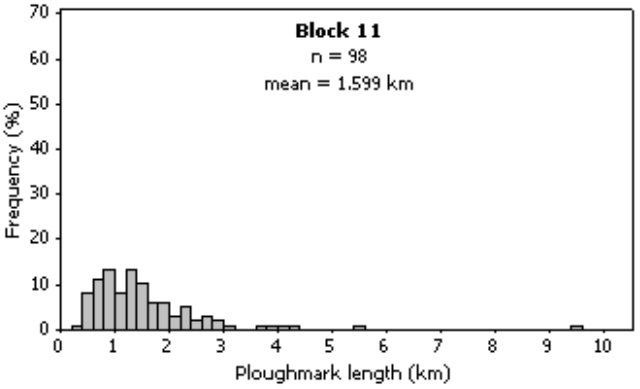
Block 11
n = 98
mean = 1.599 km
Frequency (%)
Ploughmark length (km)

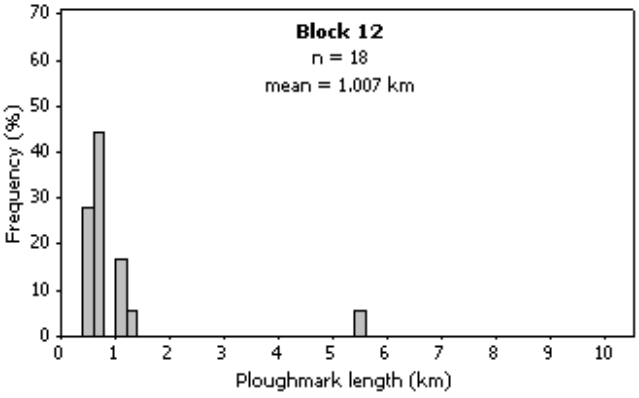
Block 12
n = 18
mean = 1.007 km
Frequency (%)
Ploughmark length (km)

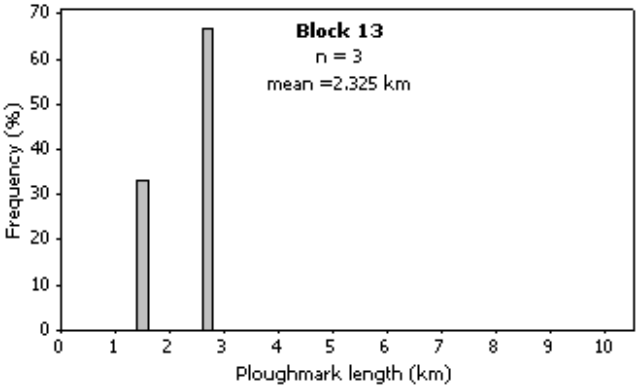
Block 13
n = 3
mean =2.325 km
Frequency (%)
Ploughmark length (km)

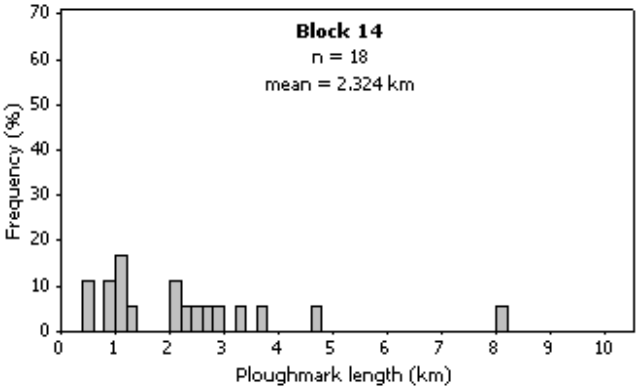
Block 14
n = 18
mean = 2.324 km
Frequency (%)
Ploughmark length (km)

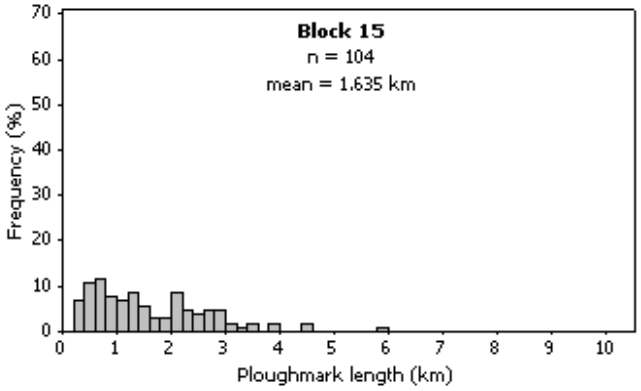
Block 15
n = 104
mean = 1.635 km
Frequency (%)
Ploughmark length (km)

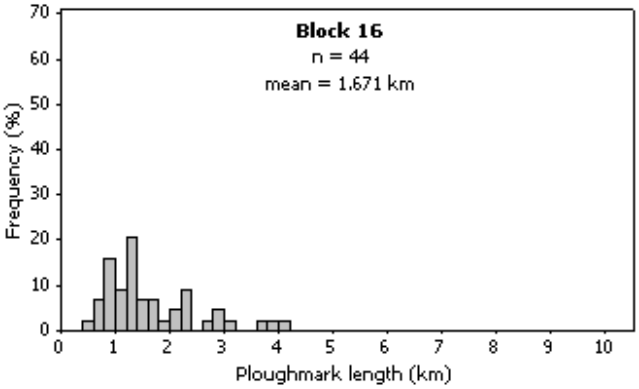
Block 16
n = 44
mean = 1.671 km
Frequency (%)
Ploughmark length (km)

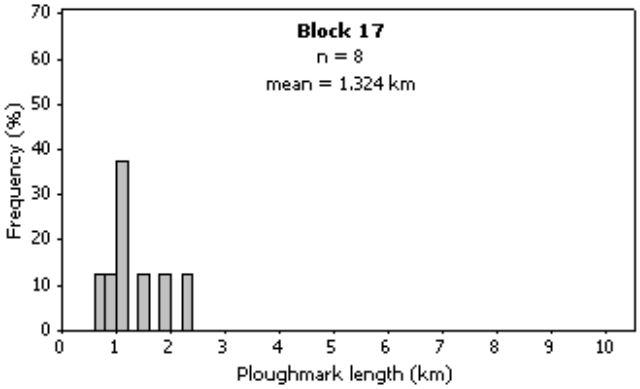
Block 17
n = 8
mean = 1.324 km
Frequency (%)
Ploughmark length (km)

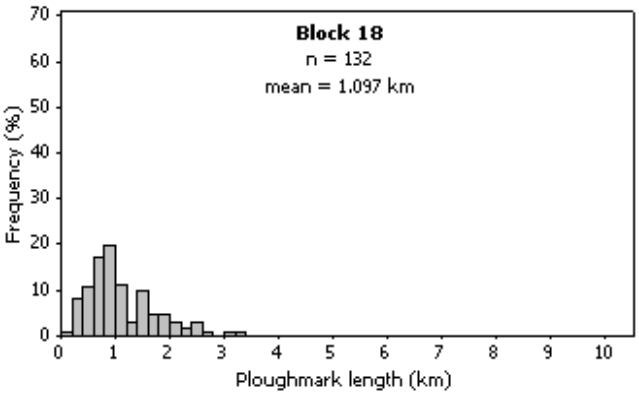
Block 18
n = 132
mean = 1.097 km
Frequency (%)
Ploughmark length (km)

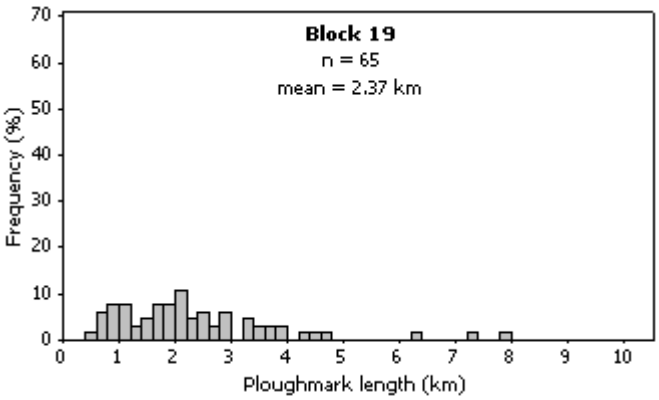
Block 19
n = 65
mean = 2.37 km
Frequency (%)
Ploughmark length (km)

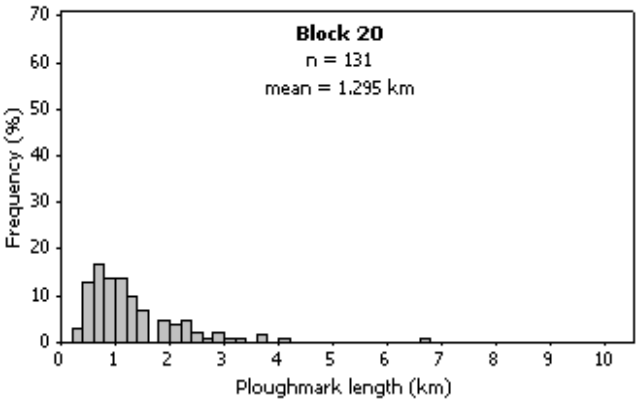
Block 20
n = 131
mean = 1.295 km
Frequency (%)
Ploughmark length (km)

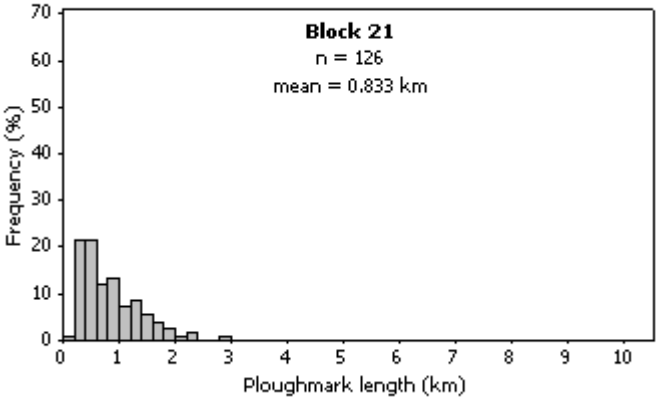
Block 21
n = 126
mean = 0.833 km
Frequency (%)
Ploughmark length (km)

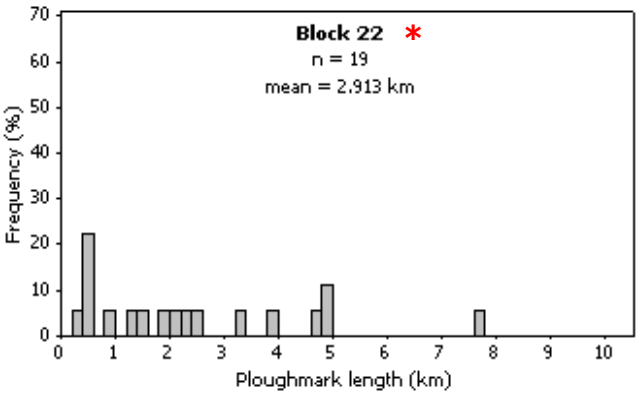
Block 22 *
n = 19
mean = 2.913 km
Frequency (%)
Ploughmark length (km)

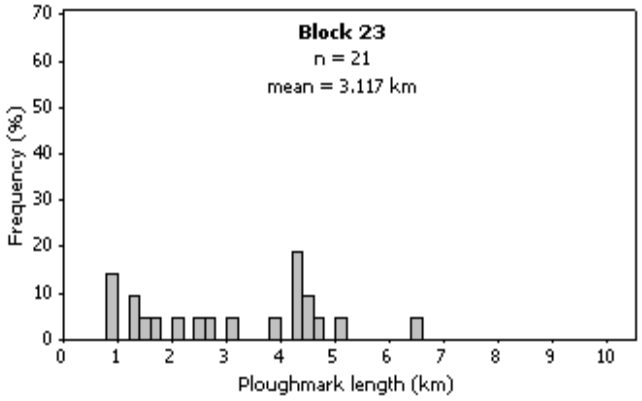
Block 23
n = 21
mean = 3.117 km
Frequency (%)
Ploughmark length (km)

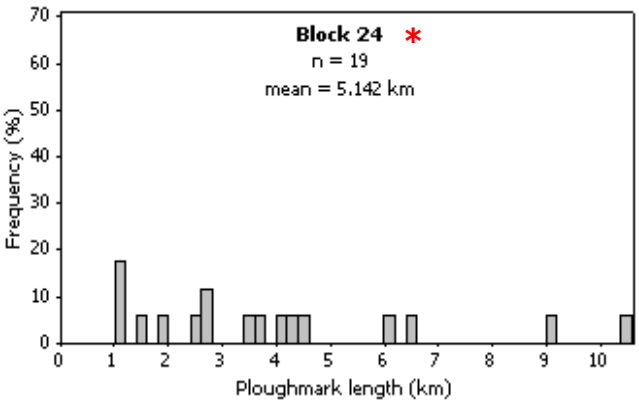
Block 24 *
n = 19
mean = 5.142 km
Frequency (%)
Ploughmark length (km)

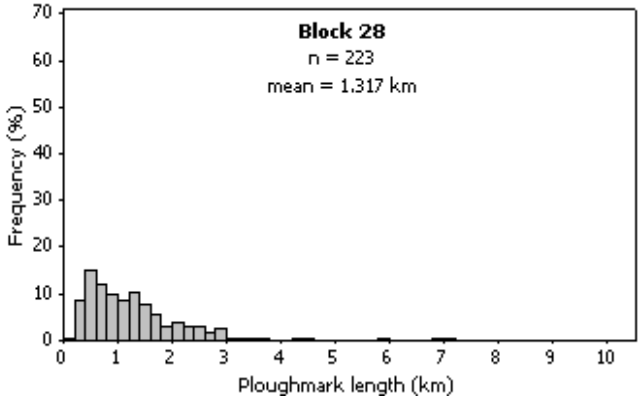
Block 28
n = 223
mean = 1.317 km
Frequency (%)
Ploughmark length (km)

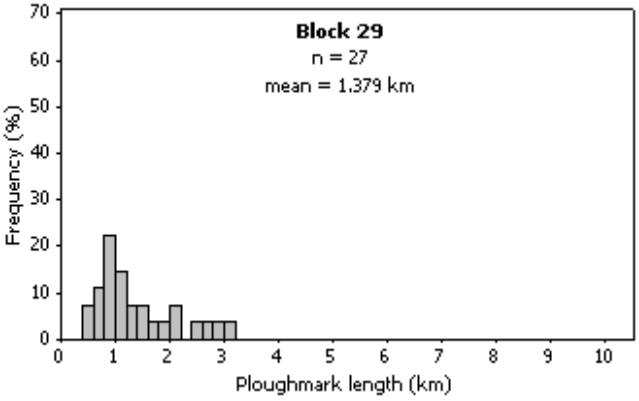
Block 29
n = 27
mean = 1.379 km
Frequency (%)
Ploughmark length (km)

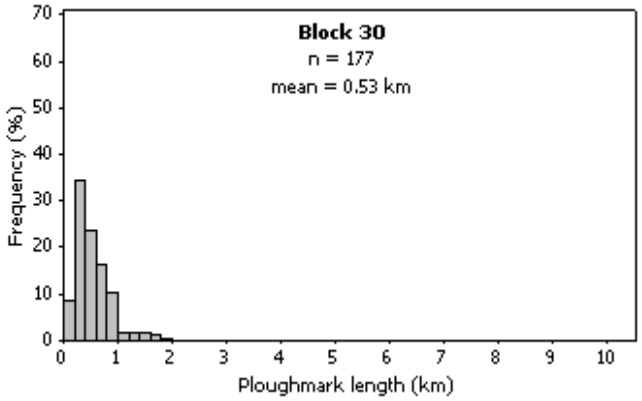
Block 30
n = 177
mean = 0.53 km
Frequency (%)
Ploughmark length (km)

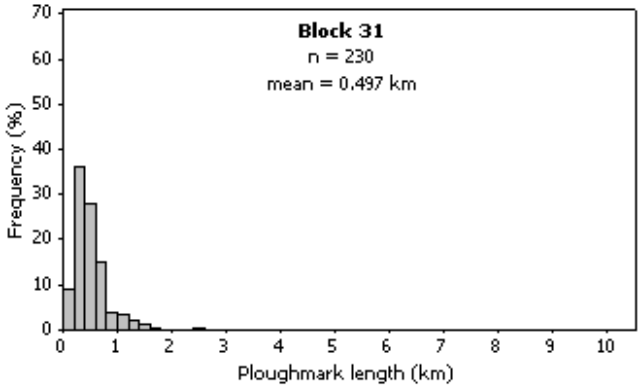
Block 31
n = 230
mean = 0.497 km
Frequency (%)
Ploughmark length (km)

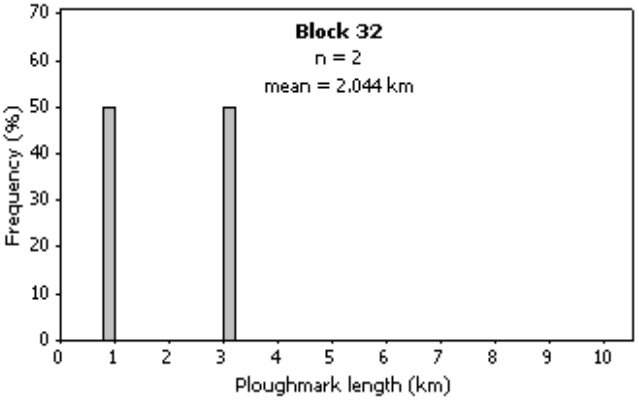
Block 32
n = 2
mean = 2.044 km
Frequency (%)
Ploughmark length (km)

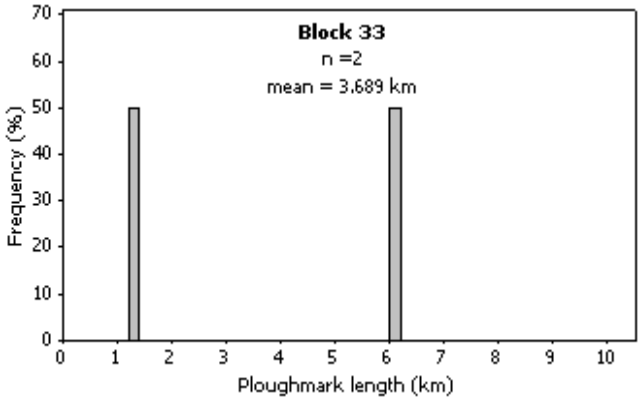
Block 33
n =2
mean = 3.689 km
Frequency (%)
Ploughmark length (km)

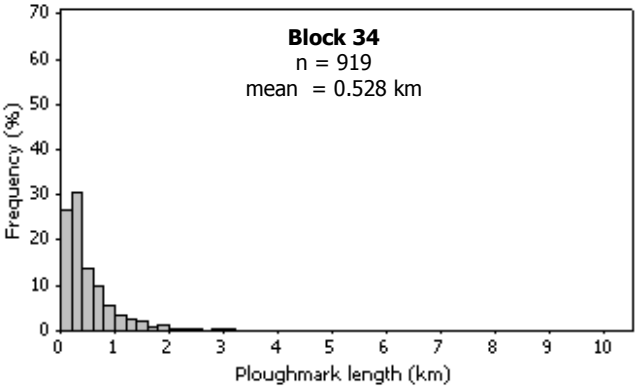
Block 34
n = 919
mean = 0.528 km
Frequency (%)
Ploughmark length (km)

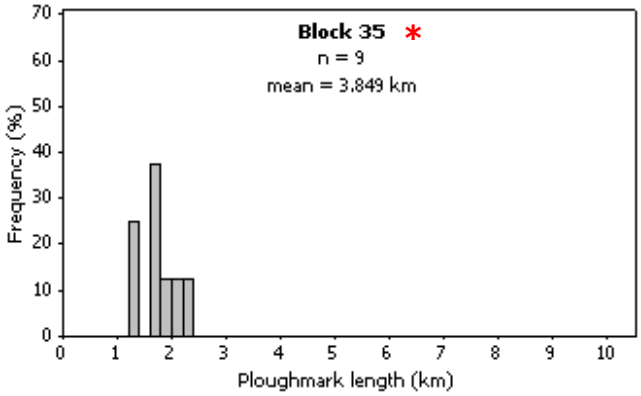
Block 35 *
n = 9
mean = 3.849 km
Frequency (%)
Ploughmark length (km)

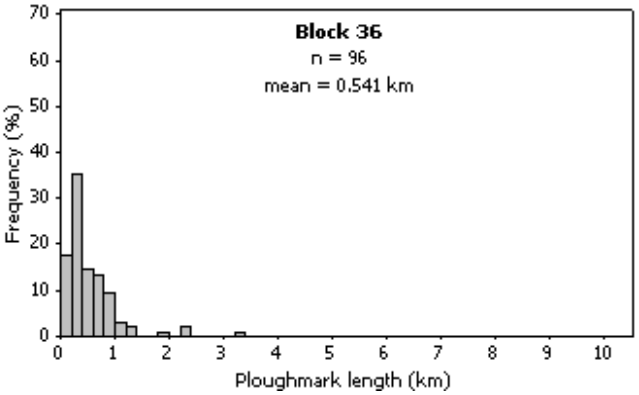
Block 36
n = 96
mean = 0.541 km
Frequency (%)
Ploughmark length (km)

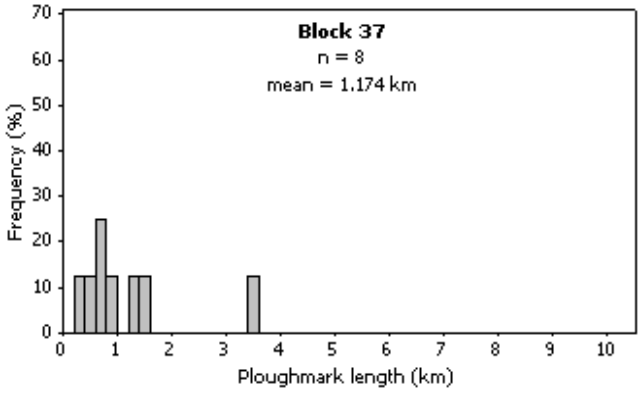
Block 37
n = 8
mean = 1.174 km
Frequency (%)
Ploughmark length (km)

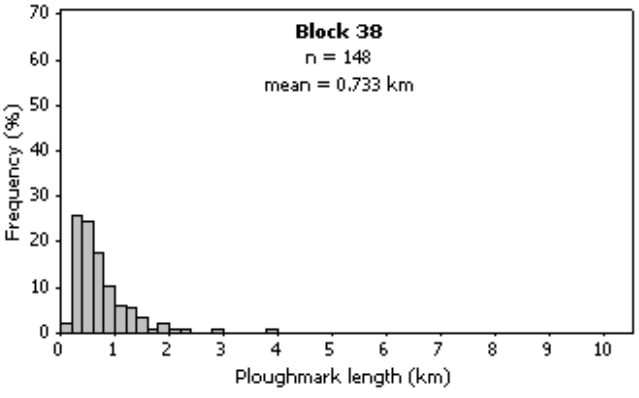
Block 38
n = 148
mean = 0.733 km
Frequency (%)
Ploughmark length (km)

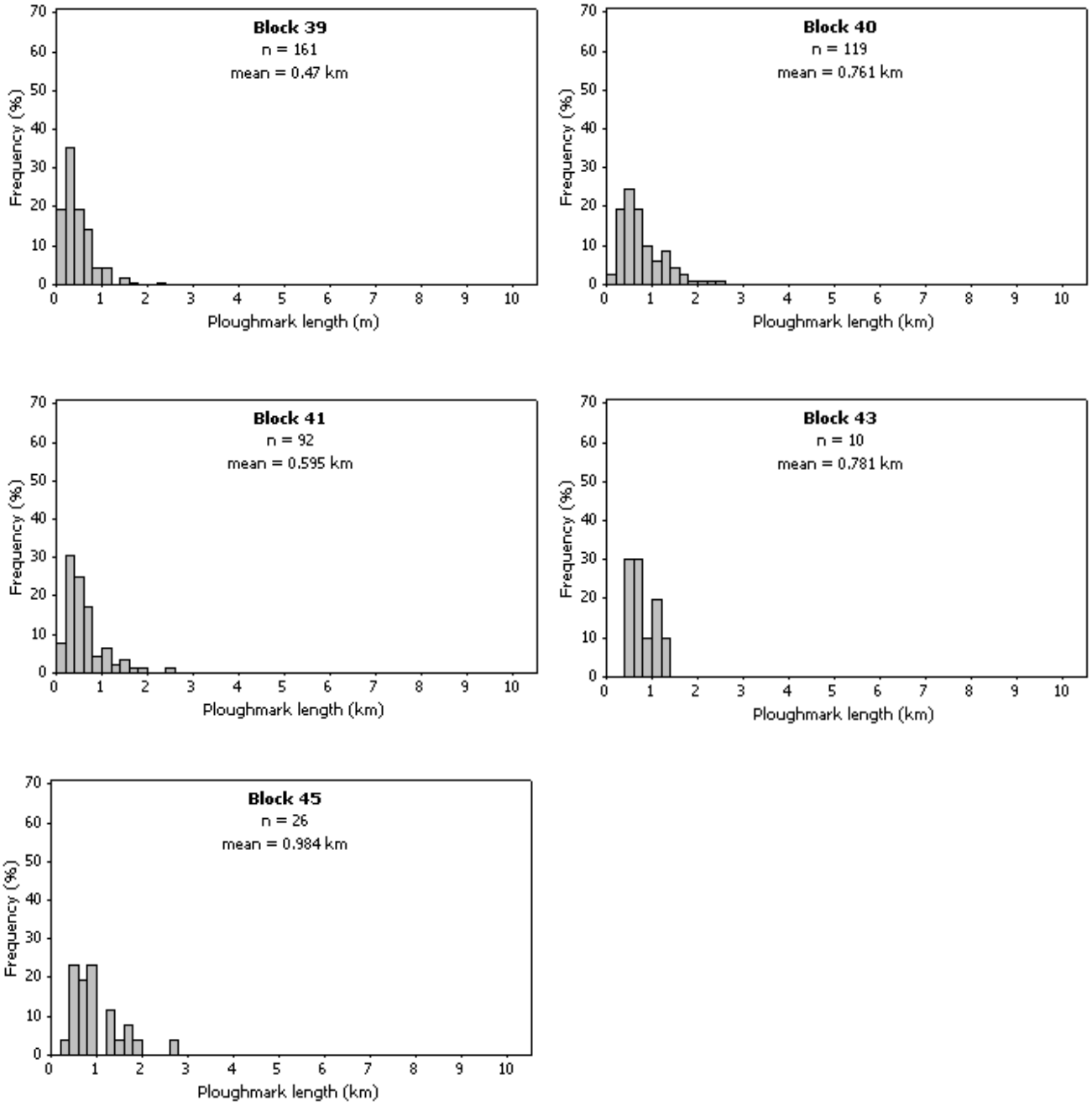


**Figure 4.1.** Histograms to show ploughmark length in kilometres for each block within the study area (blocks located in Figures 3.5 to 3.9). Blocks not illustrated contain no ploughmarks. Lengths given are the maximum observed lengths, as some of the ploughmarks extended beyond the edges of the swath coverage. Note that the histogram for Block 7 has a different vertical scale to the rest. Note also that ploughmarks with lengths in excess of 10.5 km are not shown on the histograms; a red asterix denotes areas where ploughmarks with lengths greater than 10.5 km were observed.

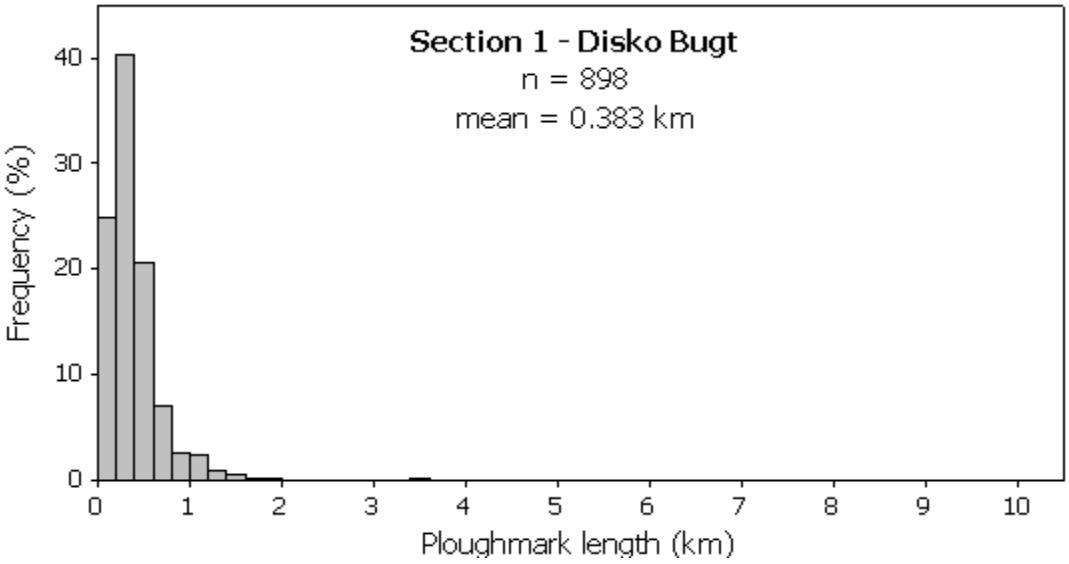
Section 1 - Disko Bugt
n = 898
mean = 0.383 km
Frequency (%)
Ploughmark length (km)

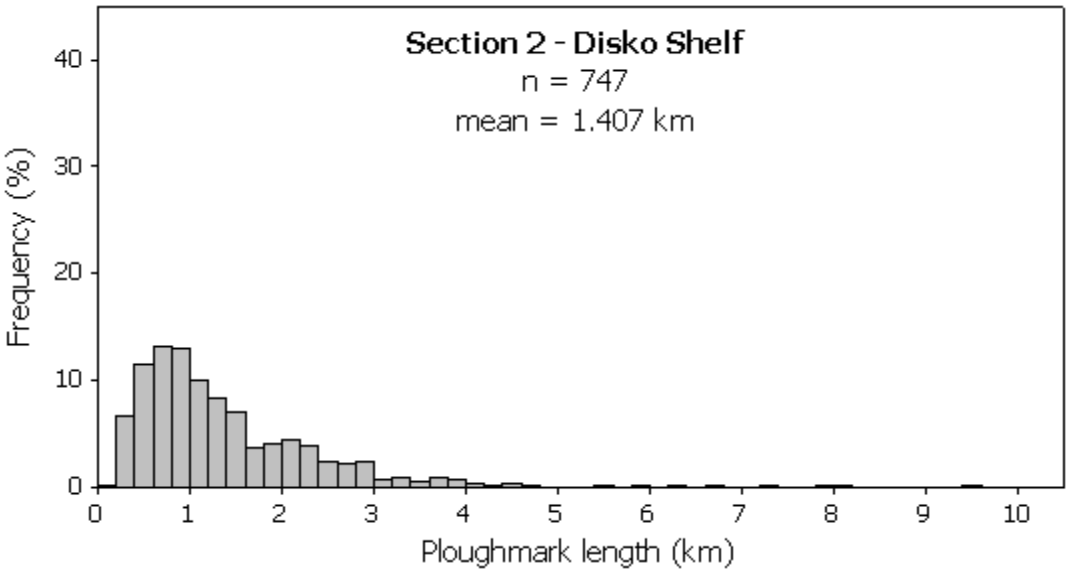
Section 2 - Disko Shelf
n = 747
mean = 1.407 km
Frequency (%)
Ploughmark length (km)

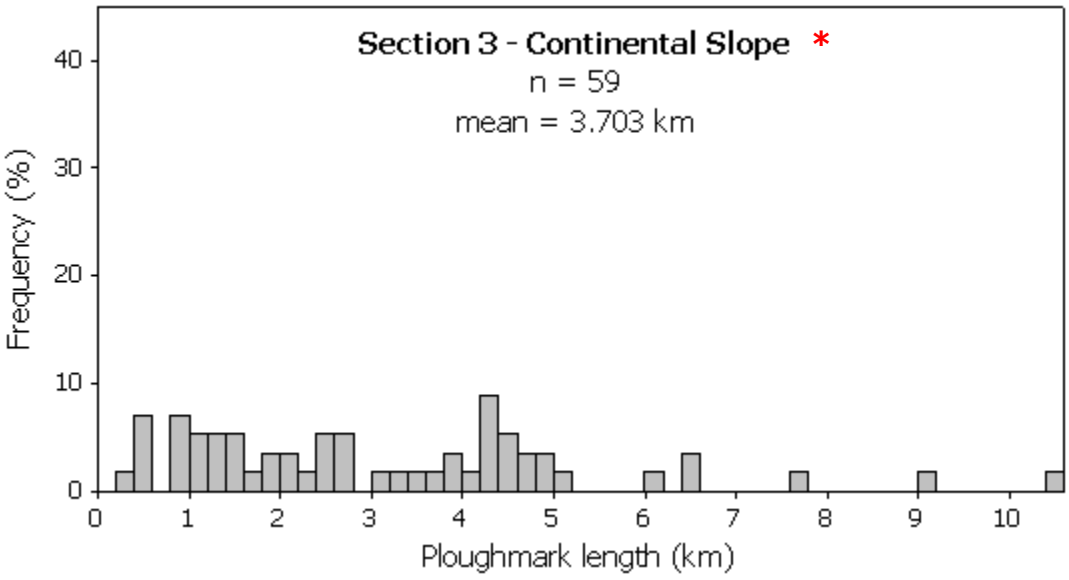
Section 3 - Continental Slope *
n = 59
mean = 3.703 km
Frequency (%)
Ploughmark length (km)

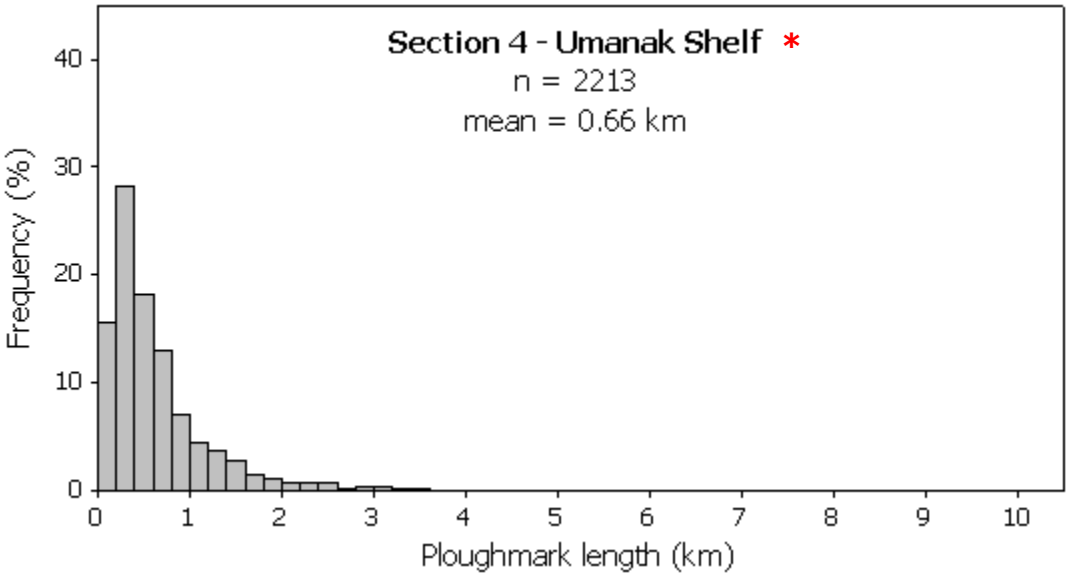
Section 4 - Umanak Shelf *
n = 2213
mean = 0.66 km
Frequency (%)
Ploughmark length (km)

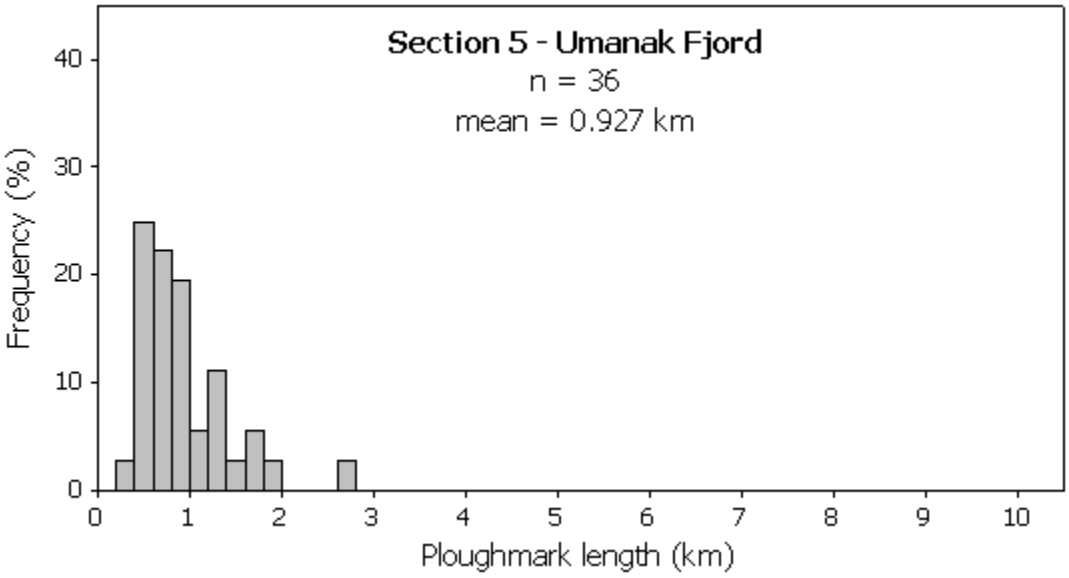
Section 5 - Umanak Fjord
n = 36
mean = 0.927 km
Frequency (%)
Ploughmark length (km)

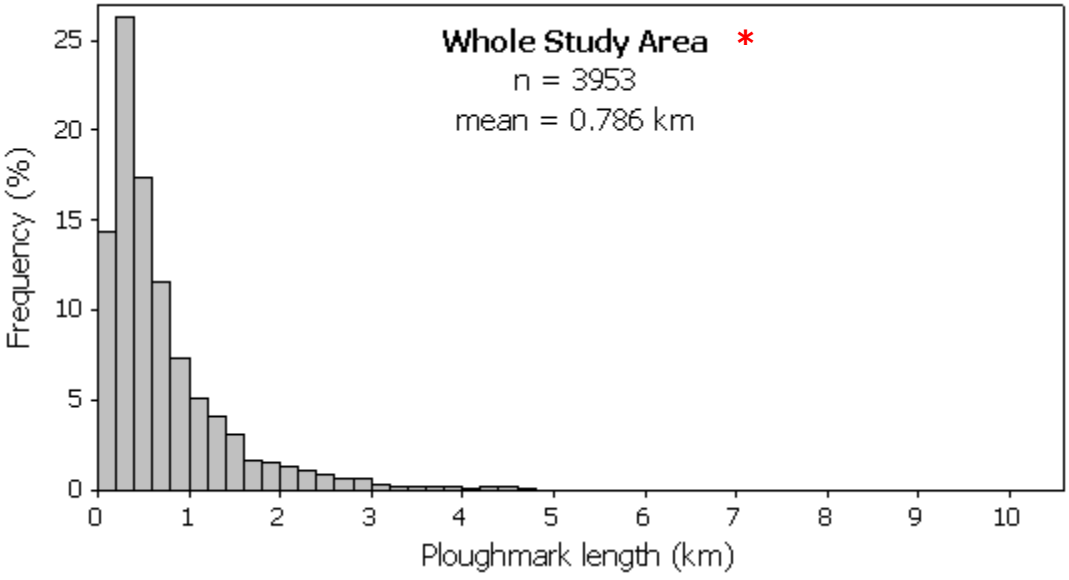
Whole Study Area *
n = 3953
mean = 0.786 km
Frequency (%)
Ploughmark length (km)

**Figure 4.2.** Histograms to show ploughmark length in kilometres for each section within the study area (sections located in Figure 3.4). A histogram to summarise ploughmark lengths for the entire study area is also shown. Note that ploughmarks with lengths in excess of 10.5 km are not shown on the histograms; a red asterix denotes areas where ploughmarks with lengths greater than 10.5 km were observed.

In Disko Bugt, the mean ploughmark length was 0.38 km (Table 4.1; Fig 4.2). The ploughmarks in Disko Bugt displayed a small range of lengths, from 0.06 km to 3.5 km, with the majority of observations clustered around the mean (Table 4.1; Fig. 4.1; Fig. 4.2). The same pattern of distribution was observed for all blocks within this section. Approximately 95% of the ploughmarks measured less than 1 km in length. The longest ploughmark was observed in block 2; at 3.5 km, this ploughmark was considerably longer than the rest of the ploughmarks in Disko Bugt, none of which exceeded 2 km in length (Fig 4.2).

A somewhat wider range of ploughmark lengths was observed across the continental shelf offshore of Disko Bugt. Ploughmark lengths ranged from 0.16 km to 9.5 km, with a mean length of 1.41 km (Table 4.1; Fig. 4.2). Approximately 95% of ploughmarks observed on the Disko Shelf measured less than 5 km in length (Fig. 4.2); ploughmarks longer than 5 km are shown on the histograms for blocks 11, 12, 14, 15, 19 and 20 as extreme outliers (Fig. 4.1). The pattern of distribution varied considerably between blocks. In blocks 12, 13, 17, 18 and 21 the majority of observations were clustered around the mean. In comparison, the histograms for blocks 11, 14, 15, 16, 19 and 20 displayed a far wider range of ploughmark lengths (Fig. 4.1).

Ploughmarks on the continental slope also displayed a wide range of lengths, from 0.35 km to 15.79 km. The mean ploughmark length was 3.7 km, although this varied between blocks, from 2.91 km in block 22, up to 5.14 km in block 24 (Table 4.1; Fig. 4.1; Fig 4.2). The distribution of ploughmark lengths on the continental slope was somewhat different to that observed for other sections within the study area, with a much wider range of ploughmark lengths and a comparatively high mean length (Fig. 4.2). This pattern of distribution was observed for all blocks on the continental slope.

The mean ploughmark length on the continental shelf offshore of Umanak Fjord was 0.66 km (Table 4.1; Fig. 4.2). This mean was dominated by the large number of short ploughmarks observed in block 34 (Fig. 4.1). Ploughmark lengths ranged from 0.03 km to 20.81 km, but in

general displayed a relatively tight distribution, with most observations clustered around the mean (Table 4.1; Fig. 4.2). The histograms for blocks 32 and 33 displayed a wider distribution; this may be explained by the fact that there were only 2 observations for each of these blocks and therefore the difference between individual ploughmark lengths was more pronounced (Fig. 4.1). Very few ploughmarks measured more than 4 km in length – so few that they did not appear on the section summary in Figure 4.2. Five ploughmarks with lengths greater than 4 km were observed in block 28, presumably because this block is located at least partly on the continental slope (Fig. 4.1). The longest ploughmark on the Umanak Shelf was located in block 35. At 20.81 km, this ploughmark was significantly longer than the other ploughmarks within the study area.

In Umanak Fjord, the mean ploughmark length was 0.93 km (Table 4.1; Fig. 4.2). The ploughmarks displayed a small range of lengths, from 0.4 km to 2.75 km, with the majority of observations clustered around the mean (Table 4.1; Fig. 4.2). The same pattern of distribution was observed for both blocks in Umanak Fjord, although the histogram for block 43 displayed a slightly tighter distribution than that for block 45 (Fig. 4.1).

A large number of short ploughmarks were observed in Disko Bugt and across the continental shelf offshore of Umanak Fjord. A smaller number of short ploughmarks were also observed within the Umanak Fjord system. The mean ploughmark length for each of these three sections was less than 1 km and in general ploughmark lengths displayed a relatively tight distribution around the mean (Fig. 4.1; Fig. 4.2). In comparison, the pattern of distribution on the continental shelf was markedly different. Here, a relatively small number of long ploughmarks were observed, as opposed to a large number of shorter ploughmarks. Mean ploughmark length on the continental slope was 3.7 km, significantly higher than the mean length of 0.79 km for the entire study area (Fig. 4.2). There was also much more variability in ploughmark lengths. The continental shelf offshore of Disko Bugt represented something of an intermediate distribution between the continental slope and the other three sections.

### 4.1.2 Interpretation

The mean and median ploughmarks lengths for the entire study area were 0.79 km and 0.49 km respectively (Table 4.1; Fig. 4.2). ~75% of ploughmarks measured less than 1 km in length (Fig 4.2), whilst only 5 ploughmarks had observed lengths in excess of 10 km. Large

icebergs are more likely to plough seafloor sediments over long distances, since the rate of iceberg melting and break-up is related to iceberg size (Weeks and Campbell, 1973; Neshyba and Josberger, 1980). On the continental slope, it is likely that many of the surviving icebergs are large, given the distance from the source of bergs at the margins of fast-flowing outlet glaciers of the Greenland Ice Sheet. In modern polar settings, the size-frequency distribution of icebergs demonstrates a progressive decay of iceberg frequency with size (Wadhams, 1988; Dowdeswell et al., 1992; Metz et al., 2008). This would account, at least in part, for the comparatively small numbers of long ploughmarks observed on the West Greenland margin.

The geographical distribution of ploughmark lengths across the study area is linked with the relationship between iceberg keel depth and bathymetry. As described in Section 2.2.1, the intensity of iceberg ploughing is inversely proportional to water depth. Therefore, small icebergs on the deep continental slope could not form ploughmarks, because their keels are too shallow to impact the seafloor. The distribution of ploughmark lengths is also linked with the proximity of the ice margin. The fjords and inner shelf are more proximal to the iceberg source, so there are a greater number of small icebergs present to form ploughmarks. Since large icebergs are more likely to survive further from the source glacier, a greater proportion of large icebergs plough the outer continental shelf and slope. This is demonstrated, for example, by the fact that there are comparatively few, longer ploughmarks on the continental slope, compared with a large number of small ploughmarks in Disko Bugt, which is in close proximity to the present-day ice margin. Although Umanak Fjord is also close to the ice margin, there are only a small number of short ploughmarks within the fjord system; this is presumably because the fjord is too deep for small icebergs to impact the seafloor.

## 4.2 Ploughmark Orientations

### 4.2.1 Observations

Ploughmark trajectories can be used as proxy indicators of iceberg drift patterns, although it is not generally possible to determine the absolute direction of travel through this method. The orientations of ploughmarks on the West Greenland margin are shown in Figures 4.3 and 4.4. It was not known whether the icebergs were drifting north or south, so in order to

maintain consistency, the orientations were all plotted from the east, from 90°N to 270°N, through the northern hemisphere of the plots.

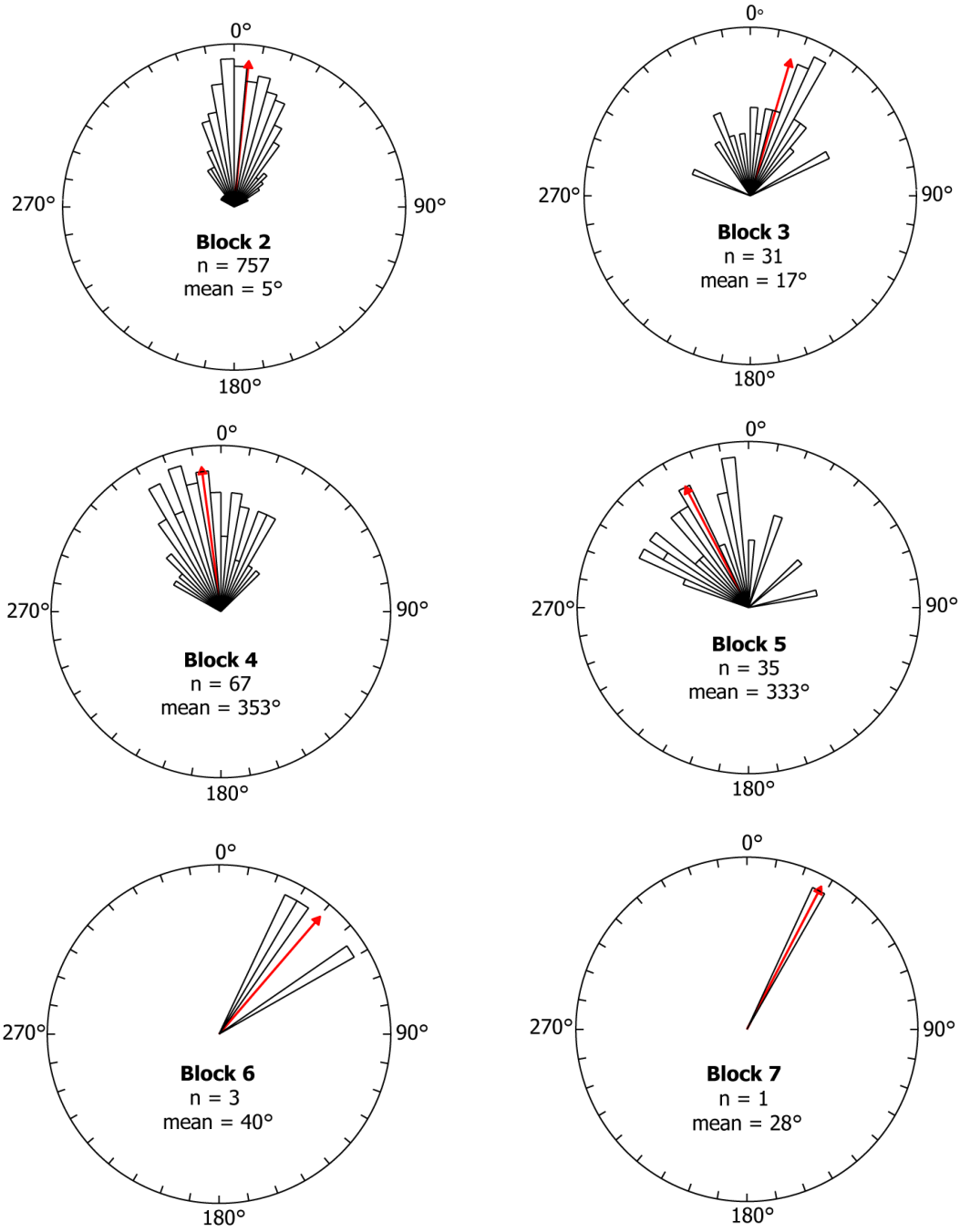

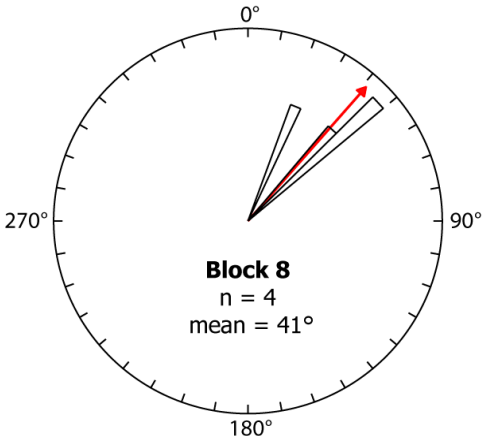
0°
270°
90°
180°
Block 8
n = 4
mean = 41°

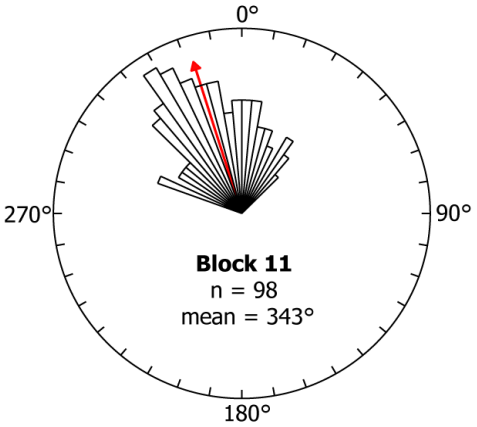
0°
270°
90°
180°
Block 11
n = 98
mean = 343°

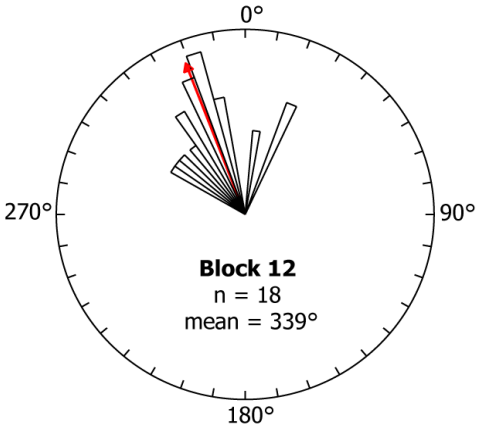
0°
270°
90°
180°
Block 12
n = 18
mean = 339°

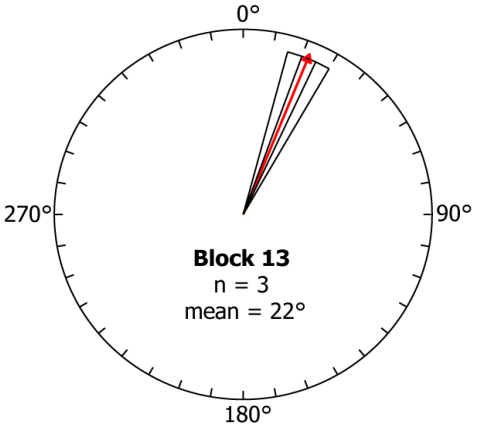
0°
270°
90°
180°
Block 13
n = 3
mean = 22°

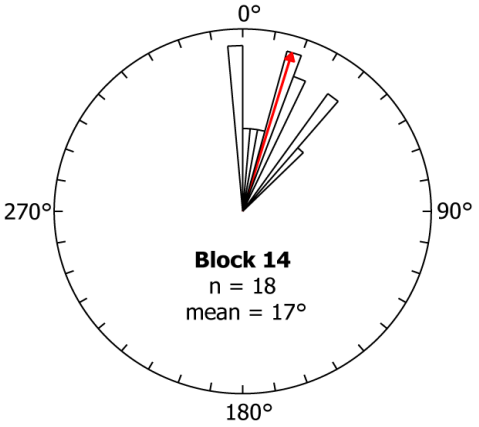
0°
270°
90°
180°
Block 14
n = 18
mean = 17°

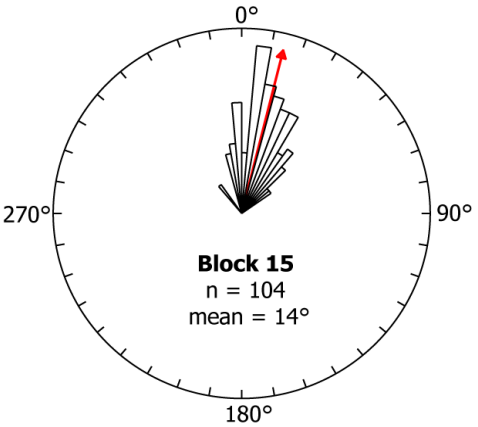
0°
270°
90°
180°
Block 15
n = 104
mean = 14°

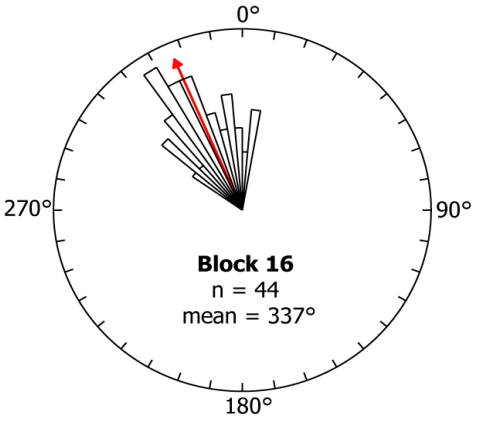
0°
270°
90°
180°
Block 16
n = 44
mean = 337°

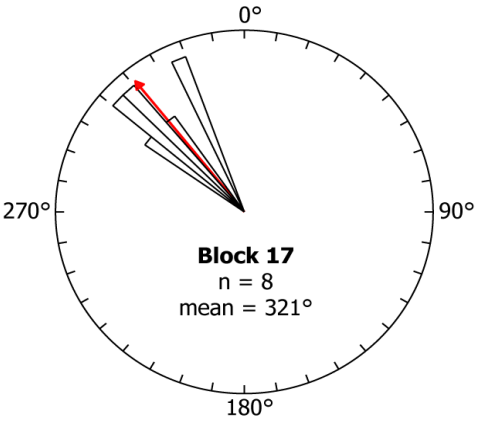
0°
270°
90°
180°
Block 17
n = 8
mean = 321°

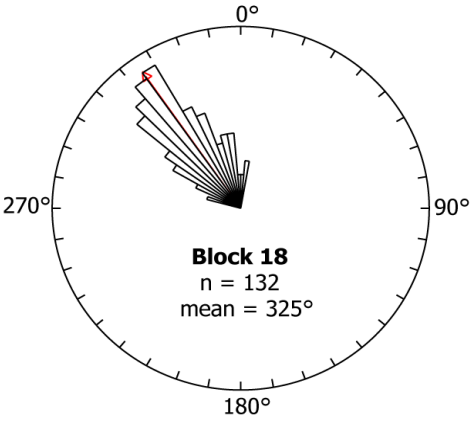
0°
270°
90°
180°
Block 18
n = 132
mean = 325°

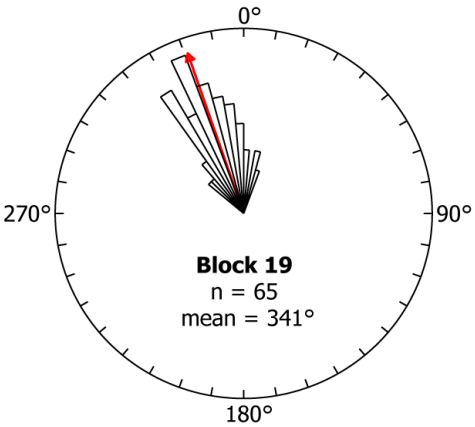
0°
270°
90°
180°
Block 19
n = 65
mean = 341°

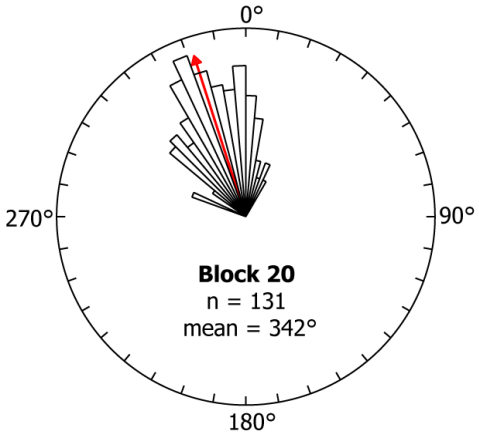
0°
270°
90°
180°
Block 20
n = 131
mean = 342°

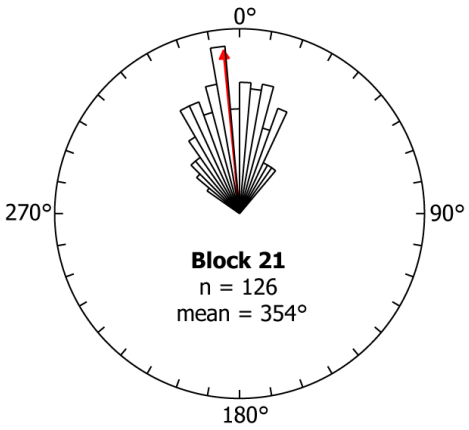
0°
270°
90°
180°
Block 21
n = 126
mean = 354°

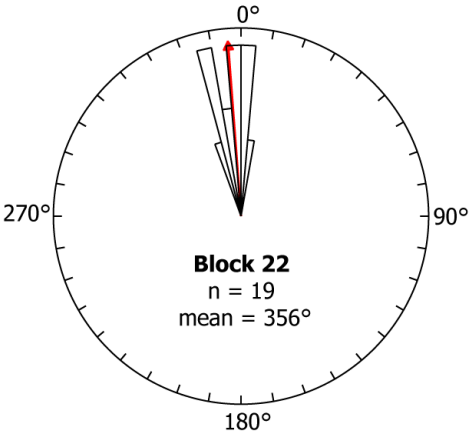
0°
270°
90°
180°
Block 22
n = 19
mean = 356°

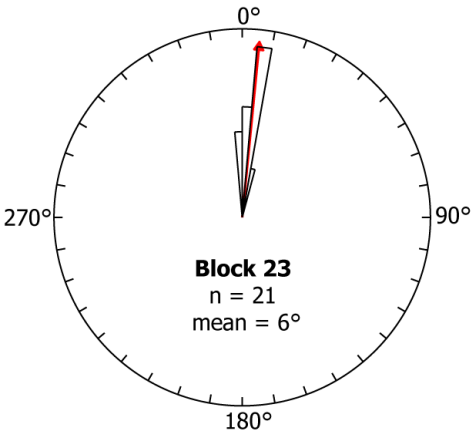
0°
270°
90°
180°
Block 23
n = 21
mean = 6°

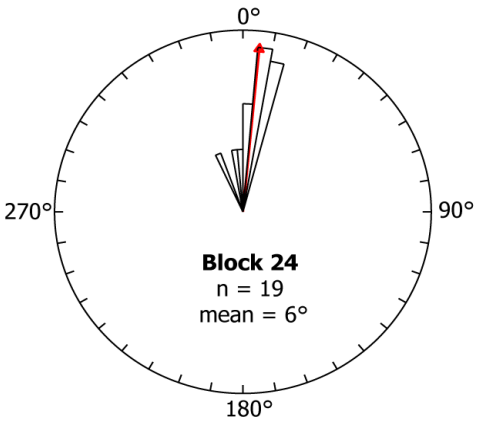
0°
270°
90°
180°
Block 24
n = 19
mean = 6°

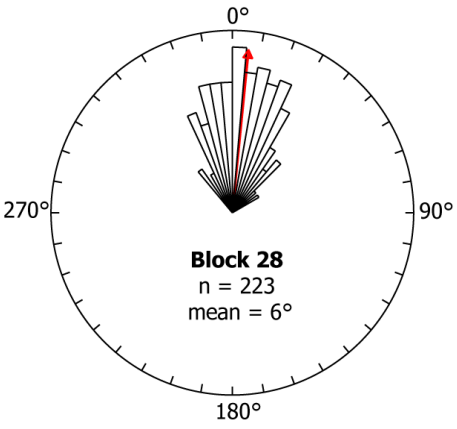
0°
270°
90°
180°
Block 28
n = 223
mean = 6°

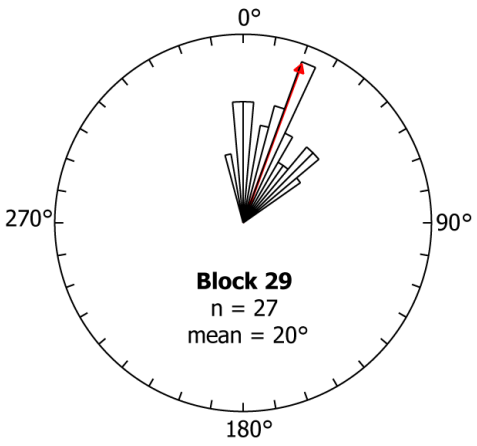
0°
270°
90°
180°
Block 29
n = 27
mean = 20°

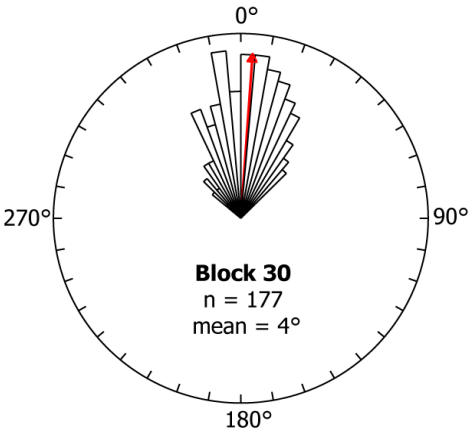
0°
270°
90°
180°
Block 30
n = 177
mean = 4°

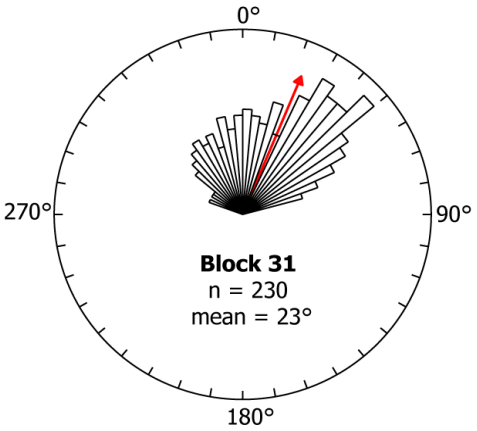
0°
270°
90°
180°
Block 31
n = 230
mean = 23°

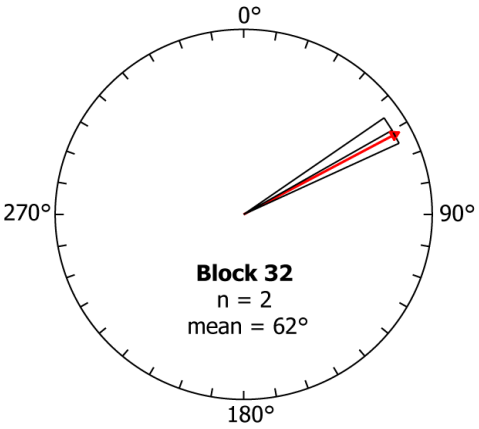
0°
270°
90°
180°
Block 32
n = 2
mean = 62°

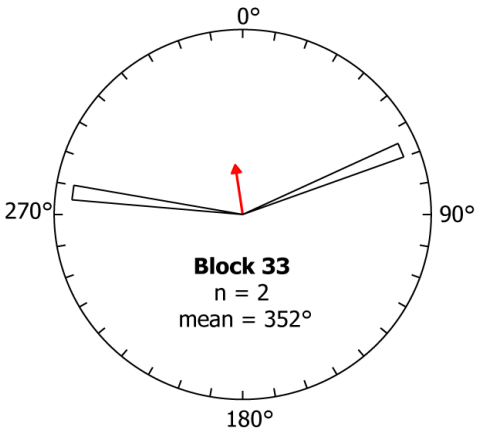
0°
270°
90°
180°
Block 33
n = 2
mean = 352°

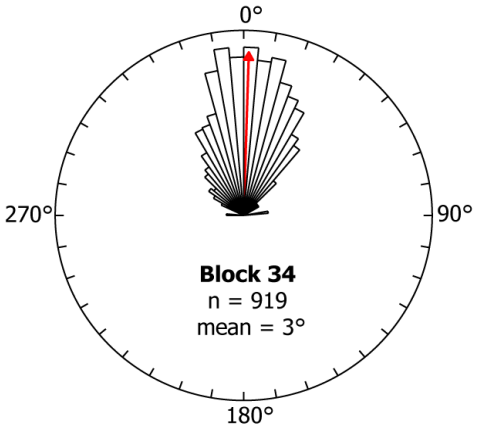
0°
270°
90°
180°
Block 34
n = 919
mean = 3°

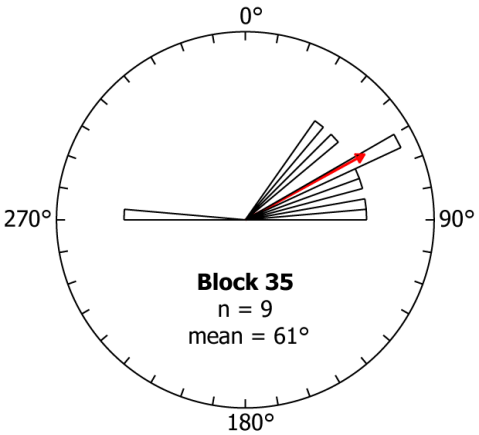
0°
270°
90°
180°
Block 35
n = 9
mean = 61°

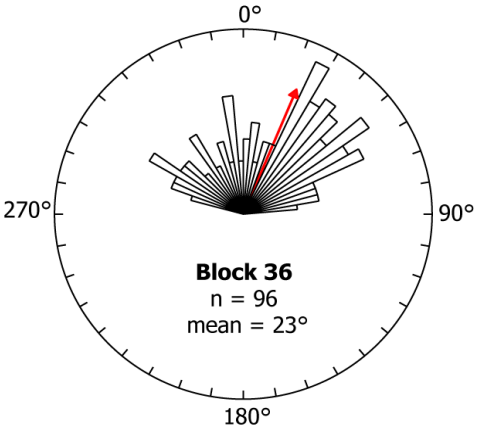
0°
270°
90°
180°
Block 36
n = 96
mean = 23°

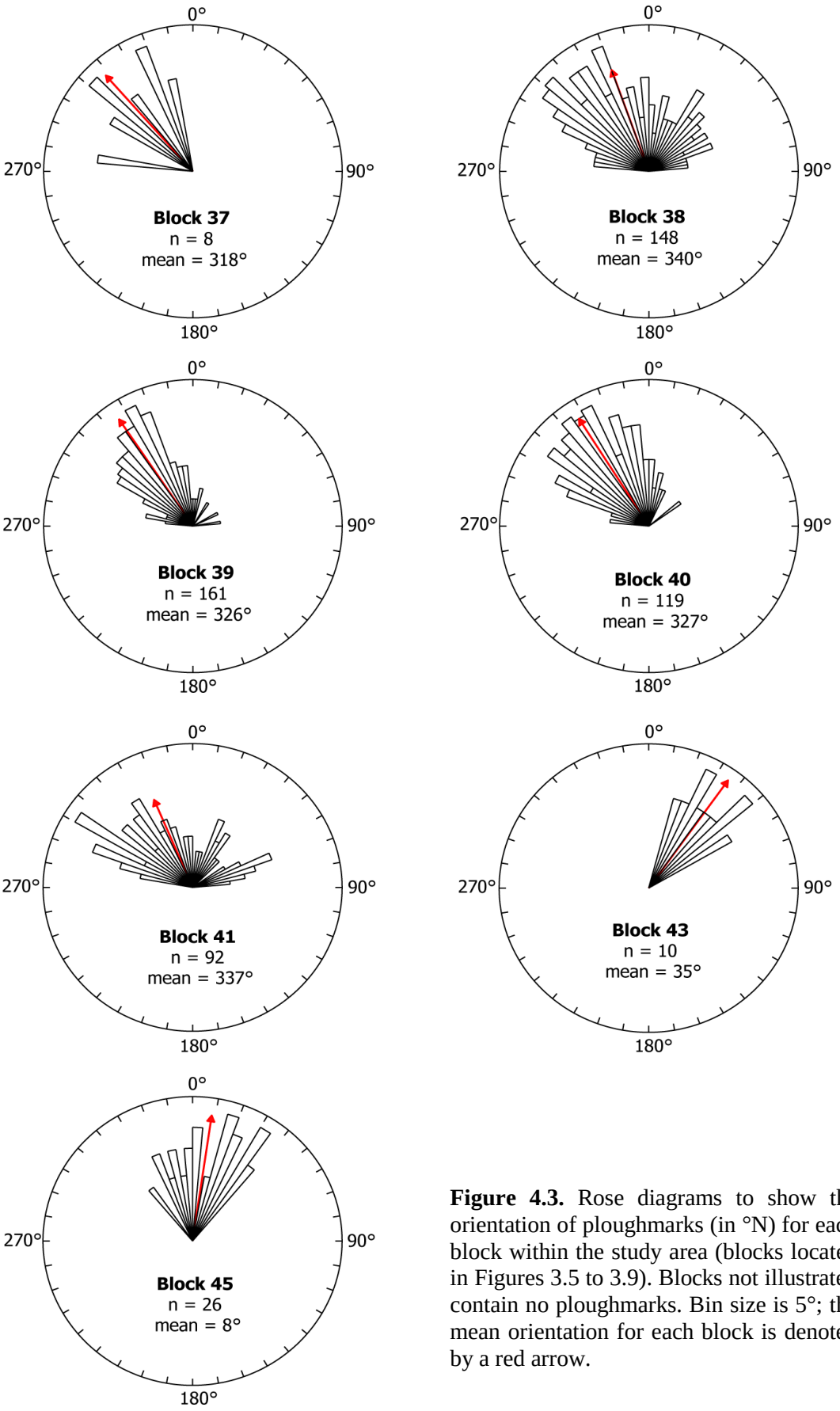


**Figure 4.3.** Rose diagrams to show the orientation of ploughmarks (in °N) for each block within the study area (blocks located in Figures 3.5 to 3.9). Blocks not illustrated contain no ploughmarks. Bin size is 5°; the mean orientation for each block is denoted by a red arrow.

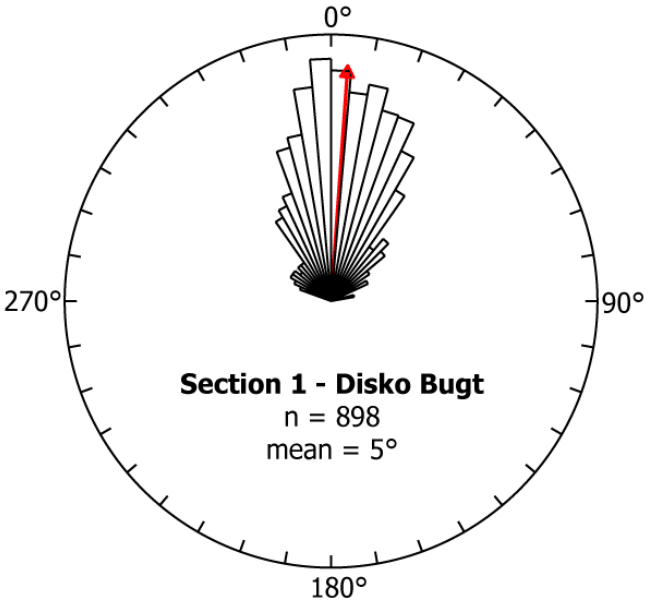
0°
270°
90°
180°
Section 1 - Disko Bugt
n = 898
mean = 5°

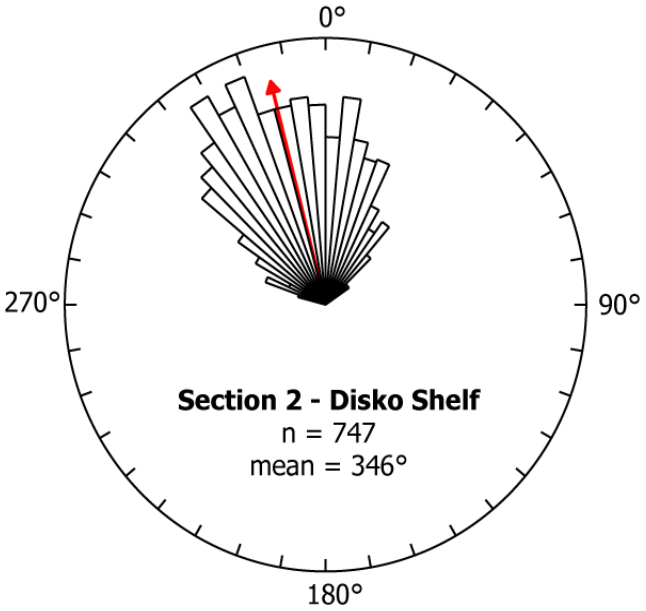
0°
270°
90°
180°
Section 2 - Disko Shelf
n = 747
mean = 346°

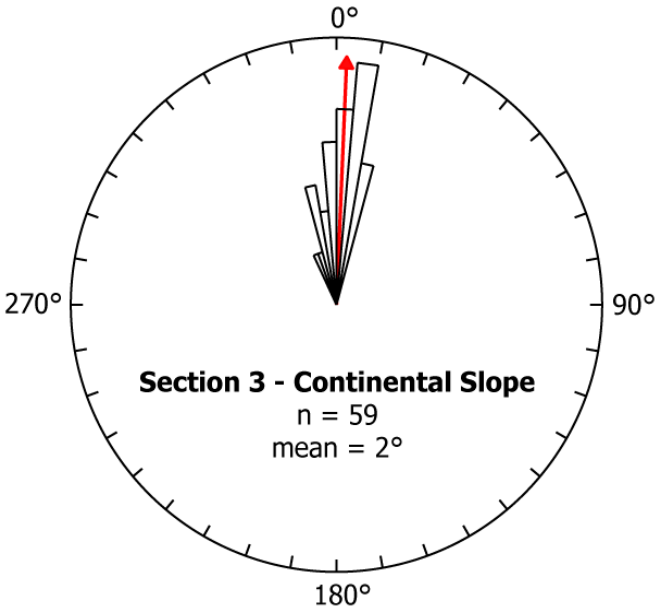
0°
270°
90°
180°
Section 3 - Continental Slope
n = 59
mean = 2°

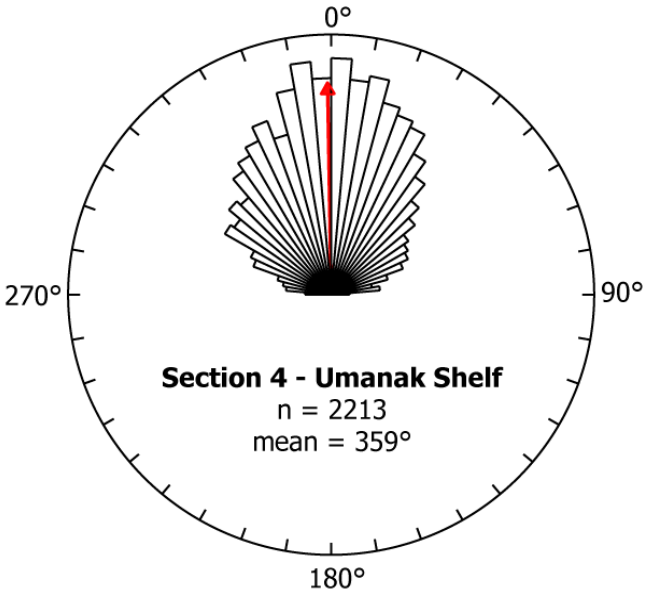
0°
270°
90°
180°
Section 4 - Umanak Shelf
n = 2213
mean = 359°

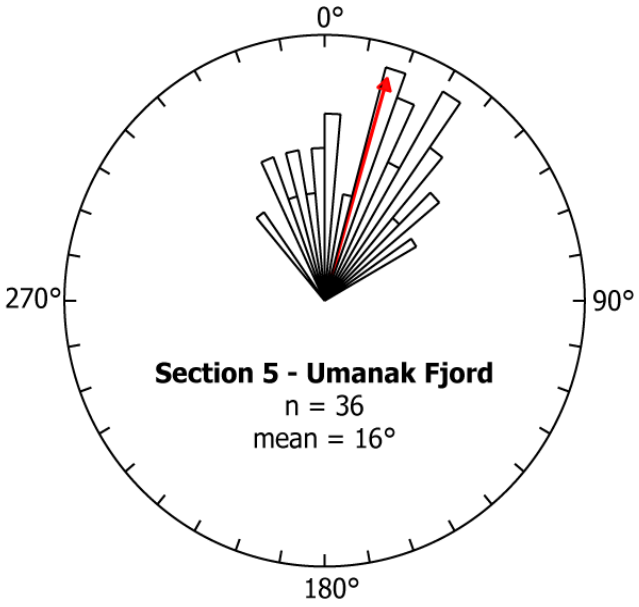
0°
270°
90°
180°
Section 5 - Umanak Fjord
n = 36
mean = 16°

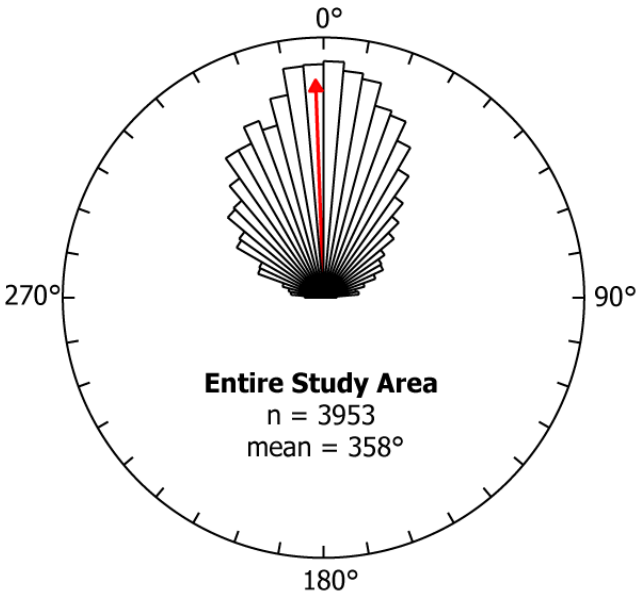
0°
270°
90°
180°
Entire Study Area
n = 3953
mean = 358°

**Figure 4.4.** Rose diagrams to show the orientations of ploughmarks (in °N) for each section within the study area (sections located in Figure 3.4). A rose diagram to summarise ploughmark orientations for the entire study area is also shown. Bin size is 5°; the mean orientation for each section is denoted by a red arrow.

The mean orientation for ploughmarks in Disko Bugt was approximately N-S (Fig. 4.4); this mean was dominated by the large number of observations from block 2. Despite the large number of observations from this block, however, the distribution was relatively tight; the majority of observations were clustered around a mean of 5°N, indicating a N-S component to iceberg drift (Fig. 4.3). In contrast, ploughmark orientations in blocks 3-6 and block 8 showed more variation (Fig. 4.3). The wide range of ploughmark orientations observed in Disko Bugt indicates that not all icebergs in this section have a N-S component to drift. Icebergs in blocks 2-4 may well be drifting northwards, to exit Disko Bugt through the Vaigat Strait to the north of Disko Island. In blocks 6-8, however, icebergs are more likely to be drifting SW rather than NE, to exit the bay via Egedesminde Dyb (Fig. 4.3).

A wide range of ploughmarks orientations were also observed across the continental shelf offshore of Disko Bugt. Mean orientation for individual blocks ranged from NNW-SSE to NNE-SSW; the mean orientation for the entire section was NNW-SSE (Fig. 4.3; Fig. 4.4). Blocks 15, 16, 17, 18, 19, 20 and 21 displayed a tight distribution, with most observations clustered around the mean, whereas blocks 11, 12 and 14 showed more variation (Fig. 4.3). This pattern of distribution suggests that ploughmark orientations became more uniform with distance across the shelf. Overall, this section of the study area showed a simpler distribution than that observed for Disko Bugt, with less variability between blocks (Fig. 4.3).

Ploughmarks on the continental slope displayed the simplest and least variable distribution of all sections within the study area. Mean orientation, both for individual blocks, and for the entire section, was N-S; the majority of observations were clustered tightly around this mean (Fig. 4.3; Fig. 4.4). The mean orientation of S-N is parallel to the main current direction on the West Greenland margin, which flows northward, indicating that iceberg drift can be related to a (palaeo)circulation pattern corresponding to the WGC. Alternatively, Kuijpers et al. (2007) suggested that ploughmarks on the West Greenland slope may have been formed by icebergs drifting south in a southward flowing counter current.

Ploughmarks on the continental shelf offshore of Umanak Fjord displayed the widest range of orientations of all sections within the study area, with a large amount of variability between individual blocks (Fig. 4.3). Although mean ploughmark orientation was N-S, not all icebergs had a northern component to drift. Ploughmarks in blocks 28 and 30 showed a mean orientation of N-S and a relatively tight distribution about the mean. A large number of N-S trending ploughmarks were also observed in block 34. In comparison, a number of ploughmarks in block 33 and blocks 35-41 were E-W trending (Fig. 4.3). However, these ploughmarks are not that apparent in the summary rose diagram for this section, because there are so few of them compared with the large number of observations from block 34. Blocks 35-41 displayed a much wider range of orientations in comparison to blocks 28-32, suggesting that in general ploughmark orientations became more uniform with distance across the shelf (Fig. 4.3).

The mean orientation for ploughmarks in the Umanak Fjord system was NNE-SSW (Fig. 4.4). Given the small number of observations from this section, the range of orientations was comparatively large. Block 43 showed a tighter distribution than block 45, with a mean orientation of NE-SW, whilst block 45 had a mean orientation of N-S (Fig. 4.3). However, icebergs in Umanak Fjord are unlikely to be drifting north, since they would just back up inside the fjord; presumably, then, the ploughmarks in blocks 43 and 45 were formed by icebergs drifting SW towards the fjord mouth.

### 4.2.2 Interpretation

Mean ploughmark orientation for the entire study area was approximately N-S (Fig. 4.4). This suggests that, in general, iceberg drift can be related to a circulation pattern corresponding to the northerly flowing WGC. However, as described above, not all icebergs had a northern component to drift. On the Umanak Shelf, for example, a number of ploughmarks in blocks 35-41 were oriented roughly E-W, whilst in Disko Bugt, ploughmarks in blocks 6-8 were mainly trending SW (Fig. 4.3). The drift tracks of individual icebergs are controlled largely by the prevailing current direction, and, to a lesser extent, by wind direction, waves and the bathymetry of the seafloor (Belderson et al., 1973; Belan et al., 2004). Variations in these factors may account, at least in part, for the wide range of ploughmark orientations observed across the study area. In the shallow waters of Disko Bugt, and across the inner continental shelf offshore of the Umanak Fjord system, large numbers of

small ploughmarks with mostly random orientations were observed. This may be explained by the fact that, in shallow areas, tidal flow tends to dominate over oceanic circulation, so that iceberg drift patterns in the shallow parts of these sections are more variable (Woodworth-Lynas et al., 1985). In contrast, ploughmarks on the deep outer shelf and continental slope displayed a more uniform orientation, with the majority of ploughmarks oriented approximately N-S (Fig. 4.3; Fig. 4.4). The small amount of variability observed for ploughmarks on the continental slope could be because these ploughmarks were formed by larger, deep-keeled icebergs, whose drift tracks were mainly influenced by the current direction. This would explain why ploughmark orientations became more uniform as water depth increased with distance across the shelf.

## 4.3 Iceberg Keel Depths

### 4.3.1 Observations

Iceberg ploughmarks were observed over a wide range of modern-day water depths within the study area, from ~140 m in Disko Bugt to a maximum depth of 1071 m on the continental slope (Table 4.2; Fig. 4.5; Fig. 4.6). The mean and median water depths for the entire study area were 457 m and 484 m respectively (Table 4.2; Fig. 4.6). The depths given are the average water depths at which ploughmarks occurred, as individual ploughmarks traversed bathymetric ranges of several to tens of metres.

| **SECTION** (Fig. 3.4) | **MEAN WATER DEPTH (m)** | **MEDIAN WATER DEPTH (m)** | **RANGE OF WATER DEPTHS (m)** |
|---|---|---|---|
| 1 Disko Bugt | 262 | 257 | 141 - 396 |
| 2 Disko Shelf | 447 | 416 | 272 - 910 |
| 3 Continental Slope | 934 | 918 | 771 - 1071 |
| 4 Umanak Shelf | 526 | 535 | 265 - 846 |
| 5 Umanak Fjord | 521 | 519 | 455 - 600 |

**Table 4.2**. Summary of the mean, median and range of modern-day water depths (in metres) at which ploughmarks occur for each section of the study area (sections located in Figure 3.4).

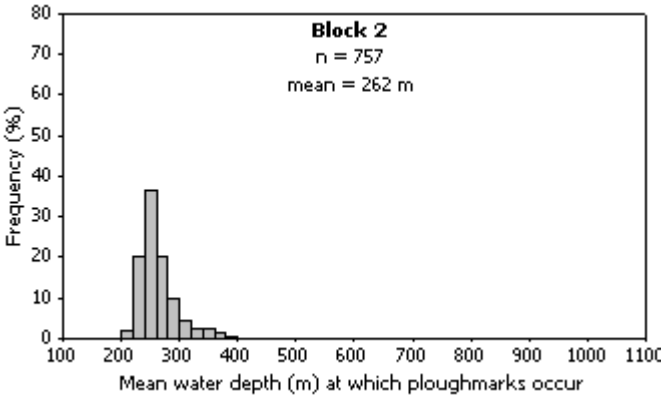
Block 2
n = 757
mean = 262 m
Frequency (%)
Mean water depth (m) at which ploughmarks occur

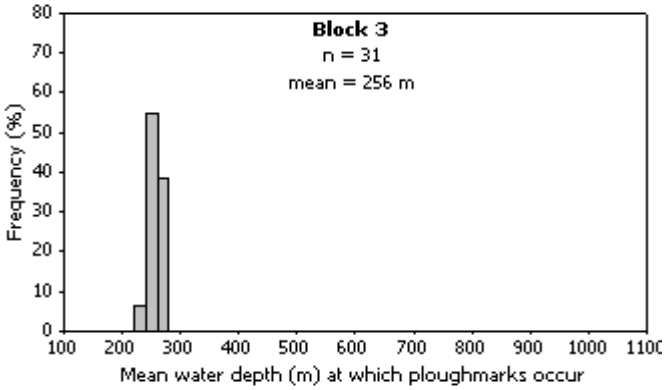
Block 3
n = 31
mean = 256 m
Frequency (%)
Mean water depth (m) at which ploughmarks occur

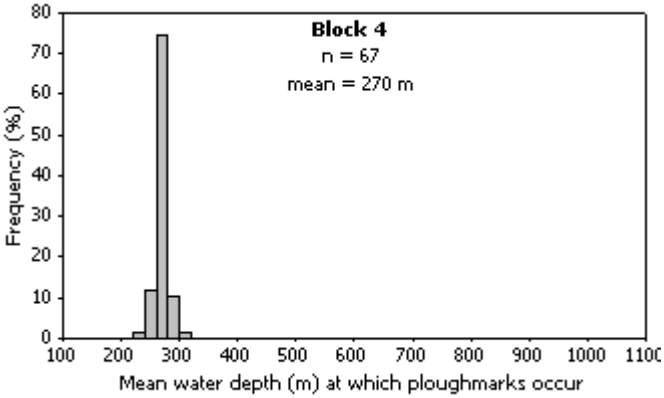
Block 4
n = 67
mean = 270 m
Frequency (%)
Mean water depth (m) at which ploughmarks occur

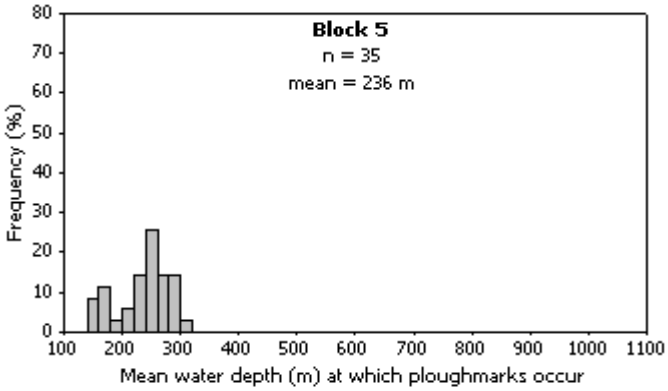
Block 5
n = 35
mean = 236 m
Frequency (%)
Mean water depth (m) at which ploughmarks occur

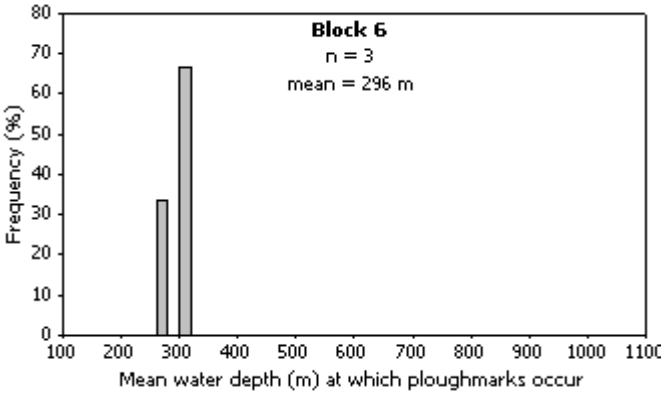
Block 6
n = 3
mean = 296 m
Frequency (%)
Mean water depth (m) at which ploughmarks occur

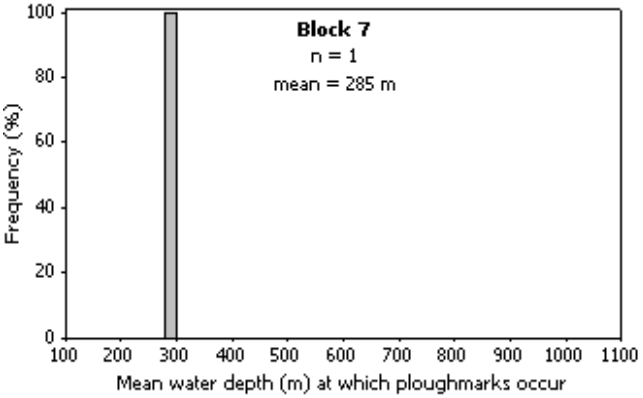
Block 7
n = 1
mean = 285 m
Frequency (%)
Mean water depth (m) at which ploughmarks occur

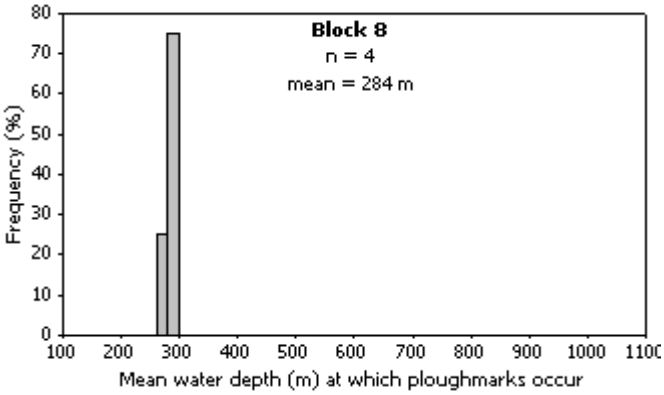
Block 8
n = 4
mean = 284 m
Frequency (%)
Mean water depth (m) at which ploughmarks occur

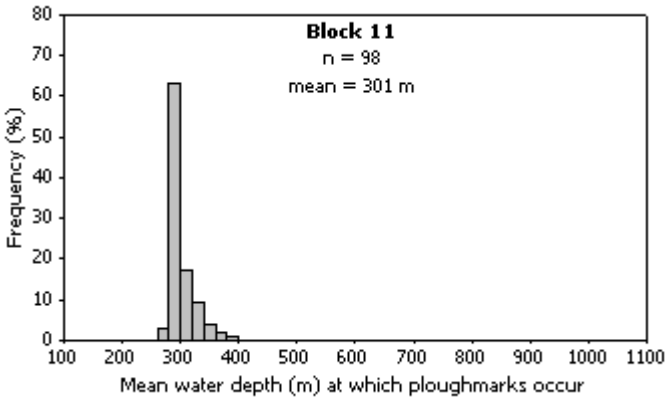
Block 11
n = 98
mean = 301 m
Frequency (%)
Mean water depth (m) at which ploughmarks occur

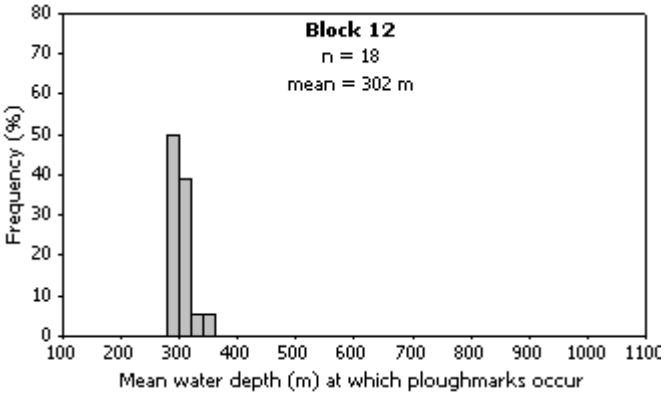
Block 12
n = 18
mean = 302 m
Frequency (%)
Mean water depth (m) at which ploughmarks occur

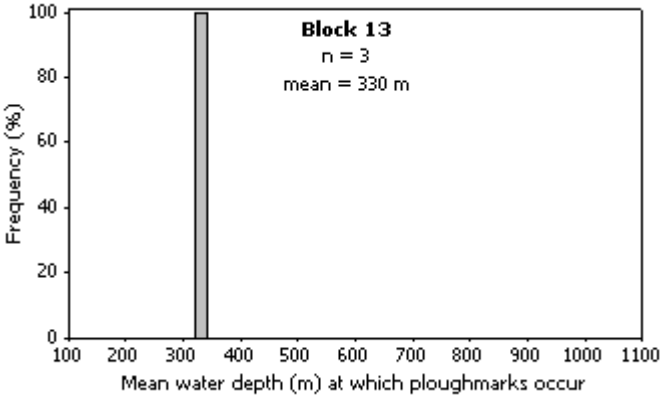
Block 13
n = 3
mean = 330 m
Frequency (%)
Mean water depth (m) at which ploughmarks occur

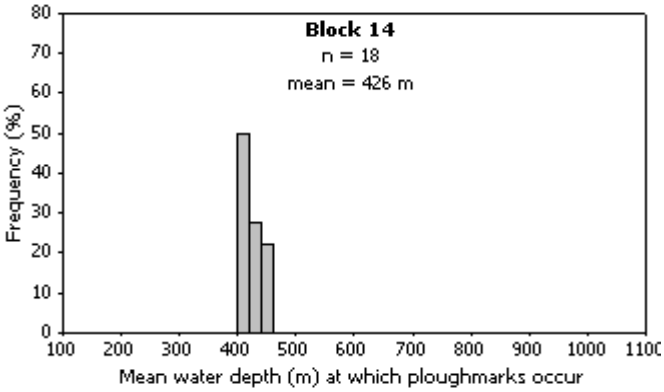
Block 14
n = 18
mean = 426 m
Frequency (%)
Mean water depth (m) at which ploughmarks occur

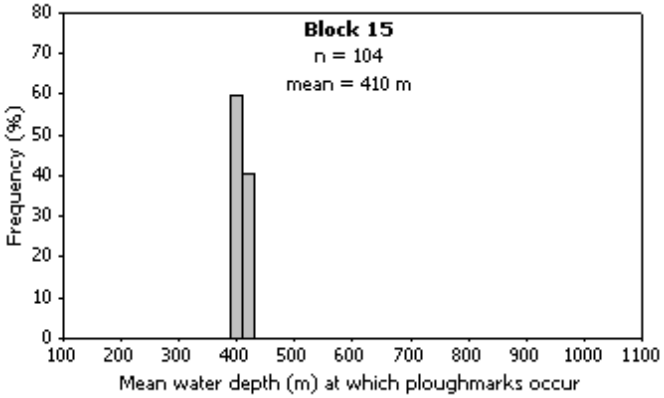
Block 15
n = 104
mean = 410 m
Frequency (%)
Mean water depth (m) at which ploughmarks occur

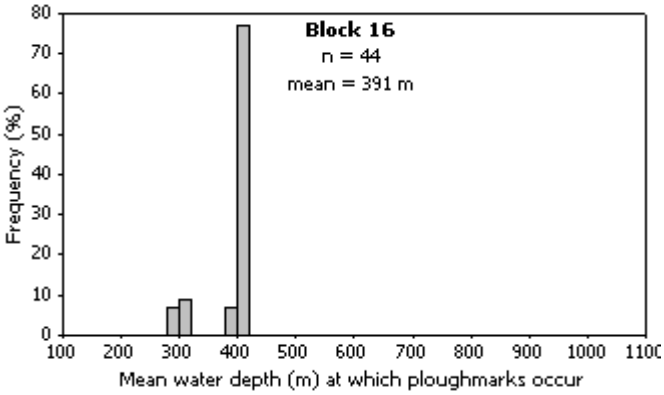
Block 16
n = 44
mean = 391 m
Frequency (%)
Mean water depth (m) at which ploughmarks occur

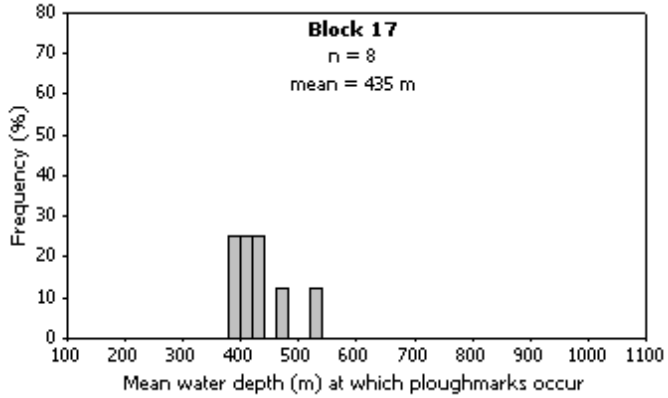
Block 17
n = 8
mean = 435 m
Frequency (%)
Mean water depth (m) at which ploughmarks occur

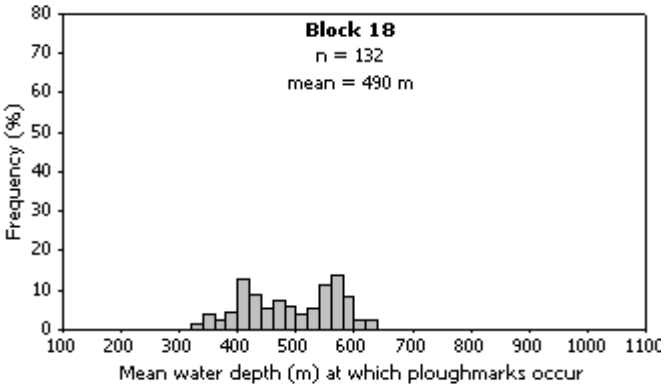
Block 18
n = 132
mean = 490 m
Frequency (%)
Mean water depth (m) at which ploughmarks occur

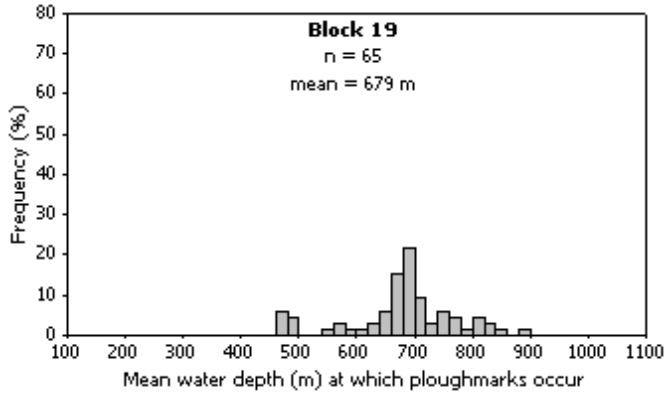
Block 19
n = 65
mean = 679 m
Frequency (%)
Mean water depth (m) at which ploughmarks occur

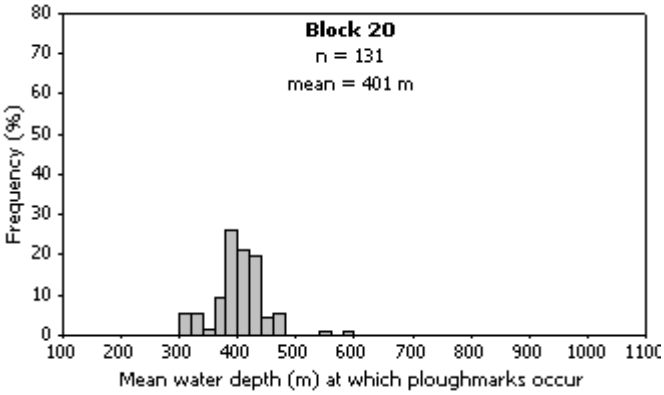
Block 20
n = 131
mean = 401 m
Frequency (%)
Mean water depth (m) at which ploughmarks occur

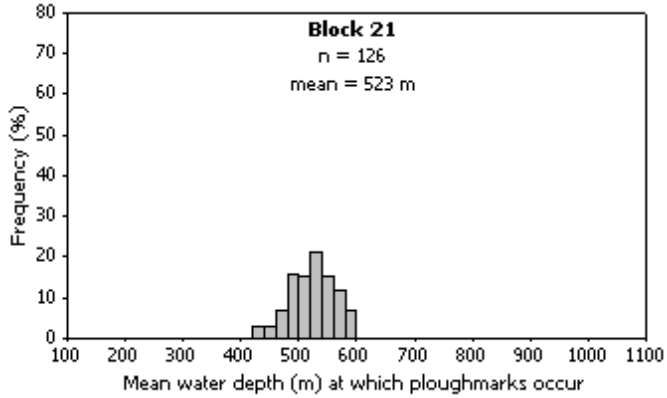
Block 21
n = 126
mean = 523 m
Frequency (%)
Mean water depth (m) at which ploughmarks occur

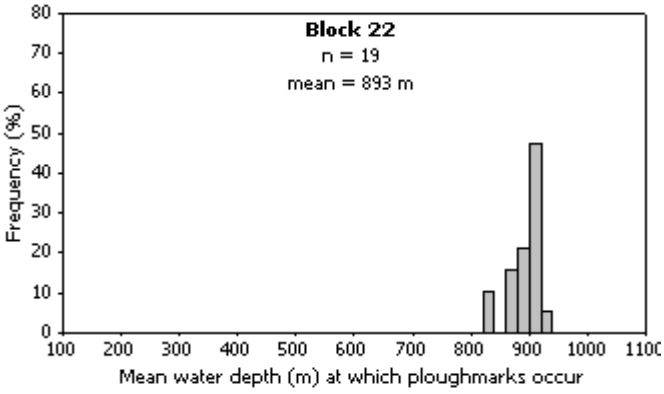
Block 22
n = 19
mean = 893 m
Frequency (%)
Mean water depth (m) at which ploughmarks occur

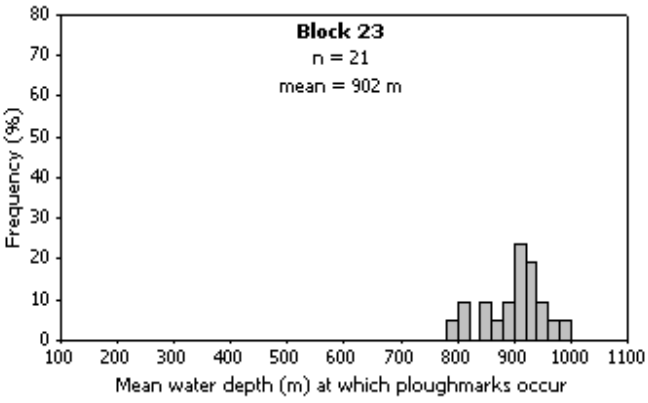
Block 23
n = 21
mean = 902 m
Frequency (%)
Mean water depth (m) at which ploughmarks occur

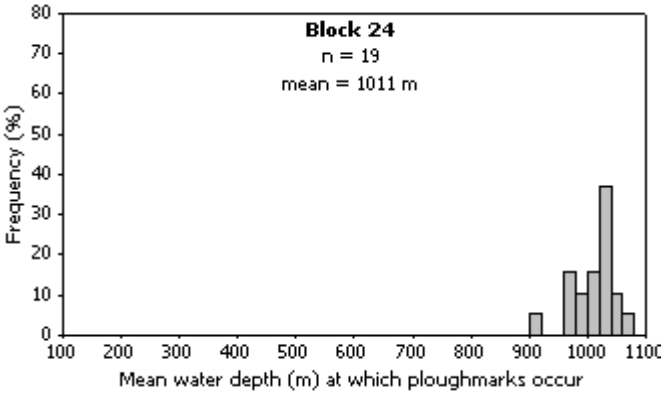
Block 24
n = 19
mean = 1011 m
Frequency (%)
Mean water depth (m) at which ploughmarks occur

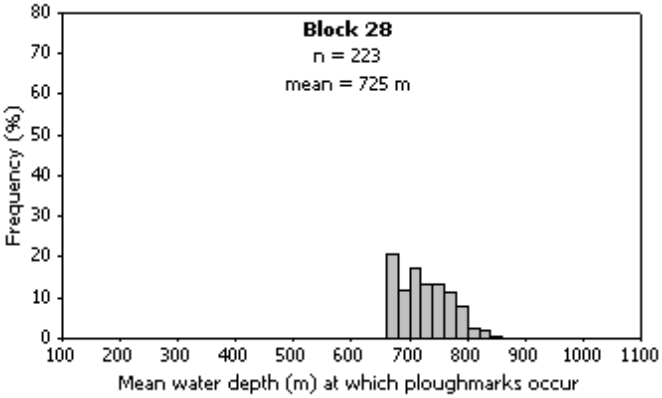
Block 28
n = 223
mean = 725 m
Frequency (%)
Mean water depth (m) at which ploughmarks occur

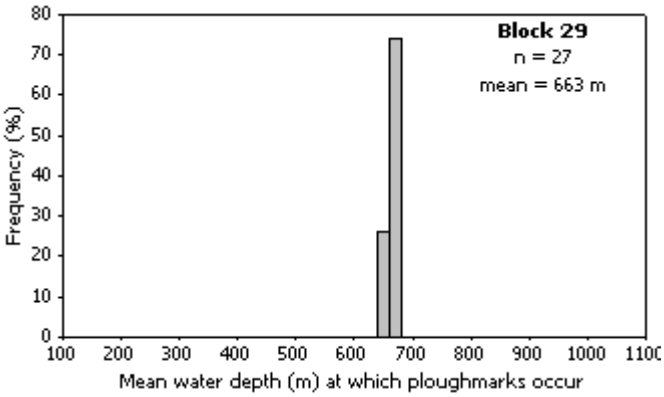
Block 29
n = 27
mean = 663 m
Frequency (%)
Mean water depth (m) at which ploughmarks occur

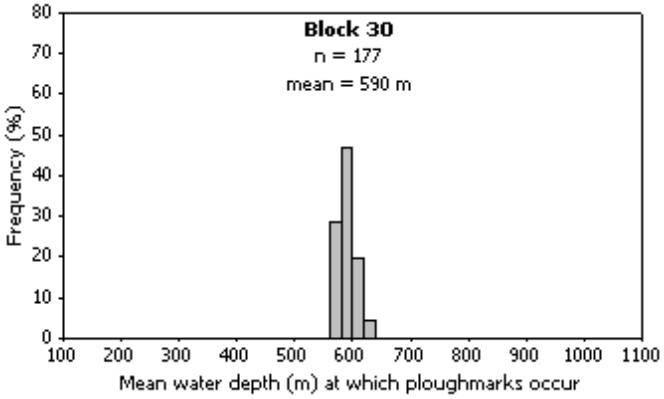
Block 30
n = 177
mean = 590 m
Frequency (%)
Mean water depth (m) at which ploughmarks occur

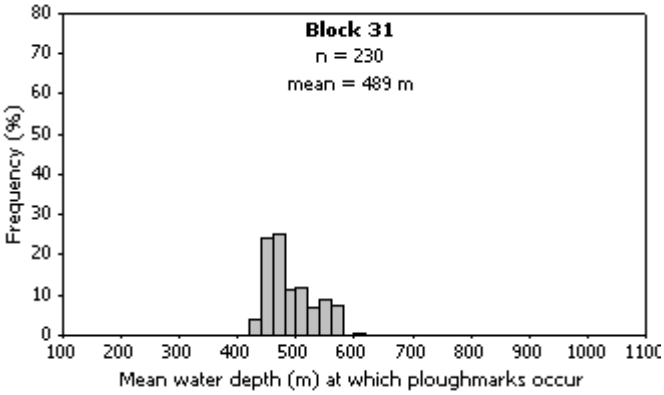
Block 31
n = 230
mean = 489 m
Frequency (%)
Mean water depth (m) at which ploughmarks occur

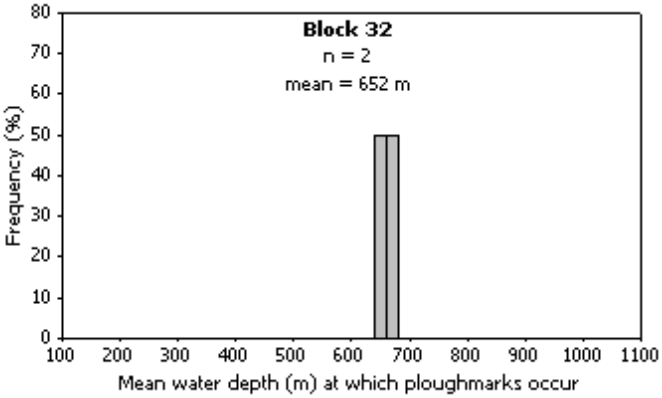
Block 32
n = 2
mean = 652 m
Frequency (%)
Mean water depth (m) at which ploughmarks occur

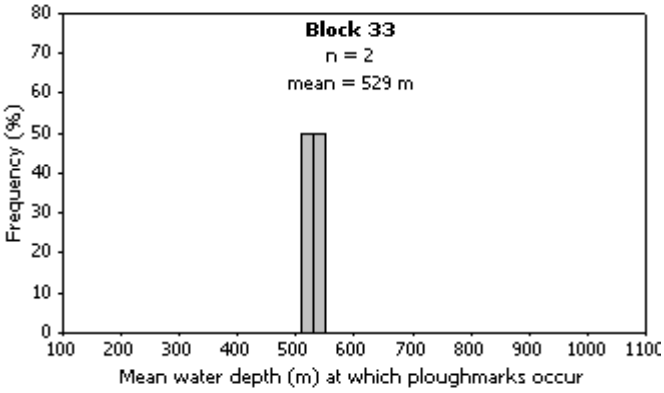
Block 33
n = 2
mean = 529 m
Frequency (%)
Mean water depth (m) at which ploughmarks occur

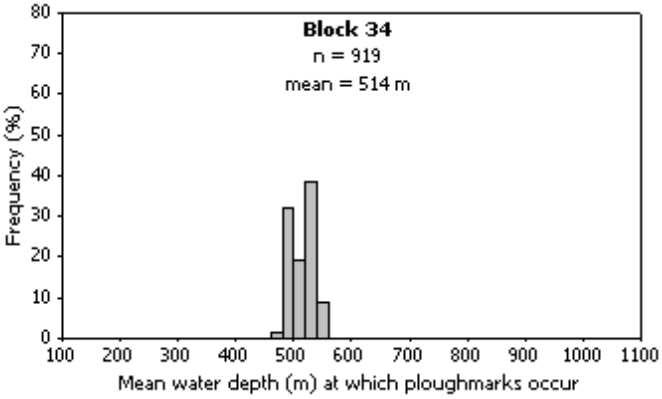
Block 34
n = 919
mean = 514 m
Frequency (%)
Mean water depth (m) at which ploughmarks occur

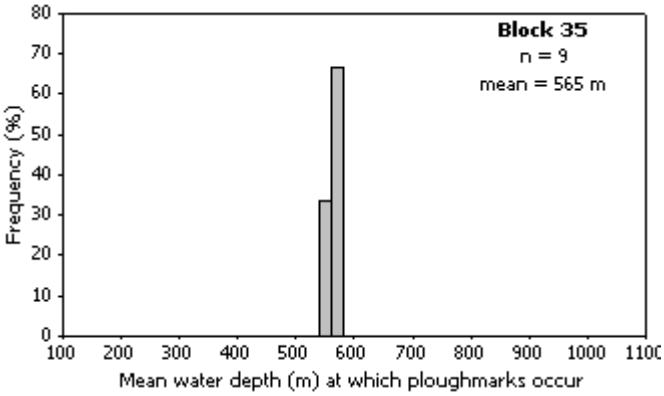
Block 35
n = 9
mean = 565 m
Frequency (%)
Mean water depth (m) at which ploughmarks occur

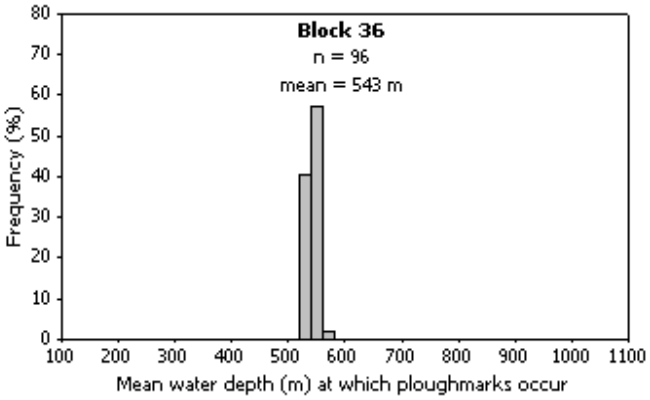
Block 36
n = 96
mean = 543 m
Frequency (%)
Mean water depth (m) at which ploughmarks occur

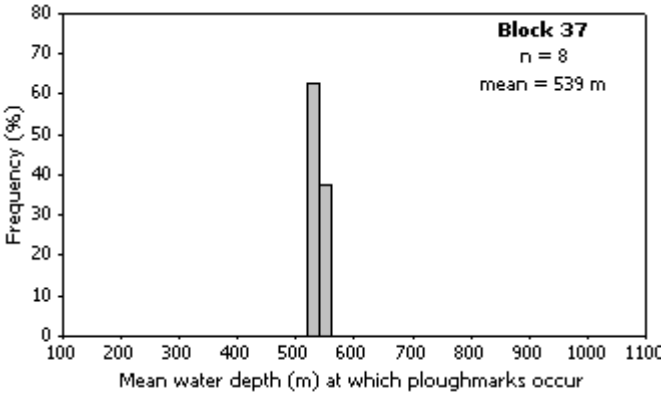
Block 37
n = 8
mean = 539 m
Frequency (%)
Mean water depth (m) at which ploughmarks occur

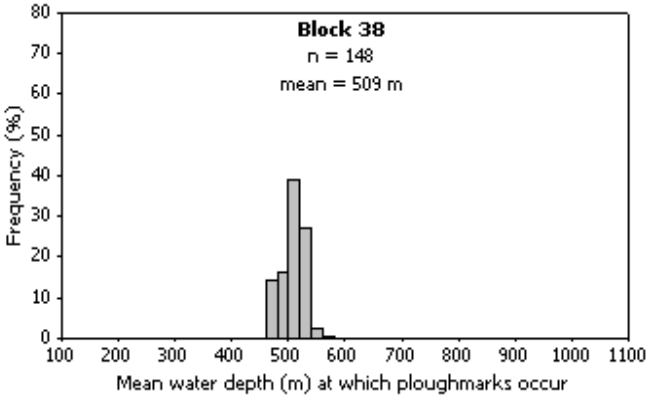
Block 38
n = 148
mean = 509 m
Frequency (%)
Mean water depth (m) at which ploughmarks occur

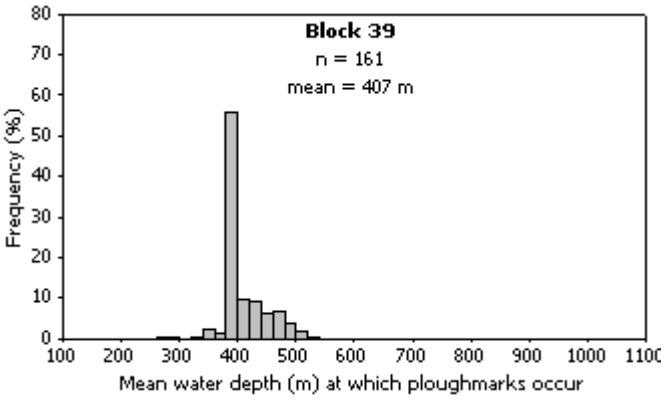
Block 39
n = 161
mean = 407 m
Frequency (%)
Mean water depth (m) at which ploughmarks occur

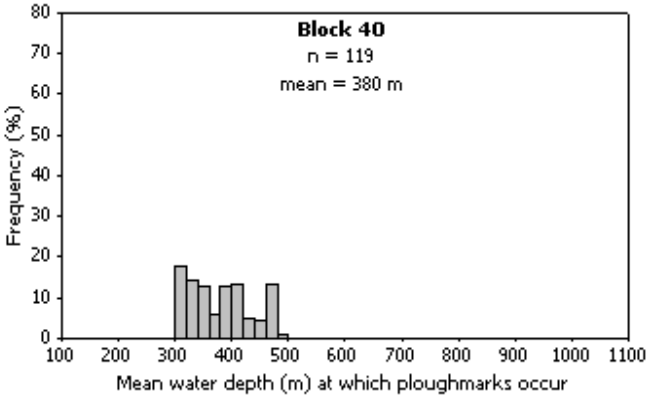
Block 40
n = 119
mean = 380 m
Frequency (%)
Mean water depth (m) at which ploughmarks occur

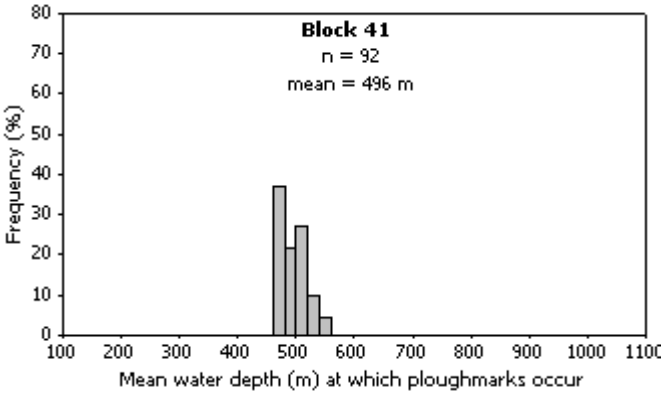
Block 41
n = 92
mean = 496 m
Frequency (%)
Mean water depth (m) at which ploughmarks occur

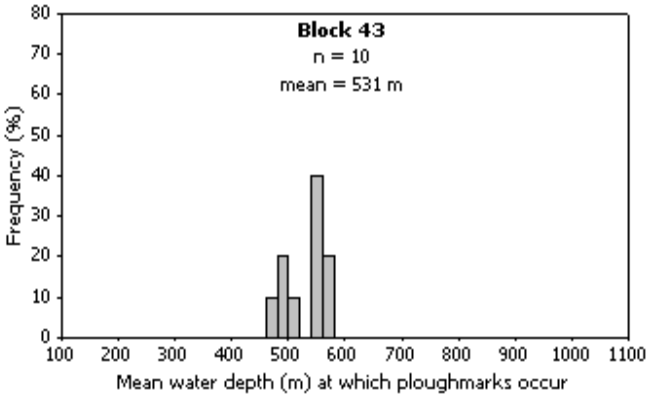
Block 43
n = 10
mean = 531 m
Frequency (%)
Mean water depth (m) at which ploughmarks occur

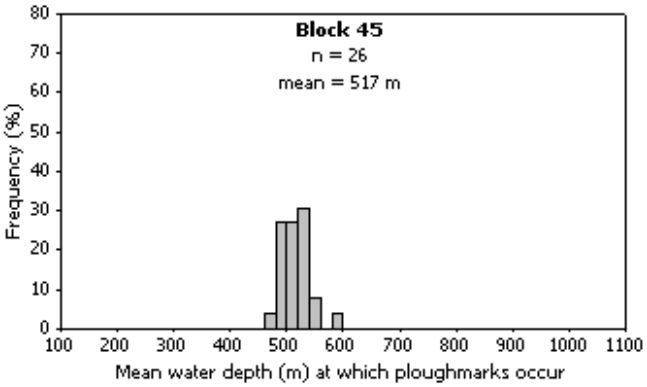


**Figure 4.5.** Histograms to show the mean water depth in metres at which ploughmarks occur for each block within the study area (blocks located in Figures 3.5 to 3.9). Blocks not illustrated contain no ploughmarks. Note that the histograms for Blocks 7 and 13 have a different vertical scale to the rest.

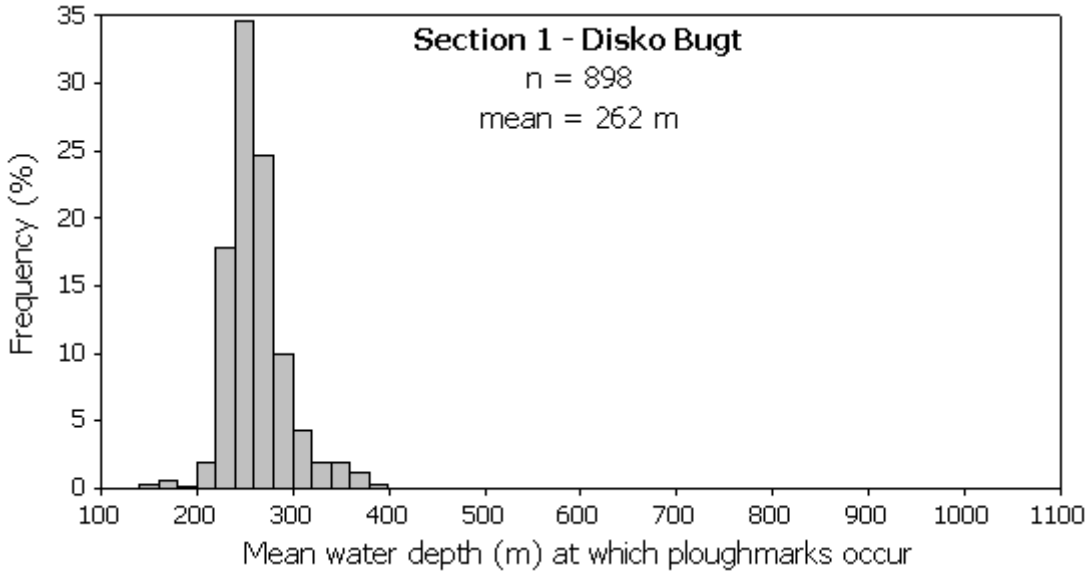


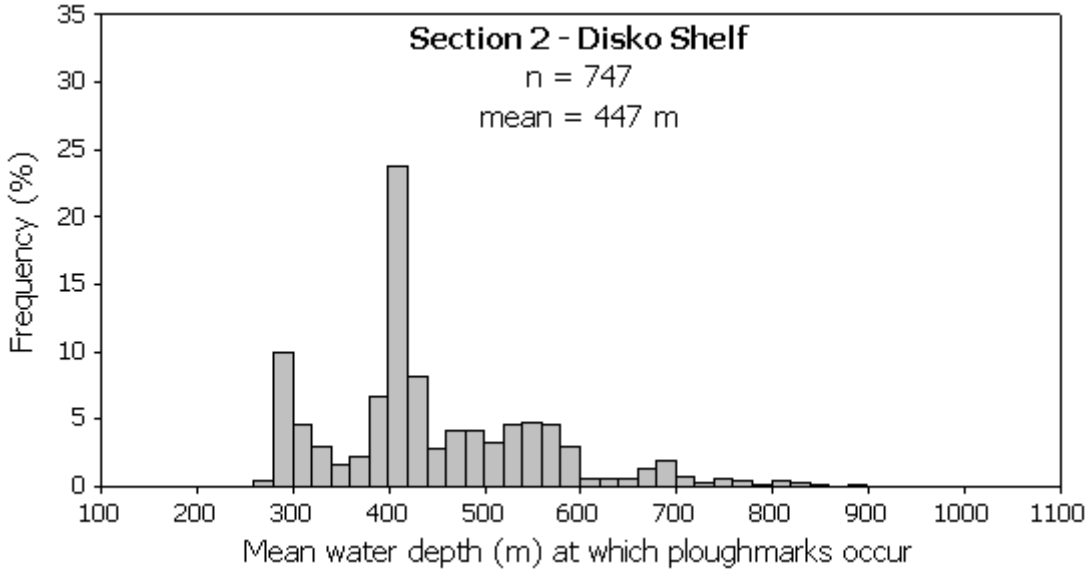

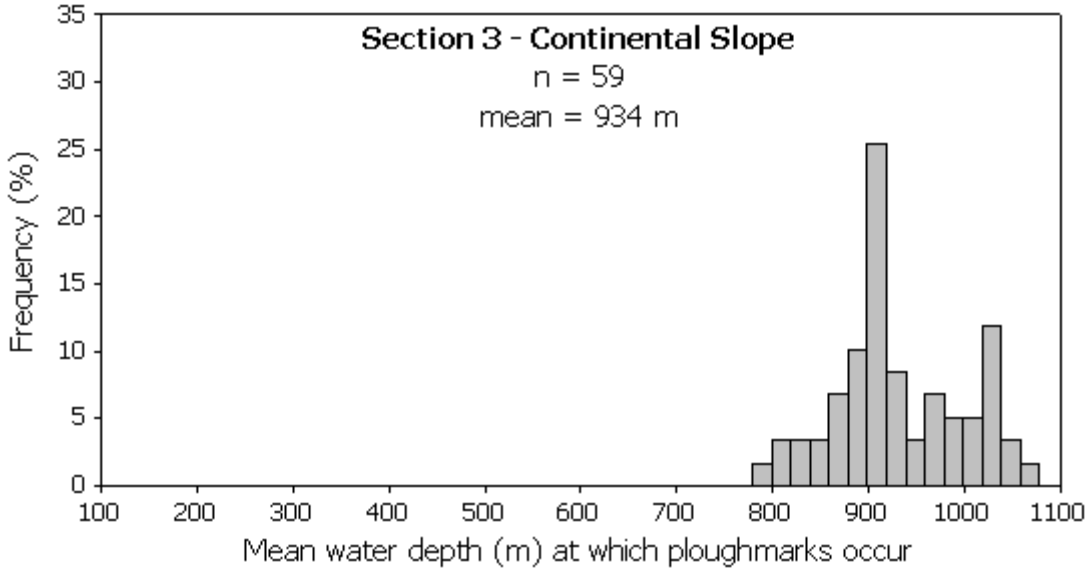
Section 3 - Continental Slope
n = 59
mean = 934 m
Frequency (%)
Mean water depth (m) at which ploughmarks occur

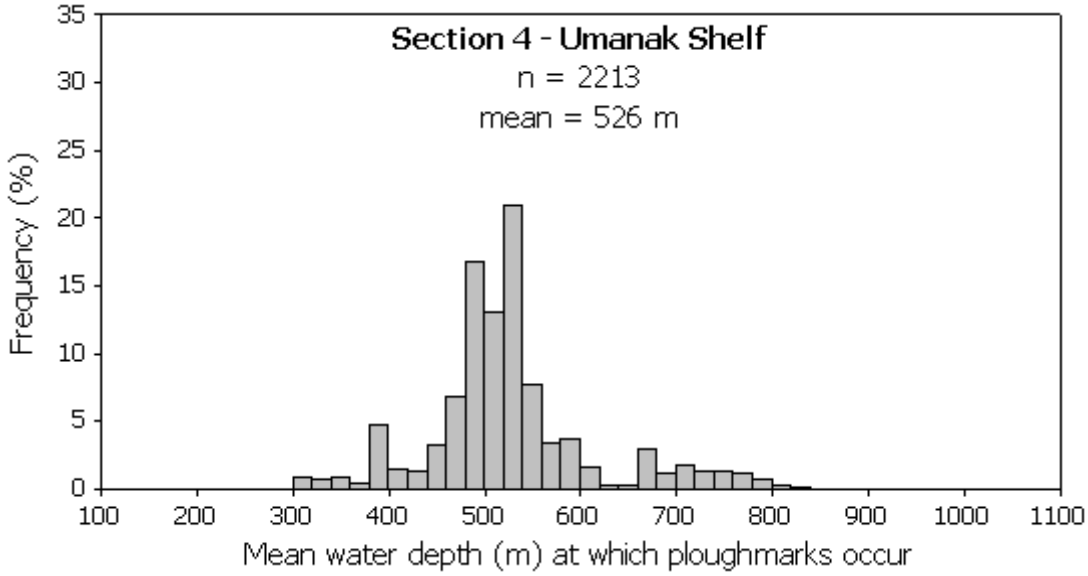
Section 4 - Umanak Shelf
n = 2213
mean = 526 m
Frequency (%)
Mean water depth (m) at which ploughmarks occur

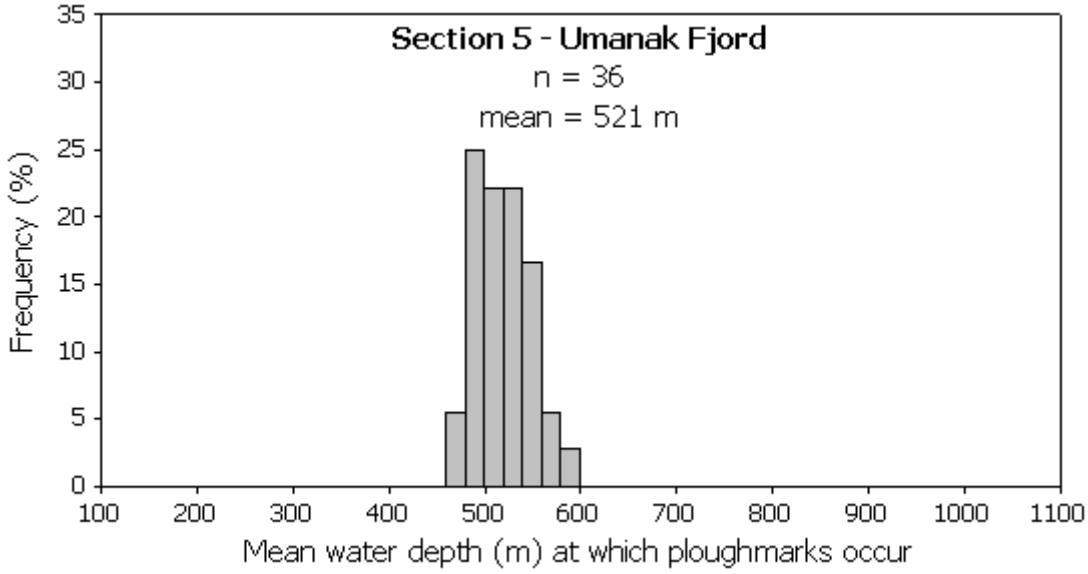
Section 5 - Umanak Fjord
n = 36
mean = 521 m
Frequency (%)
Mean water depth (m) at which ploughmarks occur

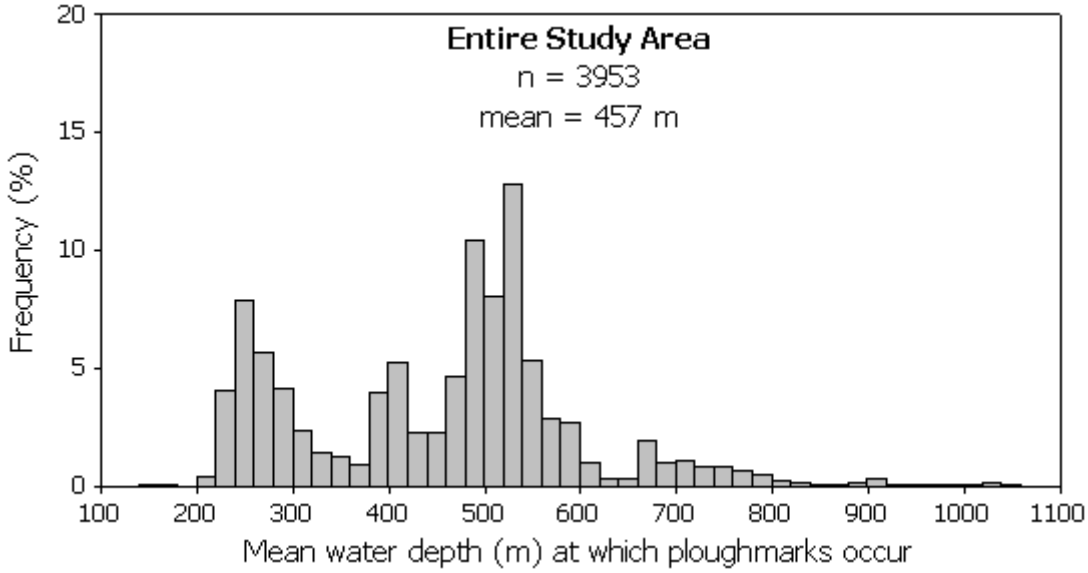


**Figure 4.6.** Histograms to shown the mean water depth in metres at which ploughmarks occur for each section within the study area (sections located in Figure 3.4). A histogram to summarise the mean water depth at which ploughmarks occur across the entire study area is also shown.

The mean water depth at which ploughmarks occurred in Disko Bugt was 262 m (Table 4.2; Fig 4.6). Depths displayed a relatively tight distribution about the mean, ranging from 141-396 m (Table 4.2). The same pattern of distribution was observed throughout Disko Bugt, with limited variation between individual blocks (Fig. 4.5). The large numbers of short ploughmarks observed at shallow water depths suggests that most ploughmarks were formed by icebergs with relatively small drafts. This makes sense, since the fjords that drain into Disko Bugt are fronted by shallow sills, which limit icebergs with keels deeper than ~350 m from entering the bay (Rignot et al., 2010). No ploughmarks were observed in blocks 1, 9 and 10, most likely because the water here is too deep for small icebergs to impact the seafloor.

On the continental shelf offshore of Disko Bugt, ploughmarks were observed over a much wider range of water depths, from 272 m, to a maximum depth of 910 m (Table 4.2). The wide spread of depths was distorted, however, by observations from block 19, which is at least partly on the continental slope. The mean water depth at which ploughmarks occurred was 447 m, but there was considerable variation between individual blocks (Fig. 4.5; Fig. 4.6). In general, the mean depth at which ploughmarks occurred increased with distance across the shelf (Fig. 4.5).

The mean water depth at which ploughmarks occurred on the continental slope was 934 m. Depths showed a relatively tight distribution about the mean, ranging from 771-1071 m (Table 4.2; Fig. 4.6). The same pattern of distribution was observed for blocks 22-24, with only a small amount of variability between individual blocks (Fig. 4.5). Ploughmarks were not observed in blocks 25-27; this is because, with depths well in excess of 1000 m, these areas are too deep for even the largest icebergs to form ploughmarks.

On the continental shelf offshore of the Umanak Fjord system, ploughmarks were observed over a wide range of water depths, from 265-846 m (Table 4.2). This wide range of depths was skewed by observations from block 28, which is located at least partly on the continental slope. The mean depth at which ploughmarks occurred within this section was 526 m (Table 4.2; Fig 4.6). Individual blocks displayed a tight distribution around the mean, but mean depth varied greatly between blocks (Fig. 4.5). In general, the mean water depth at which ploughmarks were observed increased with distance across the shelf.

The mean water depth at which ploughmarks occurred in the Umanak Fjord system was 521 m (Table 4.2; Fig. 4.6). Observations showed a comparatively tight distribution, with a range from 455-600 m (Table 4.2). A similar pattern of distribution was observed for blocks 43 and 45 (Fig 4.5). Very few ploughmarks were observed in this section, presumably because most parts of the fjord are too deep for modern icebergs to impact the seafloor (Fig. 3.9).

### 4.3.2 Interpretation

Relative and absolute sea level changes through time, but if we know what the relative sea-level was when the ploughmarks observed in this study were formed, then we can estimate the keel depths of the icebergs that carved these features. Greenland has a complex spatial and temporal sea-level history. Holocene emergence in most regions is generally less than 100 m relative to the present-day sea-level; Bitanja et al. (2005) proposed a maximum sea-level lowstand of 120 m in the Disko Bugt region. At present, outlet glaciers of the Greenland Ice Sheet produce icebergs with maximum keel depths of ~600 m (Dowdeswell et al., 1992). These drafts are not large enough to form ploughmarks at present-day water depths of up to ~1100 m; even assuming a relative sea-level lowstand of 120 m, much larger icebergs would be required to carve such features. Thus, ploughmarks at water depths in excess of about 600 m must be relict features, incised by deep-keeled palaeo-icebergs. Observations from present-

day ice margins suggest that icebergs with keel depths greater than ~600 m most likely originated from fast-flowing outlet glaciers in palaeo-ice sheets with a high mass flux (Dowdeswell et al., 1992; Dowdeswell and Bamber, 2007; Metz et al., 2008). The large-scale ploughmarks observed at water depths of up to 1071 m on the outer shelf and continental slope of central West Greenland were, therefore, most likely formed by icebergs derived from fast-flowing ice streams, at a time when the ice margin was grounded at or near the shelf break. Simpson et al. (2009) reconstructed ice sheet thickness on the West Greenland margin to ~900 m during the LGM. Assuming a relative sea-level lowstand of 120 m at this time, the ice sheet margin would have been approximately the right thickness to calve icebergs at present-day water depths in excess of 1000 m. In contrast, ploughmarks in Disko Bugt and the Umanak Fjord system are more likely to have been formed by icebergs calved from the present-day ice margin, since ploughmarks in these sections are only observed to a maximum water depth of ~600 m, which is thought to be the maximum keel depth of icebergs calved today from the margins of the Greenland Ice Sheet (Dowdewell et al., 1992).

## 4.4 Ploughmark Morphologies

A range of morphologies were observed for ploughmarks on the West Greenland margin. The ploughmarks were divided into four types, based on their morphology and distribution across the study area; these morphologies are described in more detail below.

### 4.4.1 Type I Ploughmarks

Type I ploughmarks are shallow depressions, with berms on either side of a narrow, v-shaped trough (Fig. 4.7). These features typically range from tens of metres to several kilometres long, with widths of 10-70 m at the seabed, depths of up to 5 m and berm heights in the order of 1 m. Type I ploughmarks were characterised by random orientations, which formed sinuous to criss-crossing patterns on the seafloor, reflecting the wandering drift tracks of individual icebergs. Such features were prevalent in water depths less than 200 m, but persisted to water depths of ~400 m on the West Greenland margin. Type I ploughmarks were mainly observed in Disko Bugt, and also in shallow waters on the inner continental shelf offshore of Disko Bugt and the Umanak Fjord system.

### 4.4.2 Type II Ploughmarks

Type II ploughmarks are shallow depressions flanked by small (1-2 m high) berms on either side of a u-shaped trough (Fig. 4.8). In general, these features display similar lengths to Type I ploughmarks, but their morphology is characterised by wide, flat-bottomed troughs, typically up to 100 m wide and ~10 m deep (Fig. 4.8b); this suggests that Type II ploughmarks were produced by large, wide-keeled tabular or flat-bottomed icebergs. A mega-scale Type II ploughmark was observed in block 35 on the Umanak Shelf. This ploughmark was at least 20.81 km in length, ~300 m wide and with a crest-to-trough depth of approximately 20 m (Fig. 4.9). Comparable features have been described from the Yermak Plateau by Gebhardt et al. (2011) and interpreted as ploughmarks formed by the keels of large, deep-keeled tabular icebergs. Type II ploughmarks occurred over a wide bathymetric range on the continental shelf and slope of central West Greenland, but were more common at water depths in excess of ~300 m. Sets of Type II ploughmarks were also observed to trend parallel to each other over distances of up to several kilometres (Fig. 4.10); such features were most likely formed by large, multiple-keeled icebergs derived from fast-flowing outlet glaciers of the Greenland Ice Sheet (Dowdeswell et al., 2010c).

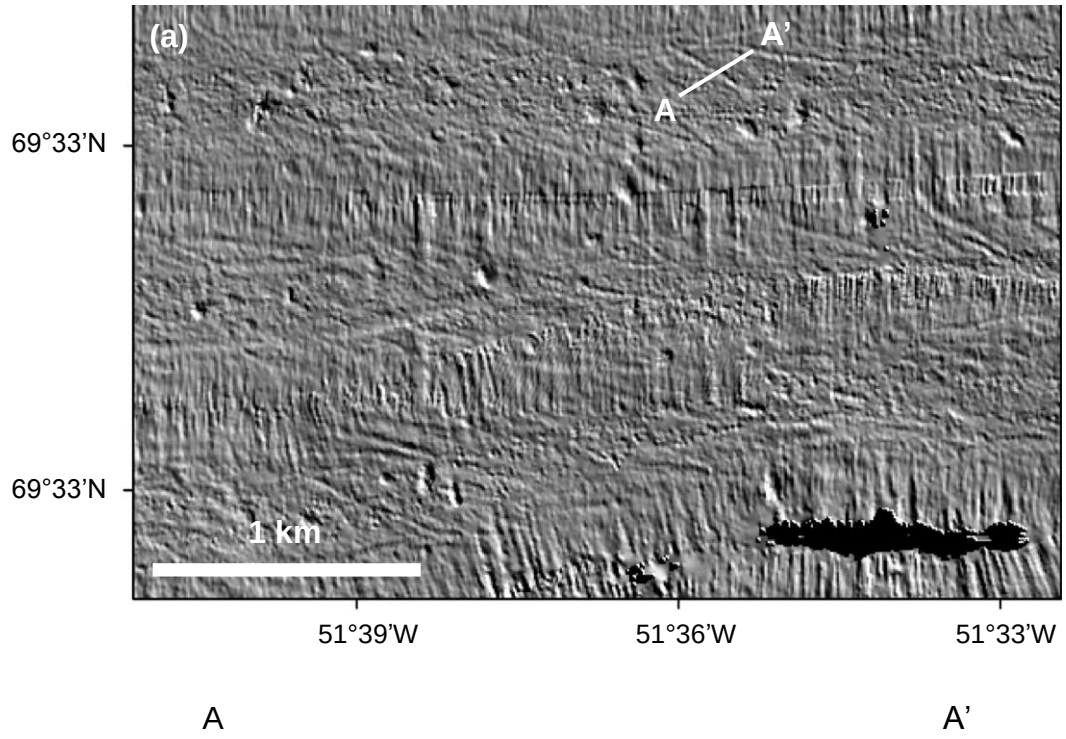

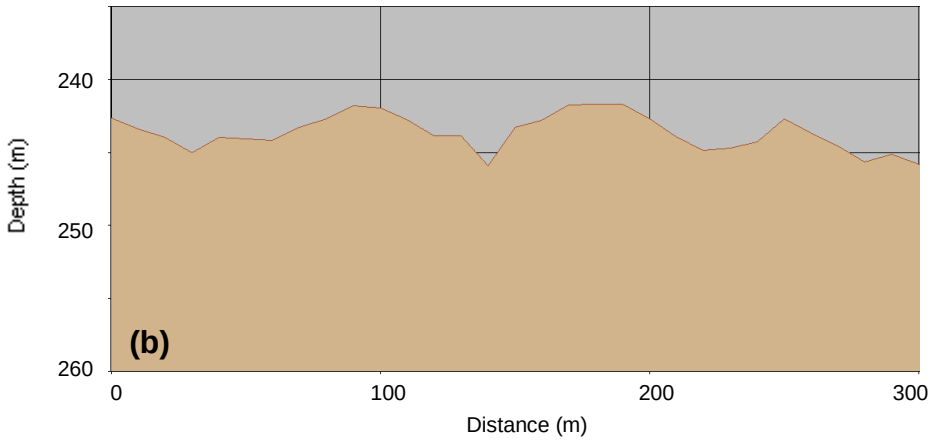


**Figure 4.7. (a)** Greyscale sun-shaded relief image of Type I ploughmarks within Disko Bugt (located in Fig. 3.4; illumination from the west; data gridded at 10 m) and **(b)** Bathymetric profile across the transect A-A'.

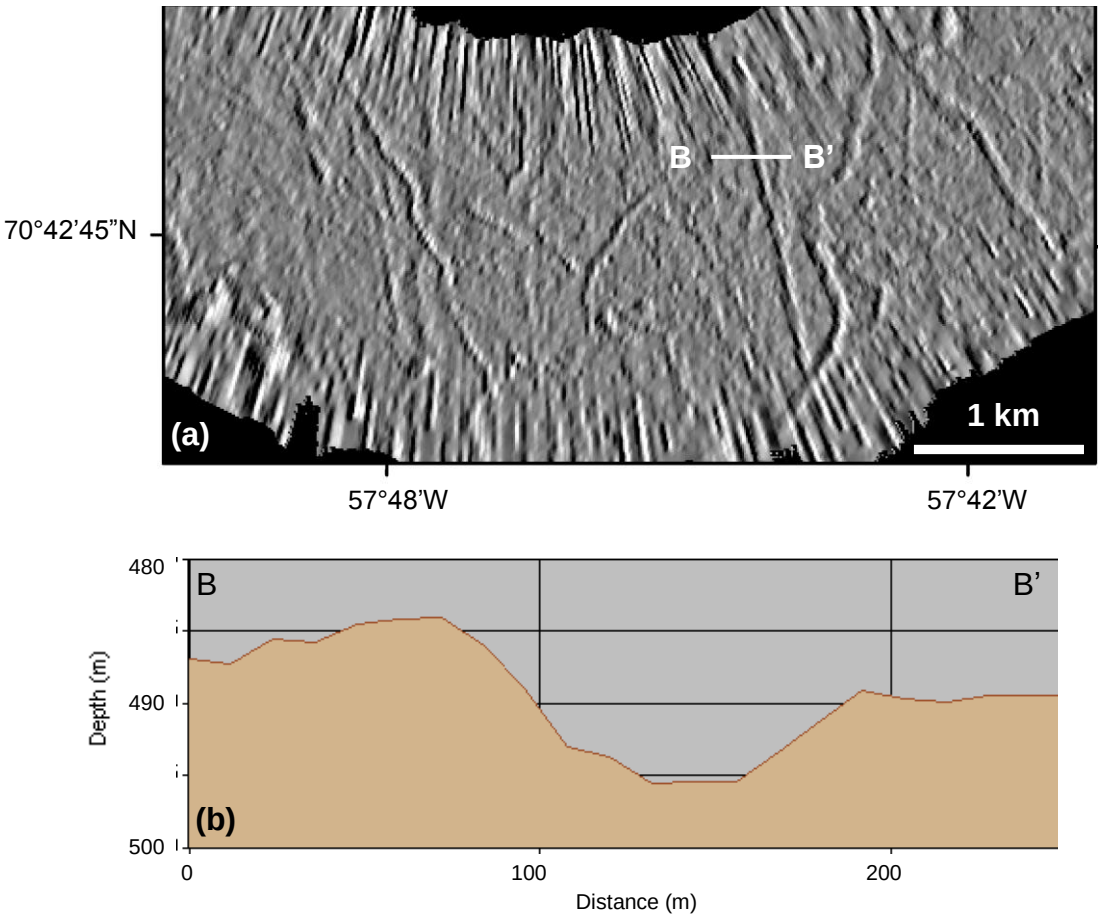


**Figure 4.8. (a)** Greyscale sun-shaded relief image of prominent Type II ploughmarks on the mid-outer continental shelf offshore of the Umanak Fjord system (located in Fig. 3.4; illumination from the west; data gridded at 12 m) and **(b)** Bathymetric profile across the transect B-B'.

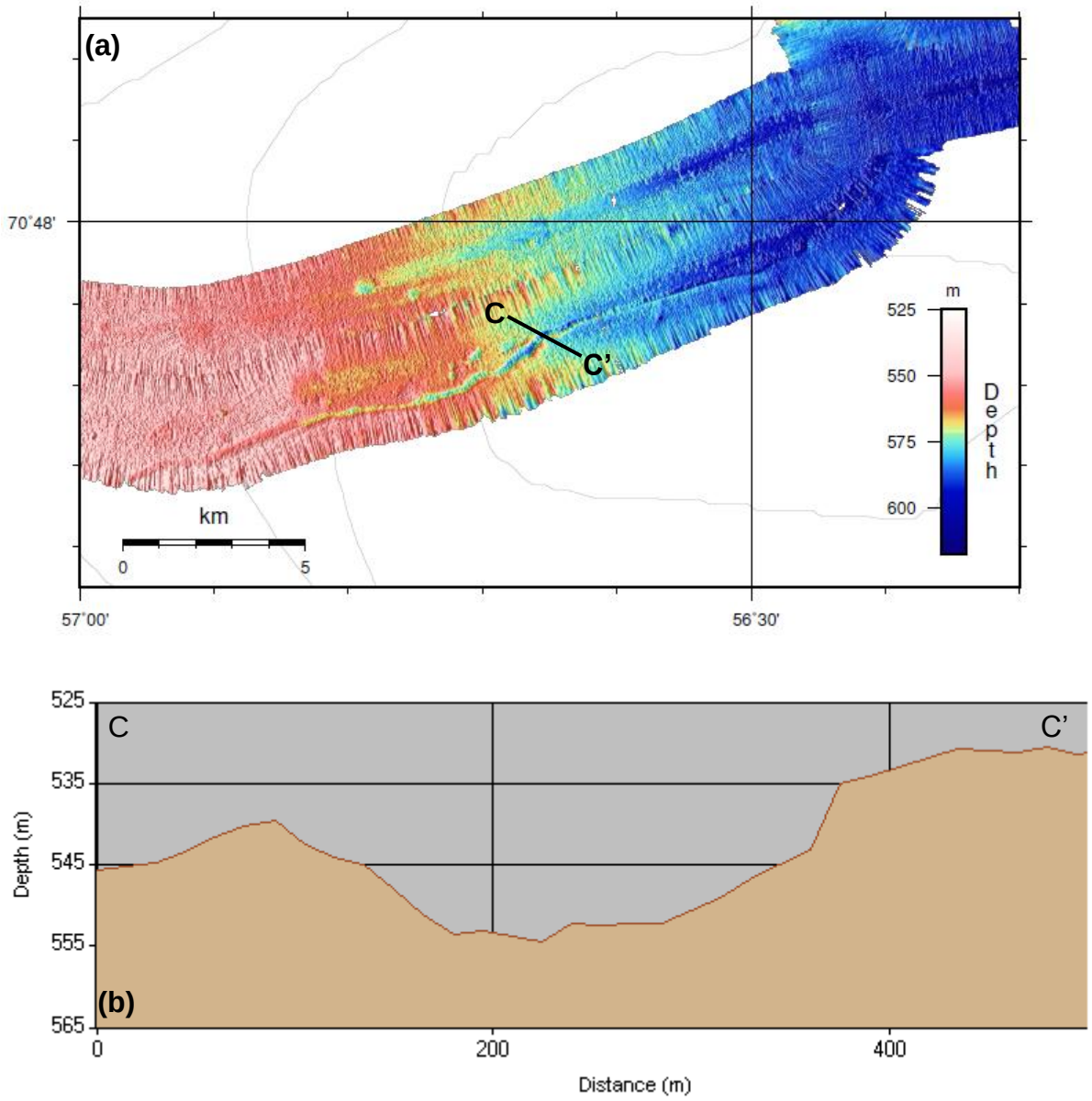


**Figure 4.9. (a)** Swath-bathymetric image of the mega-scale Type II ploughmark observed on the mid-Umanak Shelf (located in Fig. 3.4; data gridded at 15 m) and **(b)** Bathymetric profile across the transect C-C'.

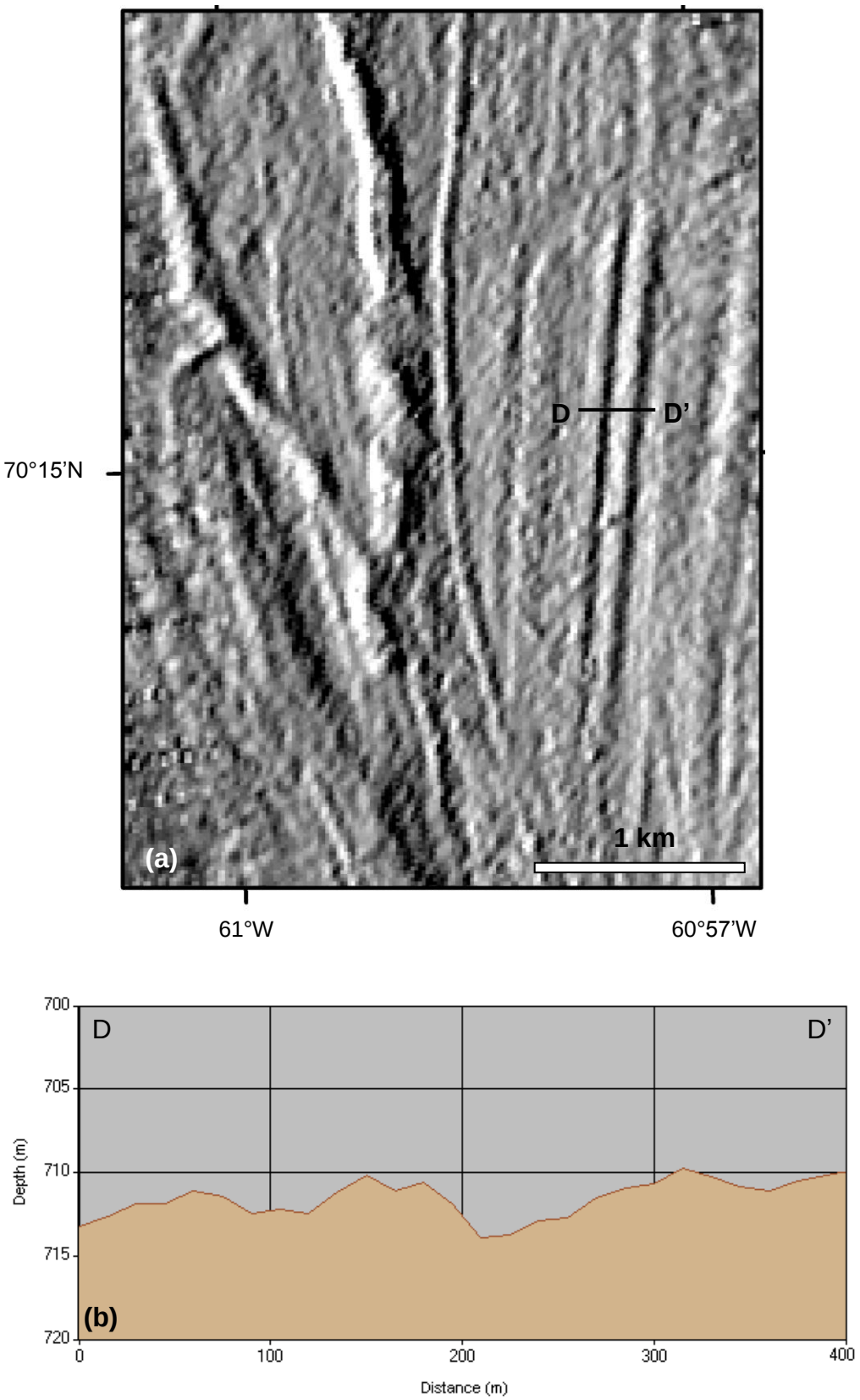


**Figure 4.10. (a)** Greyscale sun-shaded relief image of parallel Type II ploughmarks on the outer shelf/slope break offshore of the Umanak Fjord system (located in Fig 3.4; illumination from the east; data gridded at 15 m) and **(b)** Bathymetric profile across the transect D-D'.

### 4.4.3 Type III Ploughmarks

Type III ploughmarks are large, quasi-linear depressions, up to 15 km in length, ~700 m wide and 40 m deep (Fig. 4.11). The majority of Type III ploughmarks observed in this study formed sets of aligned furrows, located parallel to one another over distances of several to tens of kilometres (Fig. 4.11; 4.12).

On the West Greenland margin, Type III ploughmarks were observed only on the continental slope, at water depths between ~800-1070 m (Fig. 4.12). They displayed a more uniform orientation than Type I and II features, with a mean orientation of N-S, parallel to the slope. Comparable features have been reported from the West Greenland margin by Kuijpers et al. (2007). They documented large erosional features, up to 750 m wide, and 40 m deep, occurring at water depths between 800 m and 1085 m on the continental slope (Fig. 4.13; for location, see Fig. 4.12). These features were interpreted as giant ploughmarks, most likely carved by deep-draft icebergs derived from a fast-flowing palaeo-ice stream in the Disko region.

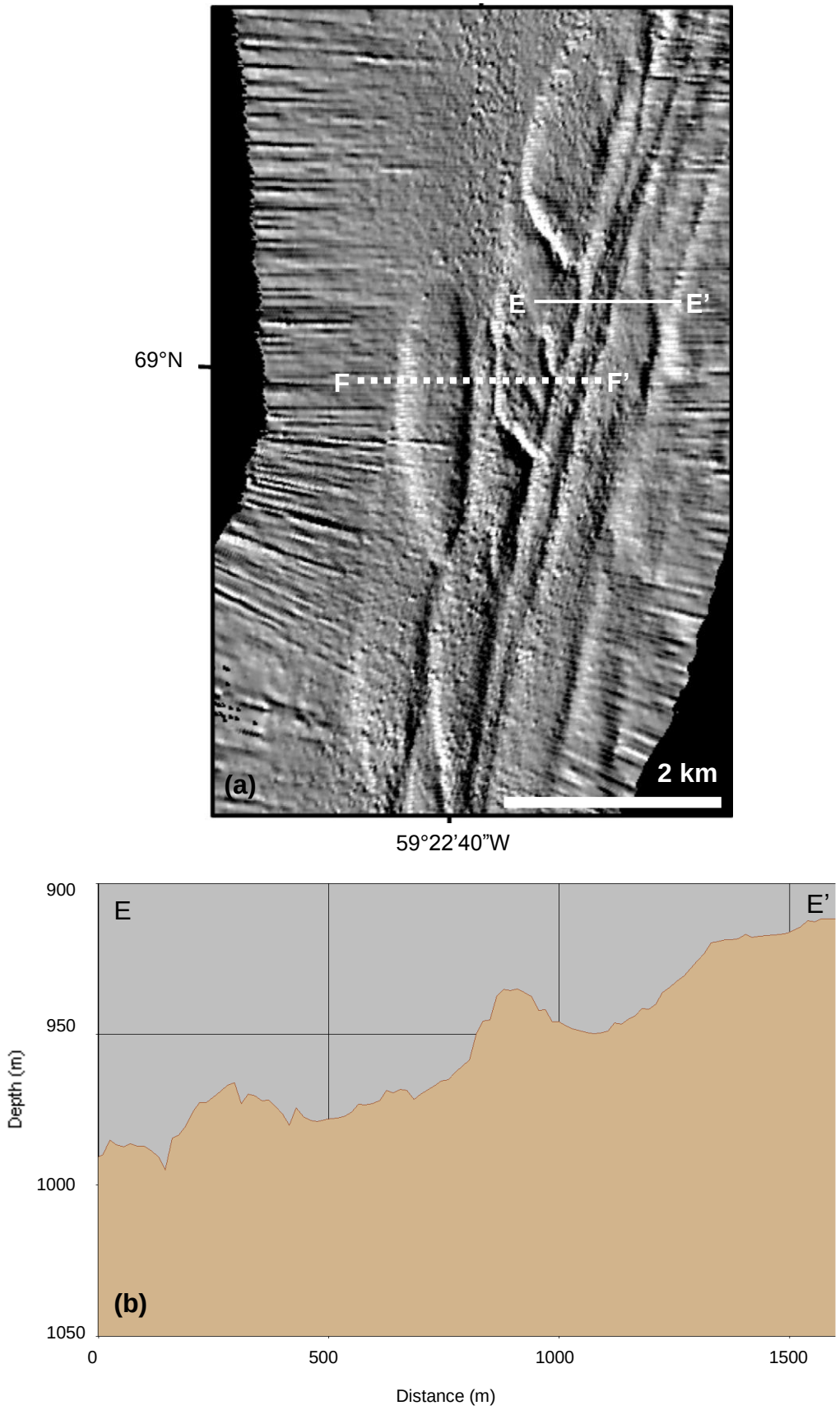


**Figure 4.11. (a)** Greyscale sun-shaded relief image of Type III ploughmarks on the West Greenland continental slope (located in Fig. 3.4; illumination from the east, data gridded at 15 m). Transect F-F'

shows the location of the slope transect investigated by Kuijpers et al. (2007). **(b)** Bathymetric profile across the transect E-E'.

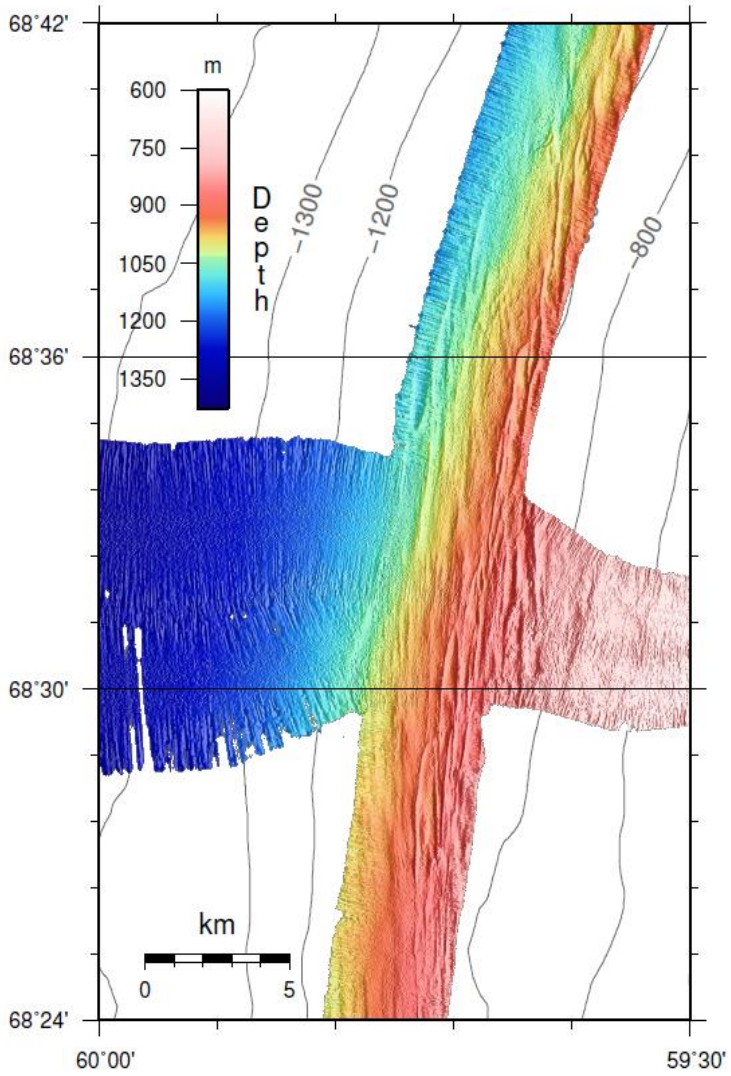


**Figure 4.12.** Swath-bathymetric image of Type III ploughmarks on the West Greenland continental slope (located in Fig. 3.4; data gridded at 50 m).

### 4.4.4 Grounding Pits

A fourth ploughmark morphology observed on the West Greenland margin is that of iceberg grounding pits, which appear on swath-bathymetric imagery as circular or semi-circular depressions in the seafloor (Fig. 4.14; Syvitski et al., 2001). These features are formed by semi-grounded icebergs, which, through the influence of ocean waves, tides and storm surges, can impact the seafloor in different location and create pits (Syvitski et al., 2001). Grounding pits typically range from 50-100 m wide and 10-15 m deep (Fig. 4.14b); on the West Greenland margin, the largest grounding pit observed was ~650 m wide. Grounding pits

were observed over a range of water depths, from 140 m, to a maximum depth of 670 m, and occurred alongside both Type I and Type II ploughmarks.

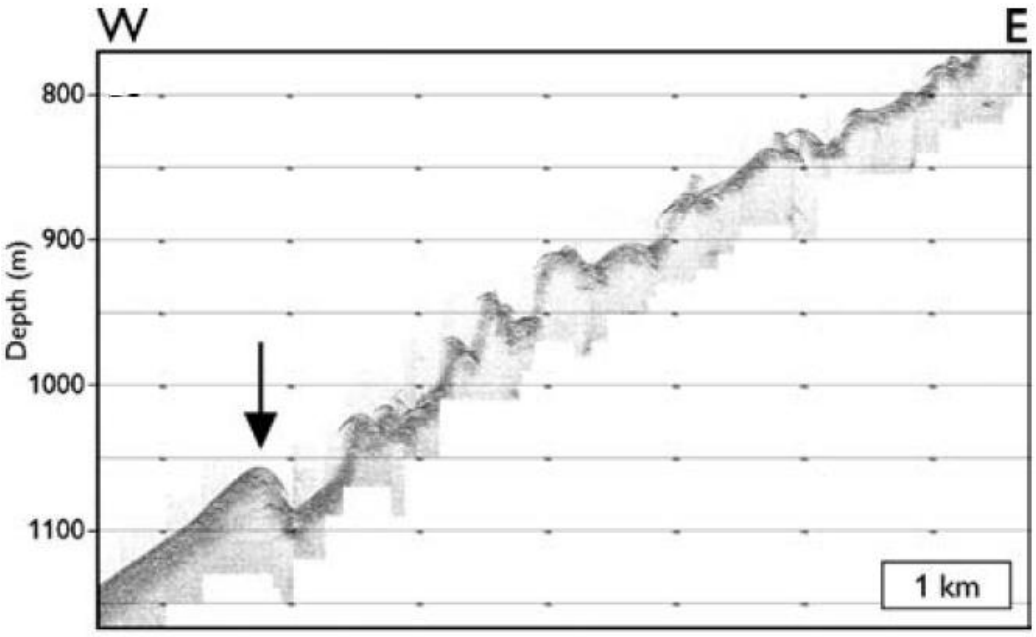


**Figure 4.13.** Sub-bottom profiler record from the 2006 cruise of R/V Dana to central West Greenland and Baffin Bay (for location, see Fig. 4.12). The profile shows an irregular and hummocky seabed topography with prominent erosional features at water depths of less than ~1100 m. The arrow marks the lower limit of iceberg ploughmarks (from Kuijpers et al., 2007).

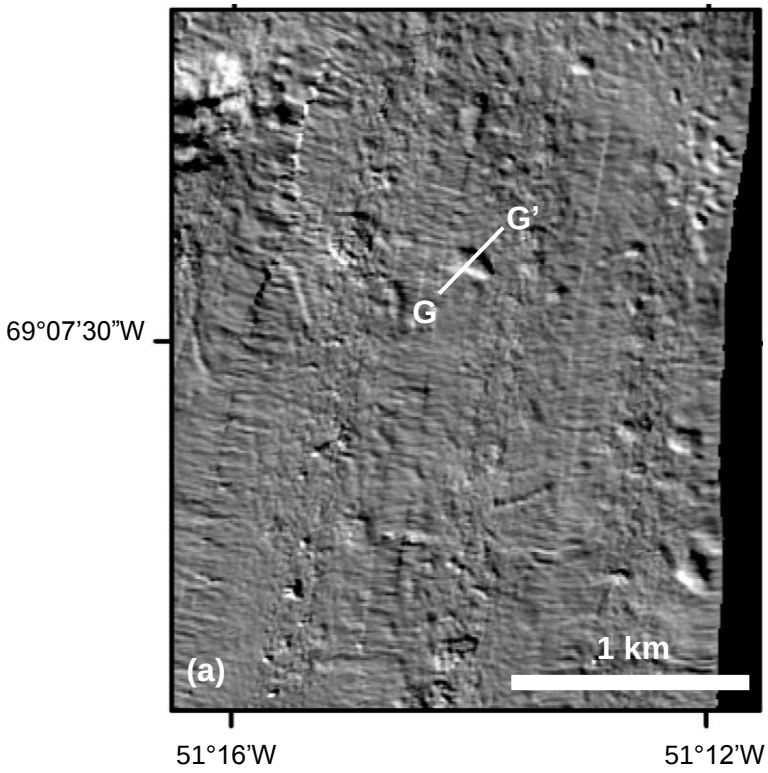

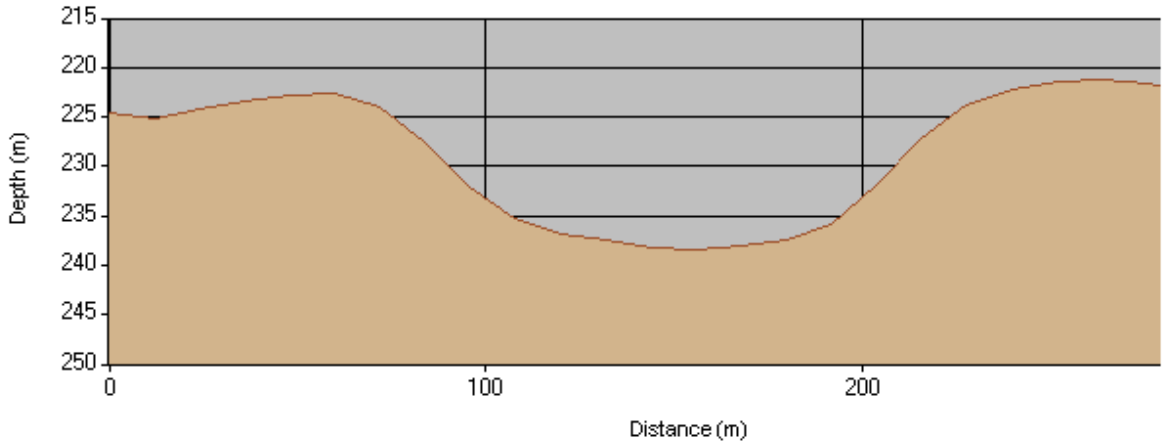


**Figure 4.14. (a)** Greyscale sun-shaded relief image of iceberg grounding pits in Disko Bugt (located in Fig. 3.4; illumination from the northwest; data gridded at 15m). Note that Type I ploughmarks can also be observed. **(b)** Bathymetric profile across the transect G-G'.

## 4.5 Ploughmark Distribution

A large number of ploughmarks with a wide range of dimensions, orientations and morphologies have been observed from the study area. In this section, the distribution of these ploughmarks on the West Greenland margin is oulined and mapped in Figures 4.15-4.19.

In Disko Bugt, a large number of Type I ploughmarks were observed in water depths of less than 400 m (Fig. 4.15). Several grounding pits, with widths of up to ~150 m, occurred alongside Type I ploughmarks in shallow (>200 m) regions of the bay (Fig 4.15). Very few Type II ploughmarks were observed; presumably, the larger, wide-keeled or tabular icebergs required to carve such features are prevented from entering Disko Bugt due to the presence of shallow sills at the mouths of fjord systems, which prevent icebergs with keels deeper than ~300 m from exiting the fjords (Rignot et al., 2010).

As shown in Fig. 4.15, the intensity of iceberg ploughing in Disko Bugt was inversely proportional to water depth. Accordingly, a high proportion of Type I ploughmarks were observed in the most shallow regions of the bay (blocks 2-5; Fig. 3.5; Fig 4.15). Few ploughmarks were observed in blocks 6-8, since average water depth in these blocks increased with distance towards Egededesminde Dyb at the western exit of the bay. Likewise, no ploughmarks were observed in block 1, since this block is located at the southeastern

entrance to the Vaigat Strait, where average water depth is approximately 600 m (Fig. 3.5; Fig. 4.15).

Three distinct patterns of ploughmark distribution were observed for the continental shelf and slope offshore of Disko Bugt (Fig. 4.16; Fig. 4.17). Type I ploughmarks were prevalent in shallow (>400) waters on the inner shelf, with a comparatively large number of ploughmarks observed for block 11 (Fig. 4.16). The intensity of iceberg ploughing in this block is likely due to the presence of a basalt escarpement, which forms a threshold with depths of 200-300 m below present-day sea-level. It is presumed that that this threshold does not allow icebergs with drafts greater than ~300 m to pass (Weidick and Bennike, 2007). On the middle-outer Disko Shelf, Type II ploughmarks were observed in large numbers at water depths in excess of ~350 m (Fig. 4.16). In general, the intensity of iceberg ploughing increased with distance across the shelf, and was greatest towards the continental shelf/slope break (Fig. 4.16). Since the basalt escarpement prevents icebergs with drafts deeper than 300 m from exiting inner Egedesminde Dyb, it is thought that ploughmarks on the outer shelf were formed at a time when the ice margin advanced beyond this threshold (Weidick and Bennike, 2007). On the continental slope offshore of the Disko region, ploughmark distribution was characterised by relatively few, large-scale (Type III) features, at water depths of up to ~1100 m. A number of large Type II ploughmarks were also observed; these persisted to water depths of around 800 m (Fig. 3.7; Fig. 4.17).

The distribution of ploughmarks on the continental shelf offshore of the Umanak Fjord system was highly variable. A large number of Type II ploughmarks were observed in block 28, towards the shelf/slope break. Comparatively few ploughmarks, however, were observed across the main swath transect on the outer shelf, although intense ploughing of seafloor sediments was noted for blocks 30-31, presumably since the mean water depth in these blocks was slightly less than that observed for adjacent blocks (Fig. 3.8; Fig. 4.18).

The largest number of ploughmarks on the Umanak Shelf was observed in block 34, which represents the most intensely ploughed region of the entire study area (Fig. 4.18; Fig. 4.19). Type II ploughmarks were prevalent, although Type I features and grounding pits were also observed. The ploughmarks in this block were superimposed on a large grounding-zone wedge (Fig. 4.19; K. Hogan, pers. comm.). A grounding-zone wedge (GZW) indicates a major still-stand in the ice margin position during general deglaciation (e.g. Dowdeswell et

al., 2008), and builds up as active ice continues to deliver sediment to the ice margin. Presumably, as the ice margin retreated from this pinning point, large numbers of icebergs were released, which ploughed the surface of the GZW, forming the extensive set of ploughmarks observed in Figure 4.19.

A large number of Type II ploughmarks were also observed across the inner Umanak Shelf (Fig. 4.18), far more than were observed on the inner Disko Shelf. Type I ploughmarks and grounding pits were present on the shelf at water depths between ~250-400 m (Fig. 4.18). In the Umanak Fjord system, only a small number of Type II ploughmarks were observed (Fig. 4.20). As previously discussed, the low intensity of iceberg ploughing in this section of the study area relates to the fact that water depths in most parts of the fjord system are relatively deep (>600 m; Fig. 3.9); therefore, the keels of modern icebergs are not large enough to impact the seafloor.

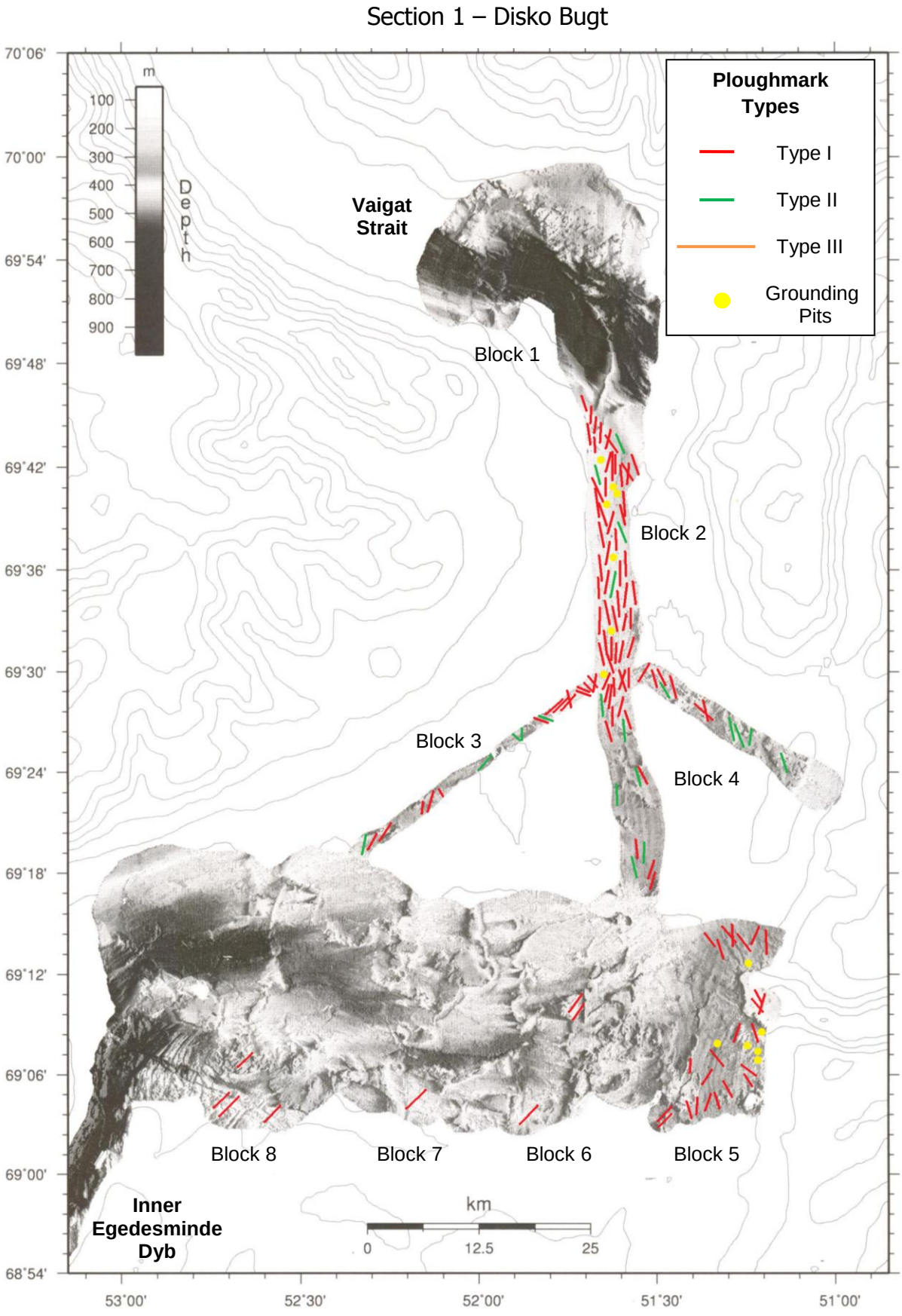


**Figure 4.15.** Greyscale swath-bathymetric map of ploughmark distribution for Section 1 of the study area on the West Greenland margin (section located in Fig. 3.4; data gridded at 50 m). Orientations

represent the mean and range of ploughmark orientations for each block within the section (blocks located in Fig. 3.5).

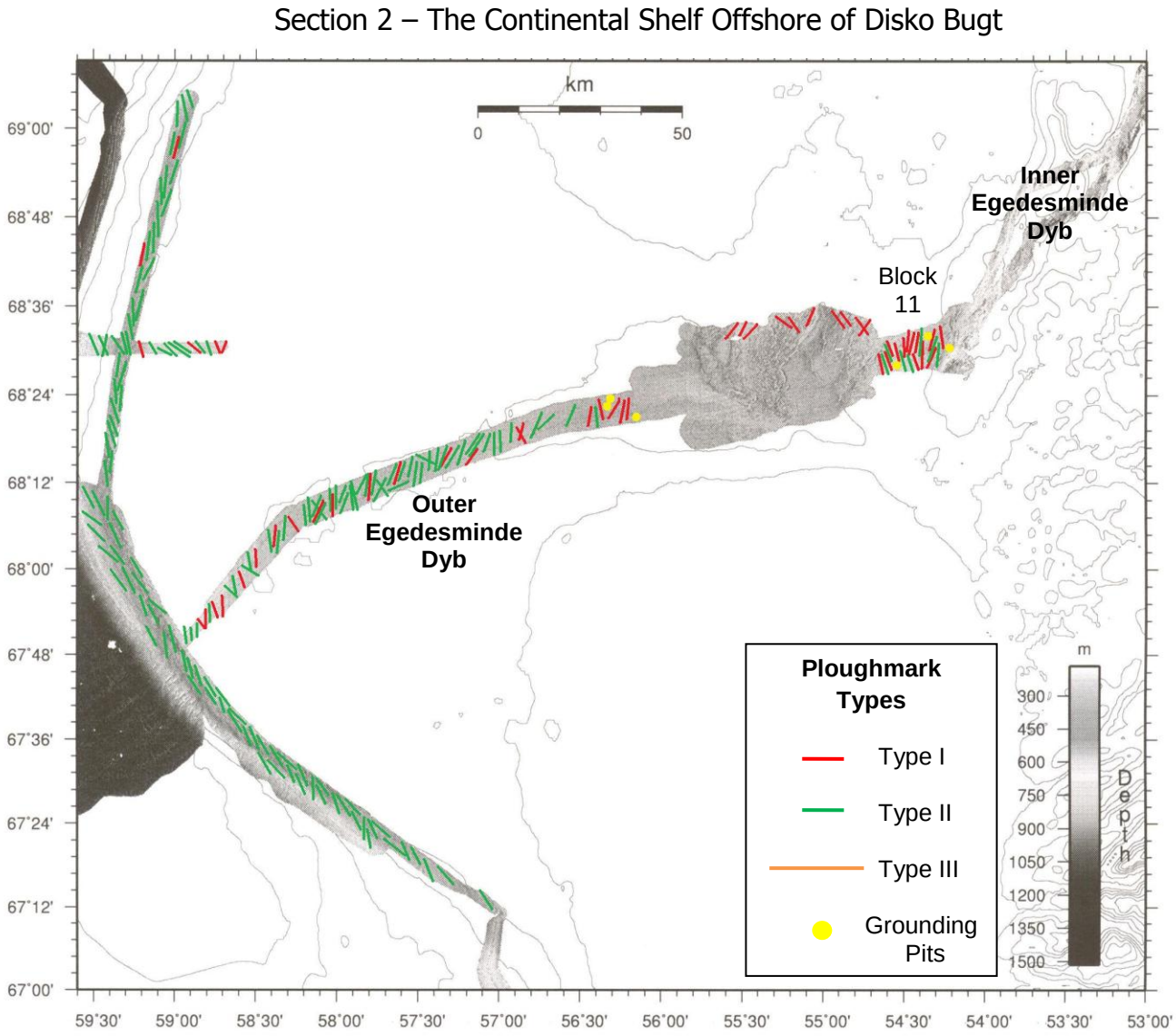


**Figure 4.16.** Greyscale swath-bathymetric map of ploughmark distribution for Section 2 of the study area on the West Greenland margin (section located in Fig. 3.4; data gridded at 30 m). Orientations represent the mean and range of ploughmark orientations for each block within the section (blocks located in Fig. 3.6).

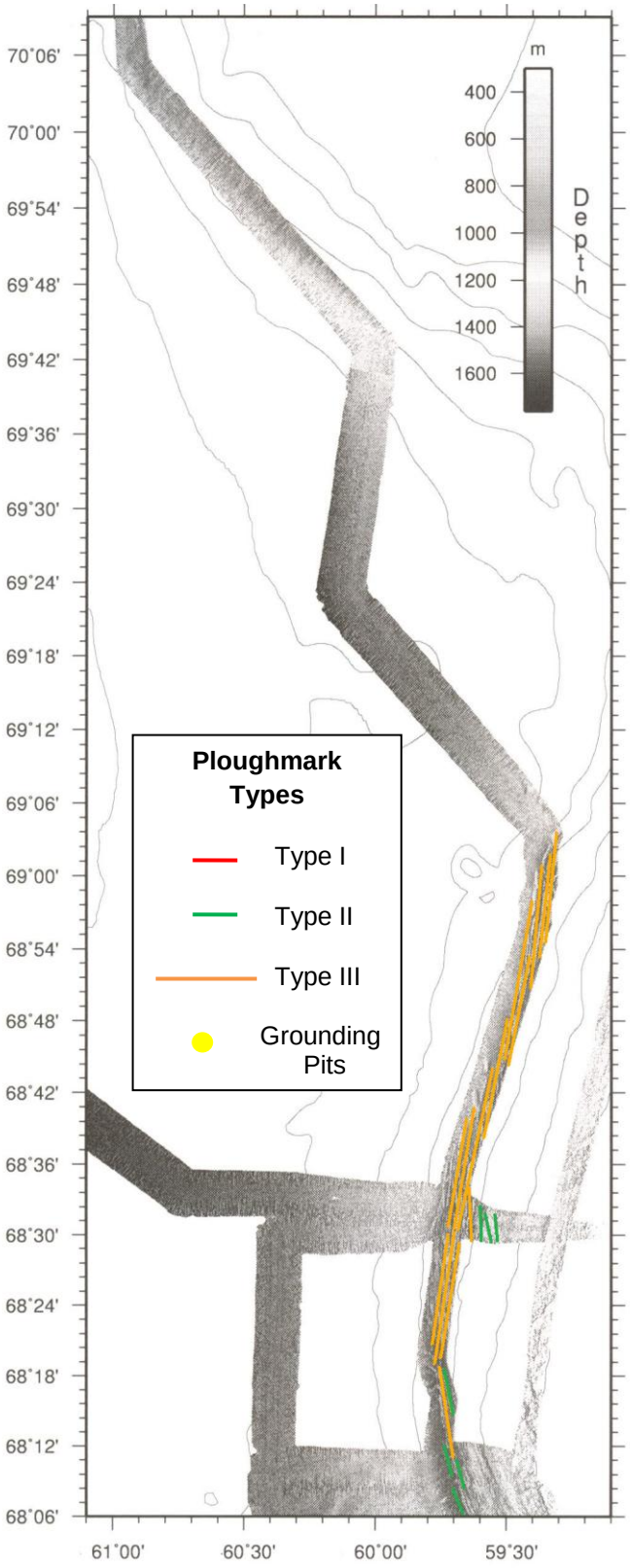


**Figure 4.17.** Greyscale swath-bathymetric map of ploughmark distribution for Section 3 of the study area on the West Greenland margin (section located in Fig. 3.4; data gridded at 50 m). Orientations represent the mean and range of ploughmark orientations for each block within the section (blocks located in Fig. 3.7).

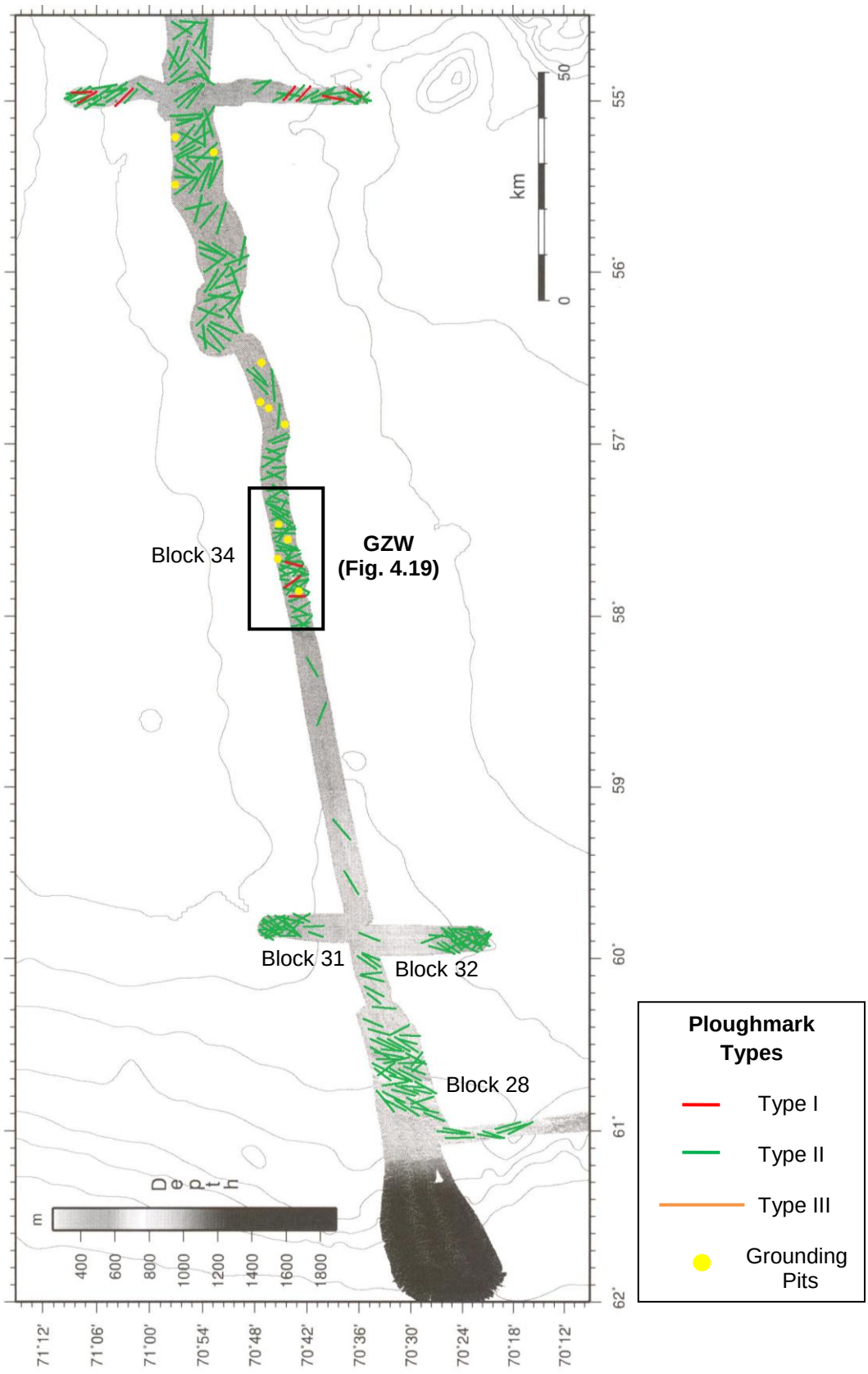


**Figure 4.18.** Greyscale swath-bathymetric map of ploughmark distribution for Section 4 of the study area on the West Greenland margin (section located in Fig. 3.4; data gridded at 30 m). Orientations

represent the mean and range of ploughmark orientations for each block within the section (blocks located in Fig. 3.8).

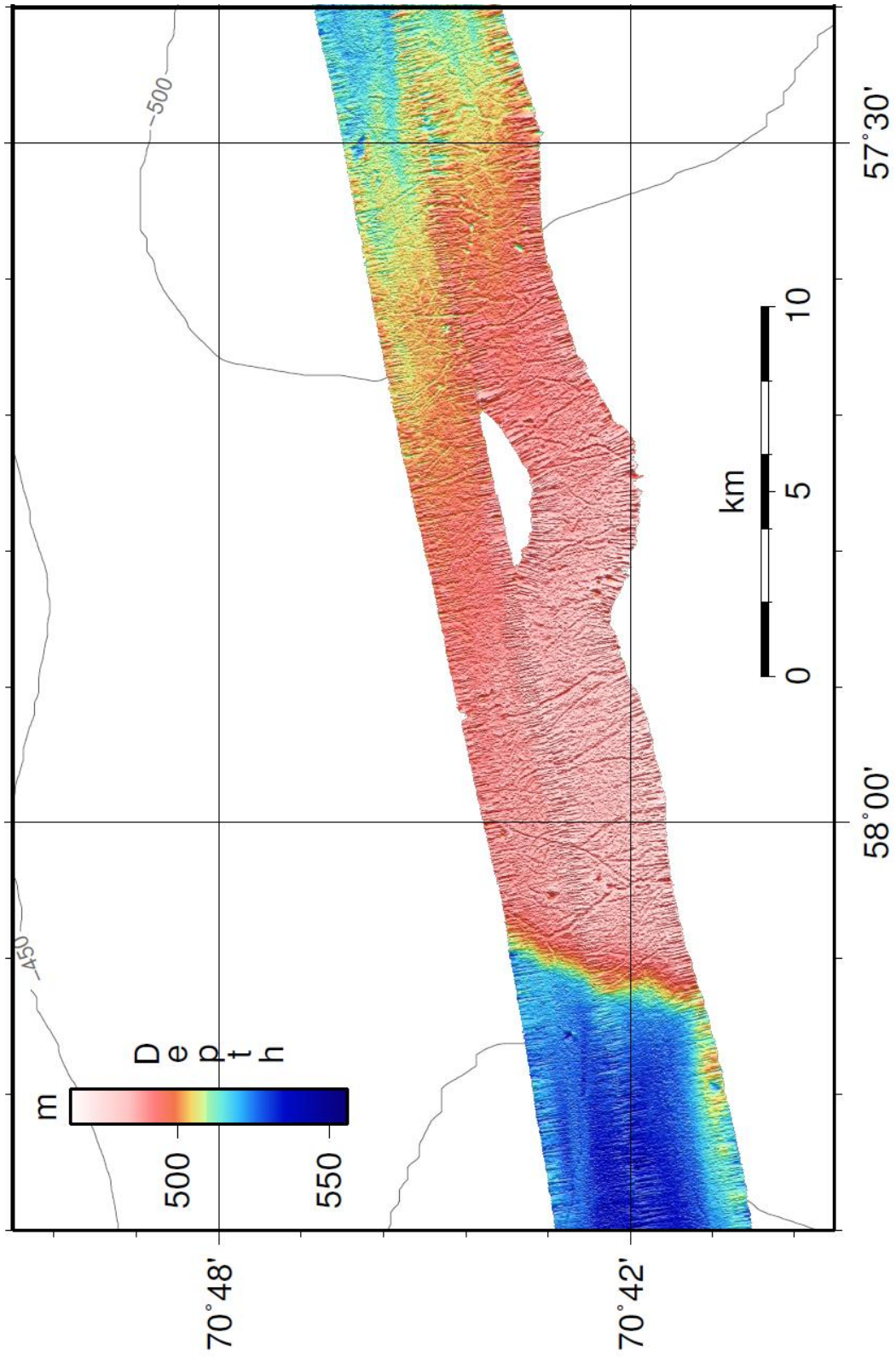


**Figure 4.19.** Swath-bathymetric image of Type II ploughmarks superimposed on the surface of a large GZW on the continental shelf offshore of the Umanak Fjord system (located in Fig. 4.18; data gridded at 12 m).

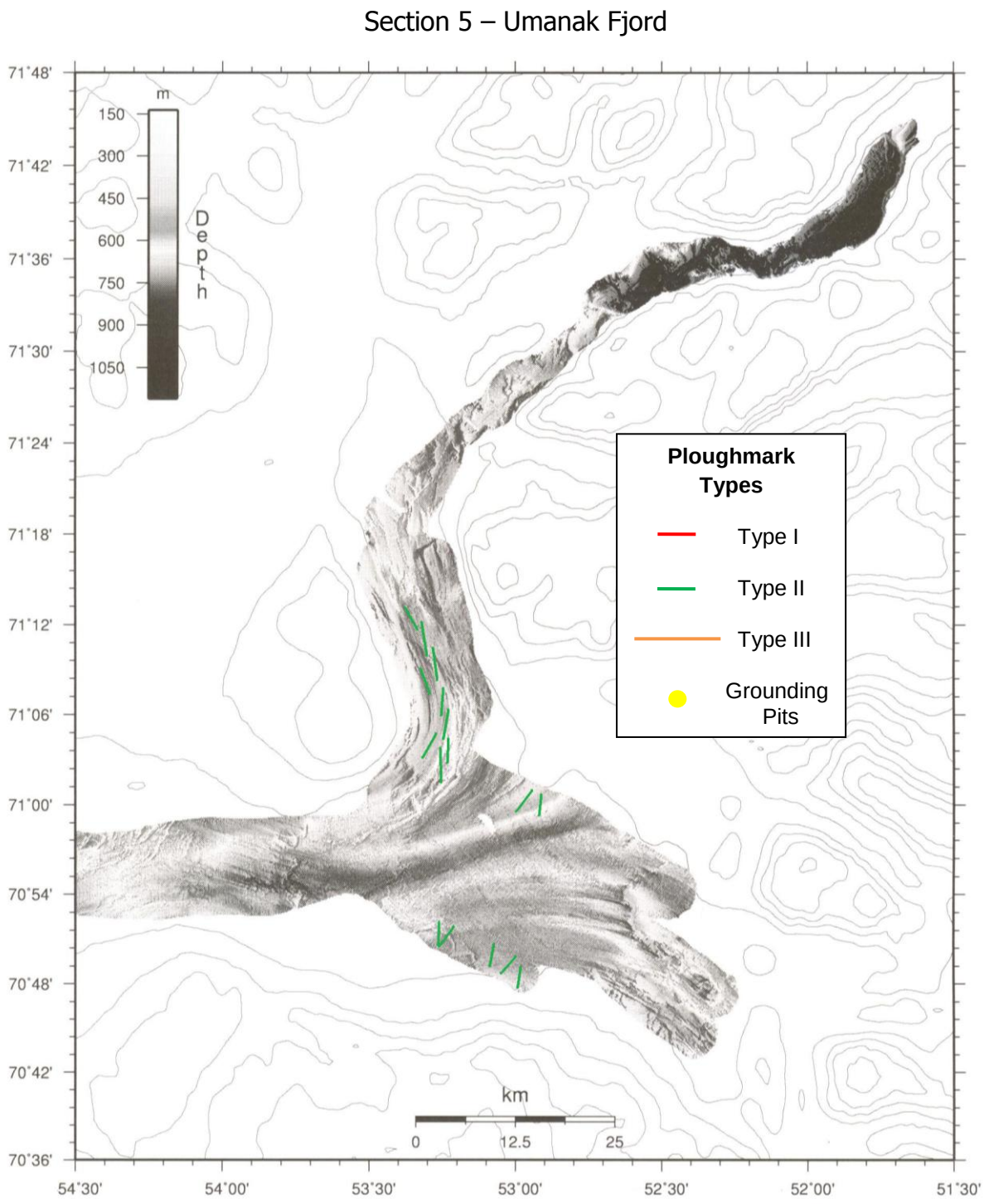


**Figure 4.20.** Greyscale swath-bathymetric map of ploughmark distribution for Section 5 of the study area on the West Greenland margin (section located in Fig. 3.4; data gridded at 30 m). Orientations represent the mean and range of ploughmark orientations for each block within the section (blocks located in Fig. 3.9).

# CHAPTER 5 – DISCUSSION

Observations on the dimensions, orientations and morphologies of iceberg ploughmarks on the West Greenland margin were presented in Chapter 4, and used to map the nature and intensity of iceberg ploughing in the region. In this Chapter, the distribution of ploughmarks across the study area is discussed and interpreted in the context of the dynamic behaviour of West Greenland outlet glaciers, both past and present.

## 5.1 Ploughmark Distribution Patterns

The distribution of ploughmark types was highly variable across the study area (Figs. 4.15-4.20). Small Type I features were observed mainly within Disko Bugt, and also at water depth of up to 400 m on the continental shelf. The distribution of these features was inversely proportional to water depth, with numerous small ploughmarks observed in the shallow (> 400 m) waters of Disko Bugt (Fig. 4.2; Fig. 4.15). Type I ploughmarks were interpreted as a combination of recent features, ploughed by icebergs calved from modern outlet glaciers of the Greenland Ice Sheet, and relict ploughmarks, incised by icebergs calved from retreating ice in the Late Weichselian. The majority of ploughmarks in Disko Bugt appeared acoustically fresh; given the high rates of deglacial sedimentation in Disko Bugt (Hogan et al., 2011), this implies a relatively young age for these ploughmarks. In contrast, Type I features at water depths of up to 400 m on the outer Disko Shelf must be relict, since the basalt escarpement which separates the inner and outer Egedesminde Dyb prevents icebergs with drafts greater than ~300 m from exiting the trough; these ploughmarks were presumably formed at a time when the ice margin was located to the west of this threshold. Ploughmarks of similar dimensions have been reported from the East Greenland shelf (Dowdeswell et al., 1993) and from the Svalbard margin (Dowdeswell et al., 2010c; Hogan et al., 2010; Batchelor et al., 2011).

Type II ploughmarks were observed over a much wider area of the shelf, and were prevalent in water depths > 300 m (Figs. 4.15-4.20). Type II features have been reported from high latitude shelves at water depths less than ~500 m by a number of workers (e.g. Hogan et al., 2010; Dowdeswell et al., 2010c; Batchelor et al., 2011). This study, however, recorded the

occurrence of large Type II features at water depths of up to ~850 m on the upper slope (Fig. 4.17; Fig. 4.18). Present-day iceberg keels touch bottom at depths of up to 500-600 m on the East Greenland margin (Dowdeswell et al., 1992), and the outlets from which these icebergs derive are dynamically similar to those releasing icebergs into the fjords of West Greenland. The occurrence of Type II ploughmarks in water depths >600 m suggests, therefore, that these features are likely to be relict in age. In addition, ploughmarks on the outermost shelf are located at a considerable distance from the present-day ice margin. Drift over hundreds of kilometres would result in appreciable melting and break-up of individual icebergs (Weeks and Campbell, 1973; Neshyba and Josberger, 1980; Dowdeswell and Dowdeswell, 1989); consequently, icebergs calved from the present day margin of the Greenland Ice Sheet are probably not responsible for the majority of Type II ploughmarks observed on the outer shelf and upper slope.

Type III ploughmarks were observed only on the continental slope, at water depths between ~800 and 1071 m (Fig 4.17). The largest of these features were up to 15 km long and 700 m wide, with a crest-trough depth of up to 40 m. Comparable features, including some of those observed in this study, have previously been described from the West Greenland slope by Kuijpers et al. (2007). The dimensions and depth of occurrence are exceptional, and indicate a time when much larger icebergs, with drafts of 900-1000 m, were produced. Iceberg ploughmarks in similarly deep water, and of similarly large dimensions, have also been observed, for example, on the Yermak Plateau and northern Svalbard margin (e.g. Vogt et al., 1994; Dowdeswell et al., 2010c).

Iceberg grounding pits were observed over a wide range of water depths on the West Greenland margin (Figs. 4.15-4.20). Grounding pits have also been observed from the Kangerlussuaq margin, East Greenland, by Syvitski et al. (2001). A bobbing iceberg (i.e. through the impact of ocean waves, tides, storm surges) can impact the sea floor in different locations and create pits; these features therefore indicate the intermittent and limited contact of iceberg keels with the sea floor.

## 5.2 Sources of Deep-Keeled Icebergs to the West Greenland Margin

Modern icebergs that impact the West Greenland margin are derived principally from outlet glaciers that drain the western sector of the Greenland Ice Sheet into Baffin Bay. The majority of these outlets are located along a ~300 km stretch of coastline between Disko Bugt and the Umanak Fjord system; a high density of icebergs has been observed for this region of the shelf. Rignot and Kanagaratnam (2006) mapped ice flow velocities for major outlet glaciers of the Greenland Ice Sheet (Fig. 5.1); these velocities were then combined with measurements of ice thickness and terminus width in order to calculate ice discharge to the ocean from each of the glaciers. South of Disko Bugt, only the Nordenskiold basin (area 19) has a significant ice flux. Nordbogletscher (area 14), Sermilik (area 15), and Kangiata nunata/Narssap sermia (area 17) have balance fluxes of only 1, 6.5 and 6 $km^3$ $yr^{-1}$ respectively, so potential mass losses from ice dynamics are small. Much larger ice discharges were calculated for outlet glaciers in central West Greenland. Ice front discharge for Nordenskiold Gletscher (area 19), Jakobshavn Isbrae (area 20) and Rinks Gletscher (area 23) was 10.7, 23.6 and 11.8 $km^3$ $yr^{-1}$ respectively (Rignot and Kanagaratnam, 2006); these glaciers are therefore the most likely sources for the large numbers of icebergs observed today on the West Greenland margin.

Observations from present-day ice margins suggest that icebergs with keel depths greater than ~500 m most likely originated from the thick, seaward margin of a fast-flowing, palaeo-ice stream (Dowdeswell and Bamber, 2007). It is inferred that the ice sheet terminus on the West Greenland margin was not a major floating ice shelf of tens or more kilometres in extent, because such features creep-thin under their own weight, and are seldom more than 300-350 m thick. In addition, at the southern entrance to Baffin Bay, the Davis Strait sill depth is approximately 650 m (Fig. 1.3). Glacial rebound data from the West Greenland margin indicate a maximum glacial subsidence of ~100 m for the Davis Strait (Kuijpers et al., 2007). This implies that the deep-keeled icebergs observed in this study must have been calved from an ice margin in the Baffin Bay region, rather than drifting round the southern tip of Greenland from the east. Thus, the most obvious sources for the deep-keeled icebergs that ploughed the West Greenland margin during the Late Weichselian and previous (de)glacial periods are the fast-flowing palaeo-ice streams that drained large basins of the Greenland Ice Sheet westwards across the shelf via Egedesminde Dyb and the Umanak cross-shelf trough.

At present, outlet glaciers of the Greenland Ice Sheet calve icebergs with maximum keel depths of ~600 m (Dowdeswell et al., 1992). These drafts are much smaller than those

required to form the largest ploughmarks observed in this study at water depths of up to 1071 m, since the keel of an iceberg must extend through the full depth of the water column in order to produce a ploughmark. The very deep observed ploughmarks must be relict, therefore, and from a time when much larger icebergs, with drafts well in excess of 600 m, were formed. The timing of ploughmark formation is not easy to date, since icebergs produce erosional features. Sub-bottom profiler records from the continental slope document no sediment infill of any significance in these very large ploughmarks (J.A. Dowdeswell, pers. comm.); this may indicate a relatively young, Late Weichselian, age. Relative sea-level at the time the ploughmarks were formed is not certain, but the LGM global lowstand value of 120 m below present sea-level can be used to estimate minimum keel depths required for ploughing. Based on this assumption, the thickness of the ice margin at the grounding line must have been at least ~900 m, in order to produce deep-draft icebergs that could plough the upper slope at the LGM. This value concurs with recent estimates of maximum LGM ice surface elevation for the West Greenland Ice Sheet of 810-1000 m (Rinterknecht et al., 2009; Roberts et al., 2009; Simpson et al., 2009). However, the ice margin itself is not likely to have been this thick. Assuming that the ice sheet was grounded on the outermost shelf, at a modern water depth of approximately 500 m, and taking into account a maximum glacial sea-level lowstand of 120 m it is difficult to see how bergs with keel depths of 900 m or more could have been calved.

An alternative process for the formation of palaeo-icebergs with keel-depths of ~900 m must be considered. One possible explanation is that large, deep-keeled icebergs were calved from the buoyant margin of a transient ice shelf with a grounding line in deeper water on the continental slope beyond the shelf break. This ice shelf may have developed as the ice sheet advanced temporarily into deeper waters on the upper slope and became ungrounded (Fig. 5.2). This would allow the development of an ice margin of sufficient thickness to calve icebergs with drafts of 900-1000 m (Fig. 5.2). There is, however, no positive evidence that such a transient advance into deep water took place.

A second possible explanation for the deep ploughmarks observed in this study is the fragmentation of large tabular icebergs. Fragmentation of an iceberg may lead to a shift in its centre of gravity, which may cause the iceberg to overturn, in some cases increasing its draft (Dowdeswell et al., 1993). Bass and Peters (1984) documented iceberg draft increases of up

to 50% through overturn, with an average increase of 25%; however, iceberg draft modelling has shown that draft changes of this magnitude are relatively rare events.

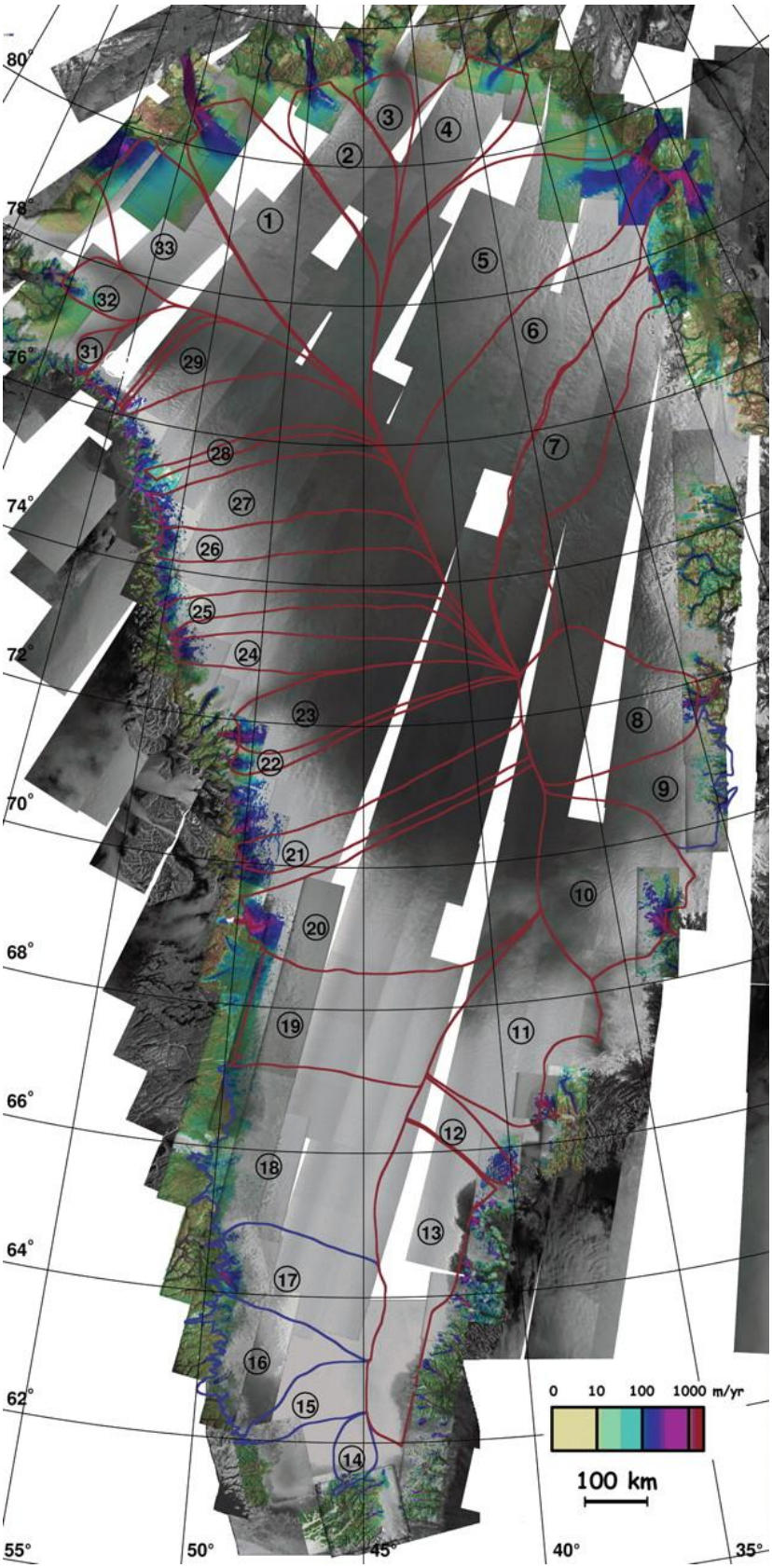

**Fig. 5.1.** Ice-velocity mosaic of the Greenland Ice Sheet assembled from year 2000 Radarsat-1 radar data, colour coded on a logarithmic scale from 1m $yr^{-1}$ (brown) to 3 km $yr^{-1}$ (purple), overlaid on a map of radar brightness from ERS-1/Radarsat-1/Envisat. Numbers refer to drainage basin areas (from Rignot and Kanagaratnam, 2006).

In addition, both Type II and Type III ploughmarks on the West Greenland margin were observed to form linear sets of multiple ploughmarks, which trended parallel to one another over distances of several kilometres (Fig. 4.11; Fig. 4.12). These features were probably formed in one of two ways: either by a single, very large iceberg, with a deep, high-relief base, or, alternatively, by individual deep-keeled icebergs trapped together in a thick, multi-year sea ice floe, which would provide a uniform pattern of drift (Dowedewell et al., 2010c). There are few direct modern analogues for this process in open marine environments. The most likely example is the melange of icebergs, bergy bits and multi-year sea ice, known as 'sikussak', which has been observed in some Greenland fjords (Dowdeswell et al., 2000; Dowdeswell et al., 2010c). At present, sikussak is rarely observed in the open ocean; it is possible, however, that during full-glacial periods, multi-year, shorefast sea ice may have extended further westward across the shelf, as has been suggested for the Arctic basin by some workers (e.g. Vogt et al., 1994).

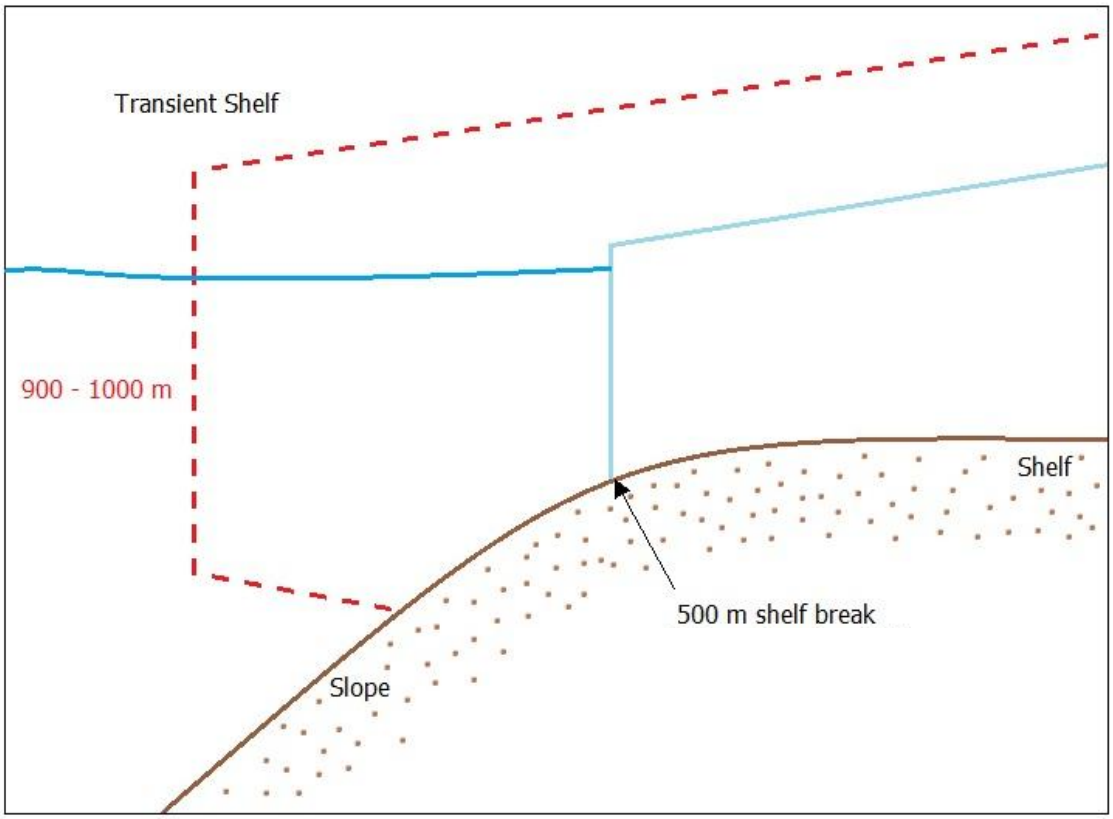

**Figure 5.2.** Conceptual diagram to show the development of a transient ice shelf with a grounding line in deeper water on the upper continental slope beyond the shelf break. This is one possible scenario for the production of very deep-keeled icebergs on the West Greenland margin during the Late Weichselian.

## 5.3 Iceberg Drift Patterns

The dominant ploughmark orientation of approximately S-N is parallel to the principal current direction on the West Greenland Margin (Fig. 4.4; Fig. 4.17). This suggests that iceberg drift is governed by the northerly-flowing WGC, which operates in Baffin Bay today. The uniform orientations of relict ploughmarks on the continental slope, which are also aligned S-N, suggest that iceberg drift during the LGM and subsequent deglaciation can also be related to a palaeo-circulation pattern corresponding to the WGC; the implication is that current direction has been relatively consistent over the Late Weischelian and Holocene.

Inshore of the slope and shelf, the drift of icebergs in Disko Bugt and the Umanak Fjord system is influenced by normal fjord circulation (Syvitski et al., 1987; Mugford and Dowdeswell, 2010), where water enters at depth and exits at the surface. This is shown by the changing mean orientation of ploughmarks which conform to the long-axis of the fjords (Fig. 4.15; Fig. 4.20). Iceberg drift in fjords is also likely to be influenced by katabatic winds from the ice sheet. This may account for the fact that ploughmarks in the southern part of Disko Bugt were oriented NE-SW (Fig. 4.15), and associated with icebergs on a SW trajectory.

The drift of icebergs across the West Greenland margin is also likely to be restricted by the bathymetric features of the continental shelf. The E-W orientation for some ploughmarks observed on the Umanak shelf (Fig. 4.18) may be related to the bathymetric constraints of the cross-shelf trough, which could have prevented deeper-keeled icebergs from exiting the trough to drift north across the shelf.

# CHAPTER 6 – SUMMARY AND CONCLUSIONS

## 6.1 Major Findings

This thesis presents new, high-resolution geophysical data from the seafloor of the West Greenland margin. Geophysical datasets are derived from multibeam swath-bathymetry and sub-bottom acoustic profiling. From analysis and interpretation of the variations in size, orientation and distribution of iceberg ploughmarks on the West Greenland margin, the following conclusions can be drawn:

- A large number of modern and relict ploughmarks were observed on the seafloor of the study area on the West Greenland margin (Figs. 4.15- 4.20), indicating that iceberg ploughing has been, and continues to be, a major glacimarine process for this region of the shelf.

- Icebergs ploughmarks were mapped at present-day water depths of up to 1071 m, implying formation in palaeo-water depths of up to 950 m. The largest features had widths of up to 700 m and were incised 40 m into the seafloor (Figs. 4.11-4.12). The deep-keeled icebergs that produced these ploughmarks were most likely derived from fast-flowing, palaeo-ice streams, which drained large basins of the Greenland Ice Sheet westwards across the shelf during the last glacial period.

- Two possible explanations for the formation of icebergs with drafts of ~900 m have been suggested: deep-keeled icebergs may have been calved from a transient ice shelf as the ice sheet advanced temporarily into deeper waters on the upper slope (Fig. 5.2), or through fragmentation and overturning of large tabular icebergs, which may in some circumstances lead to an increase in draft of up to 50% (Bass and Peters, 1984).

- Sets of aligned ploughmarks on the West Greenland margin (Fig. 4.10) were probably formed by an individual, very large iceberg, with a deep, high-relief keel, or by groups of single icebergs trapped in an extensive and thick multi-year sea-ice field, to account for the uniform pattern of drift.

- The orientation of both modern and relict ploughmarks on the West Greenland shelf and slope was predominantly S-N. This suggests that both modern and Late Weichselian iceberg drift are probably related to a circulation pattern in Baffin Bay which corresponds to a northerly flowing WGC.

## 6.2 Suggestions for Further Work

Following on from the conclusions of this thesis, summarised in Section 6.1, several possible avenues for further work are suggested below.

- To monitor icebergs through time using high-resolution satellite imagery of both calving margins and of iceberg drift. This would provide information on, for example, the processes of fragmentation and overturn, and the related changes in keel depth. Such observations could also confirm or otherwise the suggestion in Section 5.2 that overturn may temporarily produce icebergs with very deep keels.

- To extend the study area to include different areas of the Greenland margin. This would allow a wider picture of the pattern of ploughing and, hence iceberg dimensions, around Greenland to be developed.

- To measure the debris content of even a limited number of Greenland icebergs. This would provide information relevant to sedimentation rates in the fjords and on the shelves of Greenland, and assist in the interpretation of the record of ice-rafted debris around the ice sheet. This would be logistically rather difficult to achieve, as has been shown in investigations of debris in icebergs offshore of Antarctica and Svalbard (e.g. Anderson et al., 1980; Dowdeswell and Dowdeswell, 1989).

# REFERENCES


Alley, R.B., Andrews, J.T., Brigham-Grette, J., Clarke, G.K.C., Cuffey, K.M., Fitzpatrick, J.J., Funder, S., Marshall, S.J., Miller, G.H., Mitrovica, J.X., Muhs, D.R., Otto-Bliesner, B.L., Polyak, L. and White, J.W.C., 2010. History of the Greenland Ice Sheet: palaeoclimatic insights. *Quaternary Science Reviews*, 29(15-16), 1728-1756.

Andersson, J., 2008. An environmental magnetic study of a marine sediment core from Disko Bugt, West Greenland: implications for ocean current variability. Master's Thesis, Lund University.

Anderson, J.B., Domack, E.W. and Kurtz, D.D., 1980. Observations of sediment-laden icebergs in Antarctic waters: implications to glacial erosion and transport. Journal of *Glaciology*, 25(93), 387-396.

Bamber, J.L., Alley, R.B. and Joughin, I., 2007. Rapid response of modern day ice sheets to external forcing. *Earth and Planetary Science Letters*, 257(1-2), 1-13.

Barnes, P.W. and Lien, R., 1988. Icebergs rework shelf sediments to 500 m off Antarctica. *Geology*, 16(12), 1130-1133.

Bass, D.W. and Peters, G.R., 1984. Computer simulation of iceberg instability. *Cold Regions Science and Technology*, 9(2), 163-169.

Batchelor, C.L., Dowdeswell, J.A. and Hogan, K.A., 2011. Late Quaternary ice flow and sediment delivery through Hinlopen Trough, northern Svalbard margin: submarine landforms and depositional fan. *Marine Geology*, 284, 13-27.

Belan, A.B., Abbuehl, L. and Kuijpers, A., 2004. Relict Iceberg Ploughmarks on the Western Greenland Margin. Intergovernmental Oceanographic Commission, Workshop Report No. 191, 9-11.

Belderson, R.H., Kenyon, N.H. and Wilson, J.B., 1973. Iceberg plough marks in the Northeast Atlantic. *Palaeogeography, Palaeoclimatology, Palaeoecology*, 13(3), 215-224.

Benn, D.I., Hulton, N.R.J. and Mottram, R.H., 2007a. 'Calving laws', 'sliding laws' and the stability of tidewater glaciers. *Annals of Glaciology*, 46, 123-130.

Benn, D.I., Warren, C.R. and Mottram, R.H., 2007b. Calving processes and the dynamics of calving glaciers. *Earth-Science Reviews*, 82(3-4), 143-179.

Benn, D.I. and Evans, D.J.A., 2010. *Glaciers and Glaciation* (Second Edition). London: Hodder Education.

Bitanja, R., van de Wal, R.S.W. and Oerlemans, J., 2005. Modelled atmospheric temperatures and global sea levels over the past million years. *Nature*, 437(7055), 125–128.

Brett, C.P. and Zarudzki, E.F.K., 1979. Project Westmar, a shallow marine geophysical survey on the west Greenland shelf. *Rapport Grønlands Geologiske Undersøgelse*, 87.

Chalmers, J.A., Pulvertaft, T.C.R., Marcussen, C. and Pedersen, A.K., 1999. New insight into the structure of the Nuussuaq Basin, central West Greenland. *Marine and Petroleum Geology*, 16(3), 197–224.

Damuth, J.E., 1975. Echo character of the western equatorial Atlantic floor and its relationship to the dispersal and distribution of terrigenous sediments. *Marine Geology*, 18(2), 17-45.

Damuth, J.E., 1980. Use of high-frequency (3.5-12 kHz) echograms in the study of near-bottom sedimentation processes in the deep-sea. *Marine Geology*, 38(1-3), 51-75.

Denbigh, P.N., 1989. Swath Bathymetry: Principles of Operation and an Analysis of Errors. *IEEE Journal of Oceanic Engineering*, 14(4), 289-298.

Denham, L.R., 1974. Offshore geology of northern West Greenland (69°-75°N). *Rapport Grønlands Geologiske Undersøgelse*, 63.

Dowdeswell, J.A., 1989. On the nature of Svalbard icebergs. *Journal of Glaciology*, 35(120), 224-234.

Dowdeswell, J.A., 2006. The Greenland Ice Sheet and global sea-level rise. *Science*, 311(5763), 963-964.

Dowdeswell, J.A. and Bamber, J.L., 2007. Keel depths of modern Antarctic icebergs and implications for sea-floor scouring in the geological record. *Marine Geology*, 243(1-4), 120-131.

Dowdeswell, J.A. and Dowdeswell, E.K., 1989. Debris in icebergs and rates of glaci-marine sedimentation: observations from Spitsbergen and a simple model. *Journal of Geology*, 97(2), 221-231.

Dowdeswell, J.A., Evans, J. and Ó Cofaigh, C., 2010a. Submarine landforms and shallow acoustic stratigraphy of a 400 km-long fjord-shelf-slope transect, Kangerlussuaq margin, East Greenland. *Quaternary Science Reviews*, 29(25-26), 3359-3369.

Dowdeswell, J.A. and Forsberg, C.F., 1992. The size and frequency of icebergs and bergy bits derived from tidewater glaciers in Kongsfjorden, northwest Spitsbergen. *Polar Research*, 11(2), 81-91.

Dowdeswell, J.A., Hogan, K.A., Evans, J., Noormets, R., Ó Cofaigh, C. and Ottesen, D., 2010b. Past ice-sheet flow east of Svalbard inferred from streamlined subglacial landforms. *Geology*, 38(2), 163-166.

Dowdeswell, J.A., Jakobsson, M., Hogan, K.A., O'Regan, M., Backman, J., Evans, J., Hell, B., Löwemark, L., Marcussen, C., Noormets, R., Ó Cofaigh, C., Sellén, E. and Sölvsten, M., 2010c. High-resolution geophysical observations of the Yermak Plateau and northern Svalbard margin: implications for ice-sheet grounding and deep-keeled icebergs. *Quaternary Science Reviews*, 29(25-26), 3518-3531.

Dowdeswell, J.A., Kenyon, N.H. and Laberg, J.S., 1997. The glacier-influenced Scoresby Sund Fan, east Greenland continental margin: evidence from GLORIA and 3.5 kHz records. *Marine Geology*, 143(1-4), 207-221.

Dowdeswell, J.A., Maslin, M.A., Andrews, J.T. and McCave, I.N., 1995. Iceberg production, debris rafting, and the extent and thickness of Heinrich layers (H-1, H-2) in North Atlantic sediments. *Geology*, 23(4), 301-304.

Dowdeswell, J.A., Ó Cofaigh, C., Taylor, J., Kenyon, N.H., Mienert, J. and Wilken, M., 2002. On the architecture of high-latitude continental margins: the influence of ice-sheet and sea-ice processes in the Polar North Atlantic. In: Dowdeswell, J.A. and Ó Cofaigh, C. (eds). *Glacier-influenced sedimentation on high-latitude continental margins*. Geological Society of London, Special Publications, 203, 33-54.

Dowdeswell, J.A., Ottesen, D., Evans, J., Ó Cofaigh, C. and Anderson, J.B., 2008. Submarine glacial landforms and rates of ice-stream collapse. *Geology*, 36(10), 819-822.

Dowdeswell, J.A., Vilinger, H., Whittington, R.J. and Marienfeld, P., 1993. Iceberg scouring in Scoresby Sund and on the East Greenland Continental Shelf. *Marine Geology*, 111 (1-2), 37-53.

Dowdeswell, J.A., Whittington, R.J. and Hodgkins, R., 1992. The Sizes, Frequencies, and Freeboards of East Greenland Icebergs Observed Using Ship Radar and Sextant. *Journal of Geophysical Research*, 97(C3), 3515-3528.

Evans, J., Dowdeswell., J.A., Ó Cofaigh, C., Benham, T.J. and Anderson, J.B., 2006. Extent and dynamics of the West Antarctic Ice Sheet on the outer continental shelf of Pine Island Bay during the last glaciations. *Marine Geology*, 230 (1-2), 53-72.

Evans, J., Ó Cofaigh, C., Dowdeswell, J.A. and Wadhams, P., 2009. Marine geophysical evidence for former expansion and flow of the Greenland Ice Sheet across the north-east Greenland continental shelf. *Journal of Quaternary Science*, 24(3), 279-293.

Feyling-Hanssen, R. W. and Funder, S., 1990. Fauna and Flora. In: Funder, S. (ed). Late Quaternary stratigraphy and glaciology in the Thule area, northwest Greenland. *Meddelelser om Grønland, Geoscience*, 22, 19-23.

Fleming, K. and Lambeck, K., 2004. Constraints on the Greenland Ice Sheet since the Last Glacial Maximum from sea-level observations and glacial-rebound models. *Quaternary Science Reviews*, 23(9-10), 1053-1077.

Funder, S., 1989. Quaternary Geology of the ice free areas and adjacent shelves of Greenland. In: Fulton, R.J. (ed). *Quaternary Geology of Canada and Greenland*. Geological Survey of Canada, Geology of Canada 1 (also Geological Society of America, The Geology of North America K-1), 741-792.

Funder, S., Bennike, O., Böcher, J., Israelson, C., Petersen., K.S. and Símonarson. L.A., 2001. Late Pliocene Greenland – The Kap København Formation in North Greenland. *Bulletin of the Geological Society of Denmark*, 48, 117-134.

Funder, S. and Hansen, L., 1996. The Greenland ice sheet – a model for its culmination and decay during and after the last glacial maximum. *Bulletin of the Geological Society of Denmark*, 42, 137-152.

Gibbard, P., Head, M.J., Walker, M.J.C. and The Subcommission on Quaternary Stratigraphy, 2010. Formal ratification of the Quaternary System/Period and the Pleistocene Series/Epoch with a base at 2.58 Ma. *Journal of Quaternary Science*, 25(2), 96–102.

Hogan, K.A., 2008. The Geomorphic and Sedimentary Record of Glaciation on High-Latitude Continental Margins with particular reference to the Northeastern Svalbard Margin. Ph.D. Thesis, University of Cambridge.

Hogan, K.A., Dix., J.K., Lloyd, J.M., Long, A.J. and Cotterill, C.J., 2011. Seismic stratigraphy records the deglacial history of Jakobshavn Isbræ, West Greenland. *Journal of Quaternary Science*, DOI: 10.1002/jqs.1500.

Hogan, K.A., Dowdeswell, J.A., Noormets, R., Evans, J. and Ó Cofaigh, C., 2010. Evidence for full-glacial flow and retreat of the Late Weichselian ice sheet from the waters around Kong Karls Land, eastern Svalbard. *Quaternary Science Reviews*, 29, 3545-3562.

Holland, D.M., Thomas, R.H., de Young, B., Ribergaard, M.H. and Lyberth, B., 2008. Acceleration of Jakobshavn Isbrae triggered by warm subsurface ocean waters. *Nature Geoscience*, 1(10), 659-664.

Huybrechts, P., 2002. Sea-level changes at the LGM from ice-dynamic reconstructions of the Greenland and Antarctic ice sheets during the glacial cycles. Quaternary Science Reviews, 21(1-3), 203-231.

Imbrie, J., Berger, A., Boyle, E. A., Clemens, S. C., Duffy, A., Howard, W. R., Kukla, G., Kutzbach, J., Martinson, D. G., McIntyre, A., Mix, A. C., Molfino, B., Morley, J. J., Peterson, L. C., Pisias, N. G., Prell, W. L., Raymo, M. E., Shackleton, N. J. and Toggweiler, J. R., 1993. On the structure and origin of major glaciations cycles - 2. The 100000 year cycle. *Paleoceanography*, 8(6), 699-736.

Imbrie, J., Boyle, E.A., Clemens, S.C., Duffy, A., Howard, W.R., Kukla, G., Kutzbach, J., Martinson, D.G., Mcintyre, A., Mix, A.C., Molfino, B., Morley, J.J., Peterson, L.C., Pisias, N.G., Prell, W.L., Raymo, M.E., Shackleton, N.J. and Toggweiler, J.R., 1992. On the structure and origin of major glaciation cycles - 1. Linear responses to Milankovich forcing. *Paleoceanography*, 7(6), 701-738.

Jacobs, S.S., Helmer, H.H., Doake, C.S.M., Jenkins, A. and Frolich, R.M., 1992. Melting of ice shelves and the mass balance of Antarctica. *Journal of Glaciology*, 38(130), 375-387.

Jakobsson, M., Macnab, R., Mayer, L., Anderson, R., Edwards, M., Hatzky, J., Schenke, H-W., and Johnson, P., 2008. An improved bathymetric portrayal of the Arctic Ocean: Implications for ocean modelling and geological, geophysical and oceanographic analyses. *Geophysical Research Letters*, 35, L07602, doi:10.1029/2008GL033520.

Jones, E.J.W., 1999. *Marine Geophysics*. Chichester: John Wiley & Sons Ltd.

Josenhans, H.W., Zevenhuizen, J. and Klassen, R.A., 1986. The Quaternary geology of the Labrador Shelf. *Canadian Journal of Earth Sciences*, 23(8), 1190-1213.

Joughin, I., Abdalati, W. & Fahnestock, M. 2004: Large fluctuations in speed on Greenland's Jakobshavn Isbræ glacier. *Nature*, 432(7017), 608–610.

Joughin, I., Smith, B.E., Howat, I.M., Scambos, T. and Moon, R., 2010. Greenland flow variability from ice-sheet wide velocity mapping. *Journal of Glaciology*, 56(197), 415-430.

Kelly, M., 1985. A review of the Quaternary geology of western Greenland. In: Andrews, J.T. (ed), *Quaternary Environments in Eastern Canadian Arctic, Baffin Bay and Western Greenland*. Boston: Allen and Unwin, 461-501.

Kelly, M.A. and Long, A.J., 2009. The dimensions of the Greenland Ice Sheet since the Last Glacial Maximum. *PAGES News*, 17(2), 60-61.

Kenny, A.J., Cato, I., Desprez, M., Fader, G., Schüttenhelm, R.T.E. and Side, J., 2003. An overview of seabed-mapping technologies in the context of marine habitat classification. *ICES Journal of Marine Science*, 60(2), 411-418.

Kongsberg, 2010. TOPAS PS 18 parametric sub-bottom profiler: System Specification.

Kongsberg Maritime AS, 2005. EM120 Multibeam echo sounder: Product Description.

Kongsberg Simrad Subsea AS, 2001. EM120 Multibeam echo sounder: Operator Manual.

Kuijpers, A., Dalhoff, F., Brandt, M.P., Hümbs, P., Schott, T. and Zotova, A., 2007. Giant iceberg plow marks at more than 1 km water depth offshore West Greenland. *Marine Geology*, 246(1), 60-64.

Letréguilly, A., Reeh, N. and Huybrechts, P., 1991. The Greenland ice sheet through the last glacial-interglacial cycle. *Palaeogeography, Palaeoclimatology, Palaeoecology (Global and Planetary Change Section)*, 90, 385-394.

Lewis, J.C. and Bennett, G., 1984. Monte Carlo calculations of iceberg draft changes caused by roll. *Cold Regions Science and Technology*, 10(1), 1-10.

Lloyd, J.M., Park, L.A., Kuijpers, A. and Moros, M., 2005. Early Holocene palaeoceanography and deglacial chronology of Disko Bugt, West Greenland. *Quaternary Science Reviews*, 24(14-15), 1741-1755.

Long, A.J., 2009. Back to the future: Greenland's contribution to sea-level change. *GSA Today*, 19(6), 4-10.

Long, A.J. and Roberts, D.H., 2003. Late Weichselian deglacial history of Disko Bugt, West Greenland, and the dynamics of the Jakobshavns Isbrae ice stream. *Boreas*, 32(1), 208-226.

MacAyeal, D. R., Okal, E.A., Aster, R.C. and Bassis, J.N., 2008. Seismic and hydroacoustic tremor generated by colliding icebergs. *Journal of Geophysical Research*, 113, F03011, doi:10.1029/2008JF001005.

MacAyeal, D. R., Okal, E.A., Aster, R.C., Bassis, J.N., Brunt, K.M., Cathles, L.M., Drucker, R., Fricker, H.A., Kim, Y-J., Martin, S., Okal, M.H., Sergienko, O.V., Sponsler, M.P. and Thom, J.E., 2006. Transoceanic wave propagation links iceberg calving margins of Antarctica with storms in tropics and Northern Hemisphere. *Geophysical Research Letters*, 33(17), L17502.

Meier, M.F., 1997. Calving. In Van der Veen, C.J. (ed). *Calving Glaciers: Report of a Workshop, February 28 - March 2, 1997*. BPRC Report No. 15, Byrd Polar Research Center, The Ohio State University, Columbus, Ohio, 21-27.

Melles, M. and Kuhn, G., 1993. Sub-bottom profiling and sedimentological studies in the southern Weddell Sea, Antarctica: evidence for large-scale erosional/depositional processes. *Deep Sea Research Part I: Oceanographic Research Papers*, 40(4), 739-760l.

Metz, J. 2005. Marine Geophysical Investigations of the Polar North Atlantic: Sea-Floor Scouring at the Mouth of Hudson Strait by Deep-Keeled Icebergs. MPhil Thesis, University of Cambridge.

Metz, J., Dowdeswell, J.A. and Woodworth-Lynas, C.M.T., 2008. Sea-floor scour at the mouth of Hudson Strait by deep-keeled icebergs from the Laurentide Ice Sheet. *Marine Geology*, 253(3-4), 149-159.

Mikkelsen, N. and Ingerslev, T., 2002 (eds). *Nomination of the Ilulissat Icefjord for inclusion in the World Heritage List.* Copenhagen: Geological Survey of Denmark and Greenland.

Mottram, R., 2008. Processes of crevasse formation and the dynamics of calving glaciers: A study at Breiđamerkurjökull. PhD Thesis, University of St. Andrews.

Mugford, R. and Dowdeswell, J.A., 2010. Modeling iceberg-rafted sedimentation in high-latitude fjord environments. *Journal of Geophysical Research*, 115, doi: 10.1029/2009JF001564.

Neshyba, S., 1980. On the size distribution of Antarctic icebergs. *Cold Regions Science and Technology*, 1(3-4), 241-248.

Neshyba, S. and Josberger, E.G., 1980. On the Estimation of Antarctic Iceberg Melt Rate. *Journal of Physical Oceanography*, 10(10), 1681-1685.

Nick, F.M., Vieli, A., Howat, I.M. and Joughin, I., 2009. Large-scale changes in Greenland outlet glacier dynamics triggered at the terminus. *Nature Geoscience*, 2(2), 110-114.

Ó Cofaigh, C., 2009. James Clark Ross Cruise Report – JR175 West Greenland and Baffin Bay.

Ó Cofaigh, C., Dowdeswell, J., Kilfeather, A., Jennings, A., Evans, J., Noormets, R. and Walton, M., 2010. Palaeo-ice streams on the west Greenland continental margin during the last glacial cycle. *Geophysical Research Abstracts*, 12, EGU2010-4959.

Ó Cofaigh, C., Larter, R.D., Dowdeswell, J.A., Hillenbrand, C-D., Pudsey, C.J., Evans, J. and Morris, P., 2005. Flow of the West Antarctic Ice Sheet on the continental margin of the Bellingshausen Sea at the Last Glacial Maximum. *Journal of Geophysical Research*, 111, B11103, doi:10.1029/2005JB003619.

Ottesen, D. and Dowdeswell, J.A., 2009. Am inter-ice stream glaciated margin: Submarine landforms and a geomorphic model based on marine geophysical data from Svalbard. *Geological Society of America Bulletin*, 121(11-12), 1647-1665.

Ottesen, D., Dowdeswell, J.A., Landvik, J.Y. and Mienert, J. (2007). Dynamics of the Late Weichselian ice sheet on Svalbard inferred from high-resolution sea-floor morphology. *Boreas*, 36(3), 286-306.

Ottesen, D., Dowdeswell, J.A. and Rise, L., 2005. Submarine landforms and the reconstruction of fast-flowing ice streams within a large Quaternary ice sheet: The 2500-km-long Norwegian-Svalbard margin (57°-80°N). *Geological Society of America Bulletin*, 117(7-8), 1033-1050.

Otto-Bliesner, B.L., Marshall, S.J., Overpeck, J.T., Miller, G.H. and Hu, A., 2006. Simulating Arctic Climate Warmth and Icefield Retreat in the Last Interglaciation. *Science*, 311( 5768), 1751-1753.

Pedrosa, M., Andreassen, K., Winsborrow, M. and Camerlenghi, A., 2011. Seafloor geomorphology of the Storfjorden Trough outer continental shelf. *Geophysical Research Abstracts*, 13, EGU2011-4525.

Pfeffer, W.T., Harper, J.T. and O'Neel, S., 2008. Kinematic Constraints on Glacier Contributions to 21st Century Sea-Level Rise. *Science*, 321(5849), 1340-1343.

Polyak, L., 1997. Ice-keel Scouring: Overview. In: Davies, T.A., Bell, T., Cooper, A.K., Josenhans, H., Polyak, L., Solheim, A., Stoker, M.S. and Travers, J.A (eds). *Glaciated Continental Margins: An Atlas of Acoustic Images*. London: Chapman and Hall, 163-167.

Renard, V. and Allenou, J.P., 1979. Sea Beam, multi-beam echo-sounding in 'Jean Charcot': Description, evaluation and first results. *International Hydrographic Review*, 56(1), 35-67.

Rignot, E. and Kanagaratnam, P., 2006. Changes in the Velocity Structure of the Greenland Ice Sheet. *Science*, 311(5763), 986-990.

Rignot, E., Koppes, M and Velicogna, I., 2010. Rapid submarine melting of the calving faces of West Greenland glaciers. *Nature Geoscience*, 3(3), 187-191.

Rinterknecht, V., Gorokhovich, Y., Schaefer, J. and Caffee, M., 2009. Preliminary $^{10}$Be chronology for the last deglaciation of the western margin of the Greenland Ice Sheet. *Journal of Quaternary Science*, 24(3), 270-278.

Roberts, D.H. and Long, A.J., 2005. Streamlined bedrock terrain and fast ice flow, Jakobshavn Isbræ, West Greenland: implications for ice stream and ice sheet dynamics. *Boreas*, 34(1), 25-42.

Roberts, D.H., Long, A.J., Davies, B.J., Simpson, M.J.R. and Schnabel, C., 2010. Ice stream influence on West Greenland Ice Sheet dynamics during the Last Glacial Maximum. *Journal of Quaternary Science*, 25(6), 850-864.

Roberts, D.H., Long, A.J., Schnabel, C., Davies, B.J., Xu, S., Simpson, M.J.R. and Huybrechts, P., 2009. Ice sheet extent and early deglacial history of the southwestern sector of the Greenland Ice Sheet. *Quaternary Science Reviews*, 28(25-26), 2760-2773.

Robin, G. de Q., 1979. Formation, flow and disintegration of ice shelves. *Journal of Glaciology*, 24(90), 259-271.

Robinson, P.M., 2010. Dynamics of ice-cap drainage basins from marine geophysical and geological evidence: eastern Austfonna, Svalbard. MPhil Thesis, University of Cambridge.

Scambos, T., Ross, R., Bauer, R., Yermolin, Y., Skvarca, P., Long, D., Bohlander, J. and Haran, T., 2008. Calving and ice-shelf break-up processes investigated by proxy: Antarctic tabular iceberg evolution during northward drift. *Journal of Glaciology*, 54(187), 579-591.

Schmidt, V., Chayes, D. and Caress, D., 2006. The MB-System™ Cookbook [online]. Available from: http://www.mbari.org/data/mbsystem/mb-cookbook/index.html.

Siegert, M.J., 2001. *Ice Sheets and Late Quaternary Environmental Change*. Chichester: John Wiley & Sons Ltd.

Simpson, M.J.R., Milne, G.A., Huybrechts, P. and Long, A.J. Calibrating a glaciological model of the Greenland ice sheet from the Last Glacial Maximum to present-day using field observations of relative sea level and ice extent. *Quaternary Science Reviews*, 28(17-18), 1631-1657.

Solheim, A., Milliman, J.D. and Elverhoi, A., 1988. Sediment distribution and sea-floor morphology of Storbanken: implications for the glacial history of the northern Barents Sea. *Canadian Journal of Earth Sciences*, 25(4), 547-556.

Stoker, M.S., Pheasant, J.B. and Josenhans, H., 1997. Seismic Methods and Interpretation. IN Davies, T.A., Bell, J., Cooper, A.K., Josenhans, H., Polyak, L., Solheim, A., Stoker, M.S. and Stravers, J.A. (eds). *Glaciated Continental Margins: An Atlas of Acoustic Images*. London, Chapman & Hall, 9-26.

Syvitski, J.P.M., Burrell, D.C. and Skei, J.M., 1987. *Fjords: Processes and Products*. New York: Springer-Verlag.

Syvitski, J.P.M., Stein, A.B. and Andrews, J.T., 2001. Icebergs and the Sea Floor of the East Greenland (Kangerlussuaq) Continental Margin. *Arctic, Antarctic and Alpine Research*, 33(1), 52-61.

Tang, C.L., Ross, C.K., Yao, T., Petrie, B., DeTracey, B.D., and Dunlap, E., 2004. The circulation, water masses and sea-ice of Baffin Bay. *Progress in Oceanography*, 63(4), 183–228.

Tarasov, L. and Peltier, W.R., 2003. Greenland glacial history, borehole constraints, and Eemian extent. *Journal of Geophysical Research*, 108(B3), doi:10.1029/2001JB001731.

Thomas, G.S.P. and Connell, R.J., 1985. Iceberg drop, dump and grounding structures from Pleistocene glacio-lacustrine sediments, Scotland. *Journal of Sedimentary Research*, 55(2), 243-249.

Vogt, P.R., Crane, C. and Sundvor, E., 1994. Deep Pleistocene iceberg plowmarks on the Yermak Plateau: Sidescan and 3.5 kHz evidence for thick calving ice fronts and a possible marine ice sheet in the Arctic Ocean. *Geology*, 22, 403-406.

Wadhams, P., 1988. Winter observations of iceberg frequencies and sizes in the South Atlantic Ocean. *Journal of Geophysical Research*, 93(C4), 3583-3590.

Weeks, W.F. and Campbell, W.J., 1973. Icebergs as a freshwater source: an appraisal. *Journal of Glaciology*, 12(65), 207-233.

Weidick, A. and Bennike, O., 2007. Quaternary glaciation history and glaciology of Jakobshavn Isbrae and the Disko Bugt region, West Greenland: a review. *Geological Survey of Denmark and Greenland Bulletin 14*.

Weinrebe, W., Kuijpers, A., Klaucke, I. and Fink, M., 2009. Multibeam Bathymetry Surveys in Fjords and Coastal Areas off West-Greenland. Poster: AGU Fall Meeting, San Francisco, USA, 18.12.2009.

Wessel, P. and Smith, W.H.F., 1991. Free software helps map and display data. *EOS, Transactions of the American Geophysical Union*, 72(41), 441.

Williams Jr, R.S. and Ferrigno, J.G., 2009. State of the Earth's cryosphere at the beginning of the 21st century: glaciers, global snow cover, floating ice, and permafrost and periglacial environments. *Satellite Image Atlas of Glaciers of the World*. U.S. Geological Survey, Professional Paper 1368-I.

Winkelmann, D., Jokat, W., Jensen, L. and Schenke, H-W., 2010. Submarine end moraines on the continental shelf off NE Greenland - Implications for Lateglacial Dynamics. *Quaternary Science Reviews*, 29(9-10), 1069-1077.

Winsborrow, M.C.M., Andreassen, K., Corner, G.D. and Laberg, J.S., 2009. Deglaciation of a marine-based ice sheet: Late Weichselian palaeo-ice dynamics and retreat in the southern Barents Sea reconstructed from onshore and offshore glacial geomorphology. *Quaternary Science Reviews*, 29(3-4), 424-442.

Woodworth-Lynas, C.M.T. and Dowdeswell, J.A., 1994. Soft-sediment striated surfaces and massive diamicton facies produced by floating ice. In: Deynoux, M., Miller, J.M.G., Domack, E.W., Eyles, N., Fairchild, I.J. and Young, G.M. (eds). *Earth's Glacial Record*. Cambridge: Cambridge University Press, 241-259.

Woodworth-Lynas, C.M.T. and Guigné, J.Y., 1990. Iceberg scours in the geological record: examples from glacial Lake Agassiz. In: Dowdeswell, J.A. and Scourse, J.D. (eds). *Glacimarine Environments: Processes and Sediments*. Geological Society Special Publication No. 53, 217-233.

Woodworth-Lynas, C.M.T., Josenhans, H.W., Barrie, J.V., Lewis, C.F.M. and Parrott, D.R., 1991. The physical processes of seabed disturbance during iceberg grounding and scouring. *Continental Shelf Research*, 11(8-10), 939-961.

Woodworth-Lynas, C.M.T., Simms, A. and Rendell, C.M., 1985. Iceberg grounding and scouring on the Labrador Continental Shelf. *Cold Regions Science and Technology*, 10(2), 163-186.